# Naval Research Laboratory

Washington, DC 20375-5000

AD-A240 679

NRL Memorandum Report 6898

# Discharge System Tests of Halon 1301 Test Gas Simulants

H. W. CARHART, J. T. LEONARD, P. J. DINENNO,*
E. W. FORSSELL,* AND M. D. STARCHVILLE*

*Navy Technology Center for Safety and Survivability*
*Chemistry Division*

**Hughes Associates Inc.,*
*Wheaton, MD 20902*

September 19, 1991

# REPORT DOCUMENTATION PAGE

*Form Approved*
*OMB No 0704-0188*



**1. AGENCY USE ONLY** *(Leave blank)*

**2. REPORT DATE**
1991 September 19

**3. REPORT TYPE AND DATES COVERED**
Interim (June 1988 - September 1988)

**4. TITLE AND SUBTITLE**
Discharge System Tests of Halon 1301 Test Gas Simulants

**5. FUNDING NUMBERS**
61-2961-0-1
63514N; S1565-SL
DC01FFS-04
DN155-30

**6. AUTHOR(S)**
H. W. Carhart, J. T. Leonard, P. J. DiNenno,* E. W. Forssell*
M. D. Starchville*

**7. PERFORMING ORGANIZATION NAME(S) AND ADDRESS(ES)**
Naval Research Laboratory
Washington, D. C. 20375-5000

**8. PERFORMING ORGANIZATION REPORT NUMBER**
NRL Memorandum Report 6898

**9. SPONSORING/MONITORING AGENCY NAME(S) AND ADDRESS(ES)**
Naval Sea Systems Command
Washington, D. C. 20362-5100

**10. SPONSORING/MONITORING AGENCY REPORT NUMBER**

**11. SUPPLEMENTARY NOTES**
*Hughes Associates Inc., Wheaton, MD 20902

**12a. DISTRIBUTION/AVAILABILITY STATEMENT**

Approved for public release; distribution unlimited.

**12b. DISTRIBUTION CODE**

**13. ABSTRACT** *(Maximum 200 words)*

All new and retrofit installations of Halon 1301 total flooding systems in shipboard machinery spaces require an acceptance discharge test. It is desirable to use a simulant instead of Halon 1301 in view of current and future restrictions regarding the discharge of Halons into the atmosphere.

Two candidate simulants; sulfur hexafluoride ($SF_6$) and chlorodifluoromethane (R-22) were evaluated on the basis of flow through the piping networks of both modular and banked systems. A modular system with two different fill densities and six banked systems were used in this evaluation.

Sulfur hexafluoride was found to discharge at a similar rate to Halon 1301, while R-22 discharged faster in all tests. The flow splits for both candidate simulants in banked systems were similar to those of Halon 1301.

Together with work on leakage from an enclosure and initial mixing, these tests have shown that sulfur hexafluoride is an excellent simulant for Halon 1301. These conclusions will be confirmed in full scale tests.

**14. SUBJECT TERMS**

| | |
|---|---|
| Halon 1301 | Sulfur Hexafluoride |
| Halon 1301 Simulants | Chlorodifluoromethane |

**15. NUMBER OF PAGES**
115

**16. PRICE CODE**

| 17. SECURITY CLASSIFICATION OF REPORT | 18. SECURITY CLASSIFICATION OF THIS PAGE | 19. SECURITY CLASSIFICATION OF ABSTRACT | 20. LIMITATION OF ABSTRACT |
|---|---|---|---|
| UNCLASSIFIED | UNCLASSIFIED | UNCLASSIFIED | Unlimited |

NSN 7540-01-280-5500 Standard Form 298 (Rev. 2-89)

CONTENTS

CONTENTS (Con't)

FIGURES

FIGURES (Con't)

FIGURES (Con't)

## TABLES

# DISCHARGE SYSTEM TESTS OF HALON 1301 TEST GAS SIMULANTS

## 1.0 INTRODUCTION

All new and retrofit total flooding Halon 1301 fire protection systems in shipboard machinery spaces require an acceptance discharge test. It is desirable to use a simulant instead of Halon 1301 in view of current and future regulations restricting the use of Halon 1301 due to its contribution to stratospheric ozone depletion [1,2,3].

Two candidate simulants, sulfur hexafluoride ($SF_6$) and chlorodifluoromethane (R-22), were identified by DiNenno et al [4]. They were chosen on the basis of similarity in physical properties to Halon 1301. Selected physical properties of both candidate simulants and Halon 1301 are presented in Table 1 [5-9].

Both of these candidate simulants were evaluated on the basis of leakage from an enclosure and initial mixing by DiNenno et al [4,10]. Sulfur hexafluoride was found to be an excellent simulant for Halon 1301 on this basis. It leaked from an enclosure at a similar rate, as the time required for the $SF_6$-air interphase to descend was within 10% of that required for the Halon 1301-air interphase to descend in each leakage configuration tested. R-22 on the other hand, leaked

Manuscript approved June 18, 1991

## Table 1 - Chemical & Physical Properties

| | HALON 1301 | SULFURHEXAFLOURIDE | R-22 |
|---|---|---|---|
| Chemical Formula | $CBrF_3$ | $SF_6$ | $CHClF_2$ |
| Molecular Weight | 148.93 | 146.05 | 86.48 |
| Normal Boiling Point | -57.8°C(-72°F) | -50.8°C(-59.4°F)* | -40.75°C(-41.36°F) |
| Vapor Pressure at 21°C(70°F) | 1.47MPa(213.7psia) | 2.16 MPa(312.7psia) | 0.94MPa(136.12psia) |
| Critical Temp | 67°C(152.6°F) | 45.55°C(114.6°F) | 96°C(204.81°F) |
| Critical Pressure | 3.965MPa(575.0psia) | 3.759MPa(544.3psia) | 4.977MPa(721.91psia) |
| Liquid Density at 21°C(70°F) | 1567kg/m3(97.81lbm/$ft^3$) | 1378kg/$m^3$(86 lbm/$ft^3$) | 1209kg/$m^3$(75.51lbm/$ft^3$) |
| Vapor Density at 21°C(70°F) and .101MPa(14.7psia) | 6.26kg/$m^3$(0.3911lbm/$ft^3$) | 6.12kg/$m^3$(.3821lbm/$ft^3$) | 3.64kg/$m^3$(.2271lbm/$ft^3$) |
| Liquid Viscosity at 21°C(70°F) | $.00016\frac{Nsec}{m^2}(.0013\frac{lbm}{in\ sec})$ | $.00029\frac{Nsec}{m^2}(.0023\frac{lbm}{in\ sec})$ | $.0002\frac{Nsec}{m^2}(.0016\frac{lbm}{in\ sec})$ |
| Vapor Viscosity at 21°C(70°F) and .101MPa(14.7psia) | $.000016\frac{Nsec}{m^2}(.00013\frac{lbm}{in\ sec})$ | $.000015\frac{Nsec}{m^2}(.00012\frac{lbm}{in\ sec})$ | $.000013\frac{Nsec}{m^2}(.00010\frac{lbm}{in\ sec})$ |
| Thermal Conductivity of Vapor at 21°C(70°F) + .101MPa(14.7psia) air .0255W/m°K($.0147\frac{Btu}{hrft^{\circ}F}$) | .0092W/m°K($.0053\frac{Btu}{hrft^{\circ}F}$) | .0142W/m°K($.0082\frac{Btu}{hrft^{\circ}F}$) | .0105W/m°K($.006\frac{Btu}{hrft^{\circ}F}$) |
| Enthalpy of Vaporization at Boiling Point | $17,700\frac{kJ}{kgmole}(7,607\frac{Btu}{lbmole})$ | $18,840\frac{kJ}{kgmole}(8,100\frac{Btu}{lbmole})$* | $20,220\frac{kJ}{kgmole}(8,693\frac{Btu}{lbmole})$ |
| at 21°C(70°F) | $12,310\frac{kJ}{kgmole}(5,292\frac{Btu}{lbmole})$ | $9,630\frac{kJ}{kgmole}(4,140\frac{Btu}{lbmole})$ | $16,160\frac{kJ}{kgmole}(6,948\frac{Btu}{lbmole})$ |

*Triple Point 0.224 MPa -50.8°C (32.5psia -59.4°F) at a slower rate, as it took nearly 50% longer for the R-22-air interphase to descend. When the nozzle was obstructed to create a poor mixing situation, the vertical concentration profiles for both candidate simulants were similar to the vertical concentration profile of Halon 1301.

The flow of Halon 1301 through the piping network of a total flooding fire protection system is a very complex phenomenon. Halon 1301 changes phase from a liquid to a vapor in the network resulting in two-phase behavior. This causes the simplifying assumptions of many classical flow equations to be invalid as the physical properties of the fluid will not be constant. The presence of dissolved nitrogen in the flow causes an additional complication as the compositions of both phases become variables in the analysis of the flow. A further complication arises from the transient nature of the flow and its short duration. This causes time to be an additional parameter in any analysis.

A successful simulant for Halon 1301 must not only replicate the overall flow rate through the network (i.e., discharge time), it must also replicate the flow splits in the network (i.e., mass distribution between nozzles).

## 2.0 CLASSIFICATION OF NETWORKS

Pipe flow networks of total flooding fire protection systems are classified by the degree of complexity attributed to the network. The least complicated are modular systems. They are characterized by a single nozzle connected to one or more cylinders via a minimal length of pipe. The pressure difference between the discharge cylinder and the nozzle is slight so the piping network has only a minor influence on the flow. Typical applications include single chambers protected through a single cylinder and nozzle or a larger chamber protected with multiple cylinders, each directly connected to a single nozzle (common in retrofit systems).

The next classification is a balanced banked system. This allows a multicylinder and multinozzle system but the flow rate from each nozzle must be equal (within 10%) and all flow divisions must be equal (50-50). As a result of this, the pressure at each nozzle will be equal and all branches will be geometrically similar. Typical applications are a central storage area protecting several equal volume chambers or a single chamber with several evenly spaced nozzles.

The classification with the highest degree of complexity is the unbalanced banked system. These systems have either unequal flows from each nozzle or unequal flow divisions (i.e. 70-30) or both. Typical applications include a central storage area protecting several chambers of differing volumes or a single chamber with a high ceiling requiring several horizontal tiers of nozzles.

Piping networks are further characterized by a number of parameters that affect the cylinder decay curves (pressure and temperature versus outage fraction) and the relationship between those decay curves and the nozzle curves. These include the initial charge pressure, the fill density, percent of agent in piping, and the pressure drop in the network.

There are two standard initial charge pressures, 4.1 MPag (600 psig) and 2.5 MPag (360 psig) [11]. The higher initial pressure affords a greater pressure loss in the piping system and therefore smaller pipe diameters but requires a thicker walled discharge cylinder. 4.1 MPag (600 psig) initial charge pressure systems are used by the Navy [12,13].

The fill density is the mass of agent per unit volume of each discharge cylinder. This typically varies from 640 $kg/m^3$ (40 $lb/ft^3$) to 1100 $kg/m^3$ (70 $lb/ft^3$) [11]. A lower fill density causes the pressure in the cylinder to decay at a slower rate but it requires more cylinders to handle the same amount of agent. The Navy uses a standard 1100 $kg/m^3$ (70 $lb/ft^3$) fill density [12,13].

Both the percent of agent in piping and the pressure drop in the network are less tangible parameters as they can not be determined in a straight forward manner and they vary with time. The National Fire Protection Association (NFPA) in their Standard 12A provides a method for estimating both parameters at median discharge conditions (50% of initial charge mass having left the network) [11]. This method has been shown to underestimate the pressure drop for complex systems [14].

The percent of agent in piping is the difference between the mass that has left the cylinder and the mass that has left the network reported as a percentage of the initial charge mass. It typically varies from 10% to 50% with modular systems used by the Navy, restricted to the lower end.

The pressure drop in the network typically varies from 69 kPa (10 psi) in modular systems to 830 kPa (120 psi) for more complex systems.

## 3.0 OBJECTIVE

Two series of tests were conducted to evaluate sulfur hexafluoride ($SF_6$) and chlorodifluoromethane (R-22) as simulants for Halon 1301 on the basis of discharge system flow. In the first series, this evaluation was done for modular systems on the basis of similarity in discharge times between each candidate simulant and Halon 1301, at various fill densities.

Banked system flow was evaluated in the second series. In this series, the evaluation is based on similarity in flow divisions as well as discharge times.

## 4.0 MODULAR SYSTEM TESTS

### 4.1 Test Facilities

These tests were conducted at the Chesapeake Bay Detachment (CBD) of the Naval Research Laboratory, Chesapeake Beach, Maryland. A test enclosure was constructed with nominal inside dimensions of 3.7 m x 3.7 m x 3.7 m (12 ft x 12 ft x 12 ft) providing a floodable volume of approximately 48.9 $m^3$ (1728 $ft^3$). The test enclosure was built using conventional 5.1 x 10.2 cm (2 x 4 in.) framing, with 5.1 x 16.2 cm (2 x 6 in.) floor and ceiling joists. The enclosure was located indoors to facilitate easier testing and eliminate ambient weather effects. To ensure an airtight environment, two layers of 1.3 cm (.5 in.) painted gypsum wallboard were attached to all interior surfaces. All wallboard joints were then taped and spackled prior to the application of two coats of water based interior paint. The enclosure was also fitted with a 203 x 91.4 cm (80 x 36 in.) steel door assembly that utilized magnetic seals and two 45.7 x 81.3 x .6 cm (18 x 32 x .25 in.) plexiglass observation windows.

## 4.2 Halon 1301 Total Flooding System

The enclosure was fitted with a roof-mounted modular Halon 1301 total flooding system. A FENWAL Cylindrical Agent Storage Container (P/N 31-192007-251) was utilized in this system. It has an internal volume of .0125 $m^3$ (.442 $ft^3$) and is rated for 9.2 kg (20 lb) to 13.8 kg (30 lb) of Halon 1301. A manual activation valve was used to initiate the discharge. A discharge pipe from this system penetrated the ceiling at its center and terminated at the nozzle, which was approximately 20.3 cm (8 in.) below the finished ceiling. The discharge pipe had a nominal pipe size of 3.8 cm

(1.5 in.) and provided approximately 1.5 m (5 ft) of flow length. The nozzle was a Bete (P/N TF48FC) Spiral Nozzle. This same system was used for the simulants, $SF_6$ and R-22.

## 4.3 Procedure

In these tests, the Halon 1301 fill density was varied with the two candidate simulants being tested at fill densities that would result in the same percent by volume concentration as the Halon 1301 tests.

### 4.3.1 Test Sequence

A. Discharge cylinder was filled with desired agent and super pressurized with nitrogen to 2.41 MPag (350 psig).

B. Data logging was initiated and discharge started.

C. Test ended when concentration profile had remained stable for five minutes.

D. Enclosure was purged.

## 4.4 Instrumentation

The location of the instrumentation is shown in Figure 1.

### 4.4.1 Temperature

Temperature of the fluid was monitored in the discharge cylinder and just before the nozzle. Two Inconel sheathed thermocouples were used to accomplish this.

### 4.4.2 Pressure

The pressure was monitored at the same locations as the temperature. Two 0 to 6.9 MPag (0 to 1000 psig) range

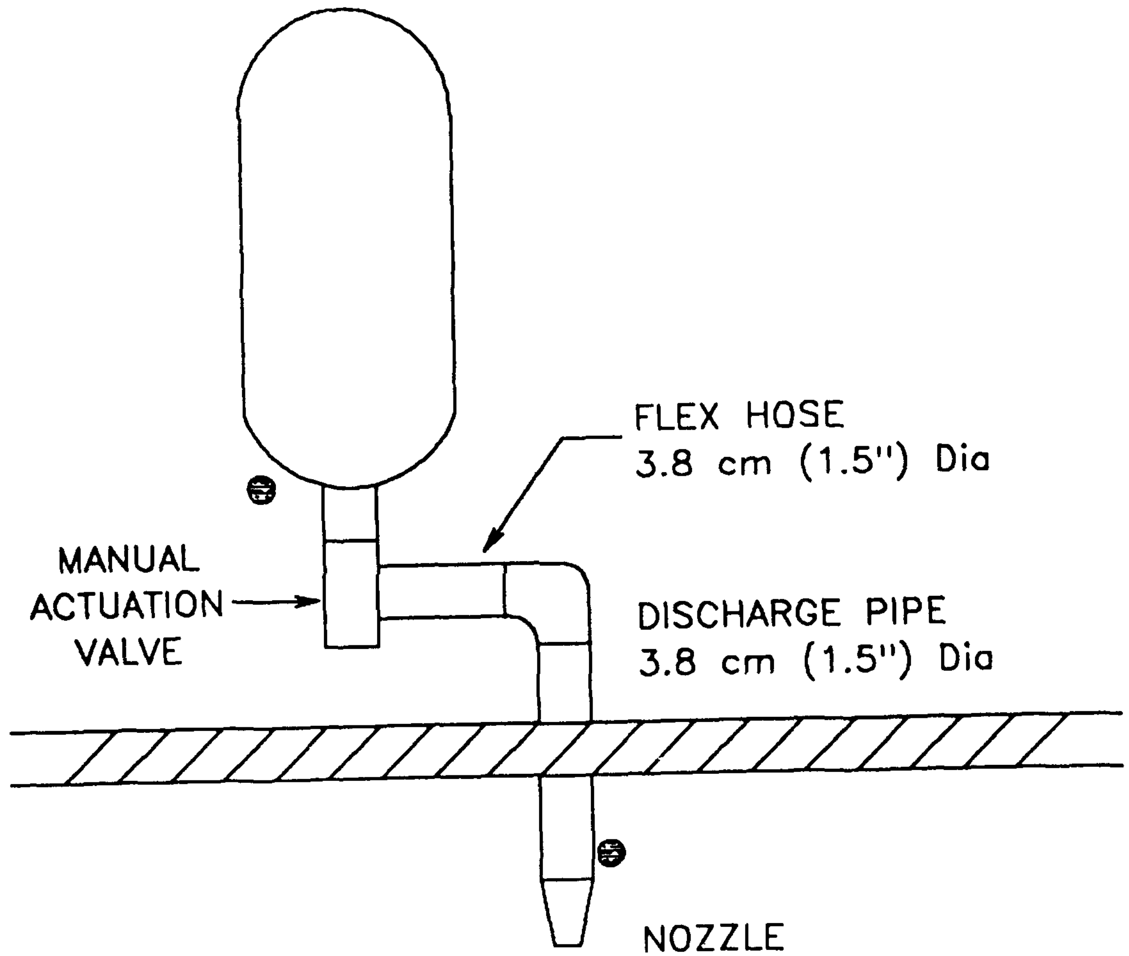


● TEMPERATURE, PRESSURE

Fig. 1 – Modular system

Genisco Technology Corporation Model SP500 vented gage pressure transducers were used to accomplish this.

### 4.5 Results

In the experiments performed, two different Halon 1301 fill densities were used; 800 kg/m$^3$ (50 lb/ft$^3$) and 1100 kg/m$^3$ (70 lb/ft$^3$). The peak nozzle pressures and discharge times are given in Tables 2 and 3 for the lower and higher fill densities respectively. The discharge time is defined by the National Fire Protection Association in their standard 12A as the time between the cylinder actuation and when the flow from the nozzle becomes predominately vapor [11]. Two methods were used to determine when this point is reached. In the first method, the inflection in the nozzle pressure curve when the flow changes from predominately liquid to predominately vapor is utilized. In the second method, the drop in the nozzle flow temperature at this point is utilized. In addition, the discharge time was determined by the time required for the nozzle pressure to return to the ambient pressure signifying the end of the flow. A nozzle pressure of 345 kPag (50 psig), which is 5% of the full scale reading of the pressure transducers used, was taken as ambient in order to stay well above the noise level of the transducers.

Figures 2 and 3 show the nozzle pressure, and nozzle temperature, for the lower fill density. The nozzle pressure and temperature for the higher fill density are shown in Figures 4 and 5.

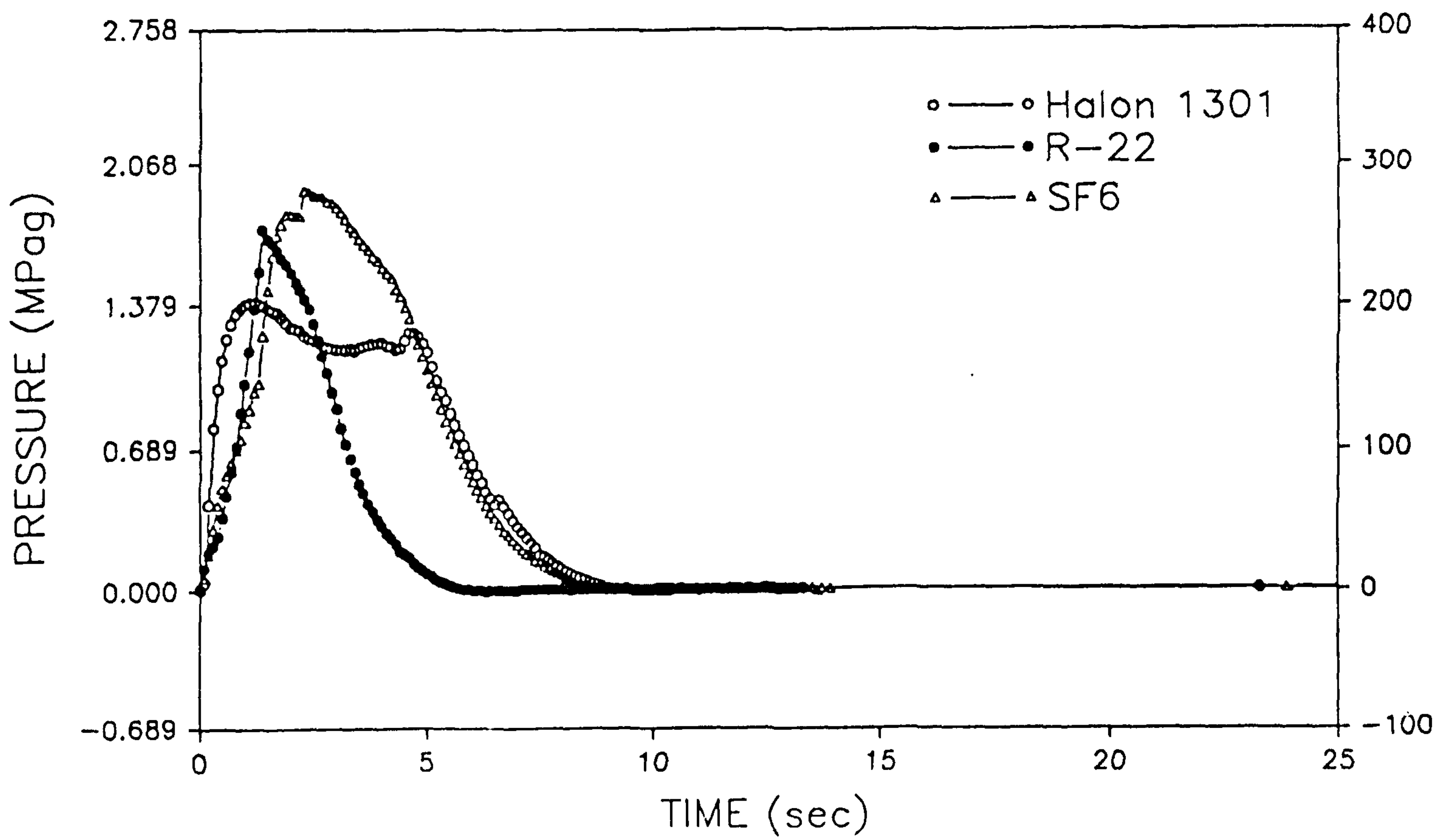


Fig. 2 – Nozzle pressure with fill density of 800 kg/m3 (50 lb/ft3)

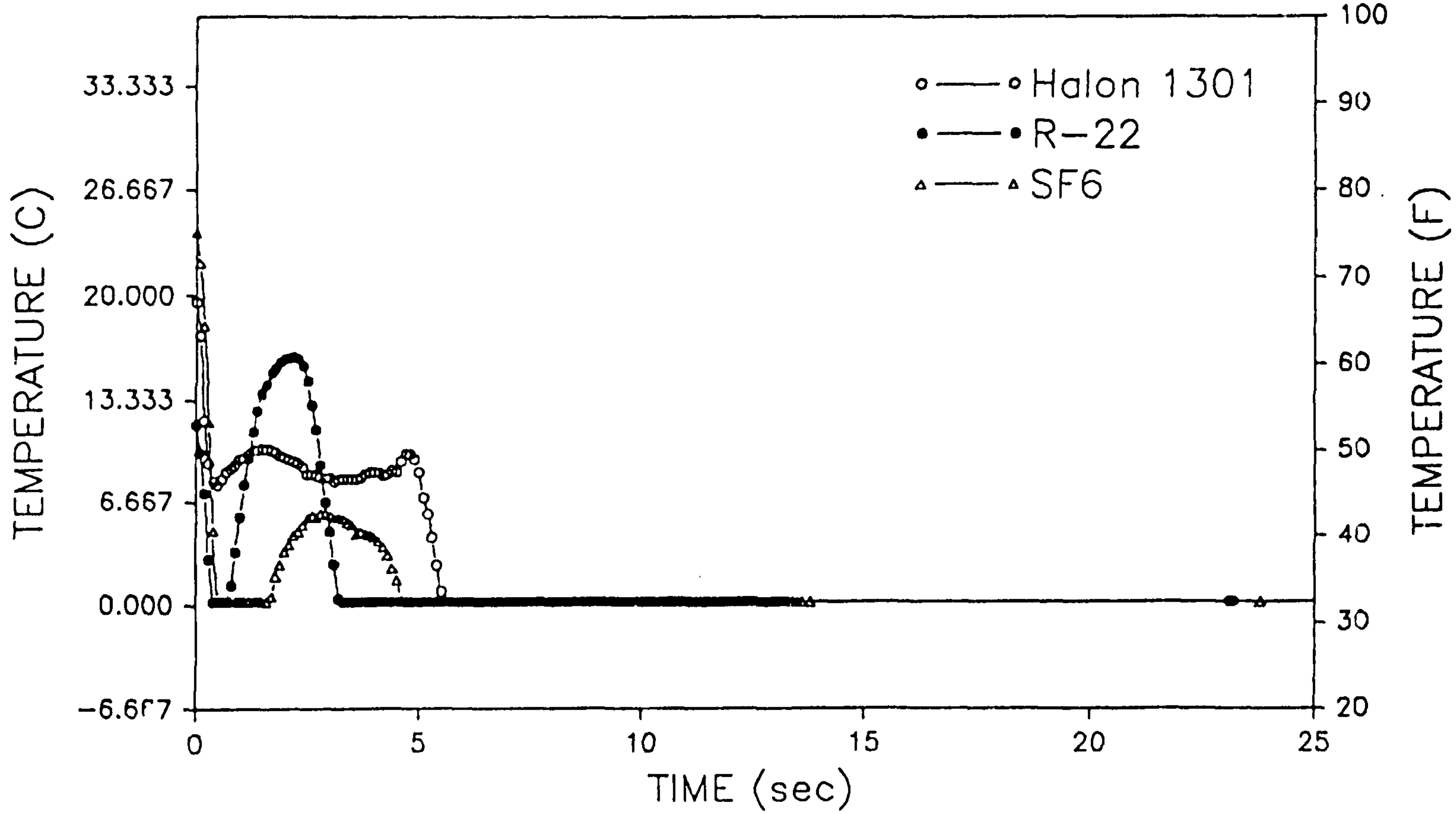


Fig. 3 -- Nozzle temperature with fill density of 800 kg/m3 (50 lb/ft3)

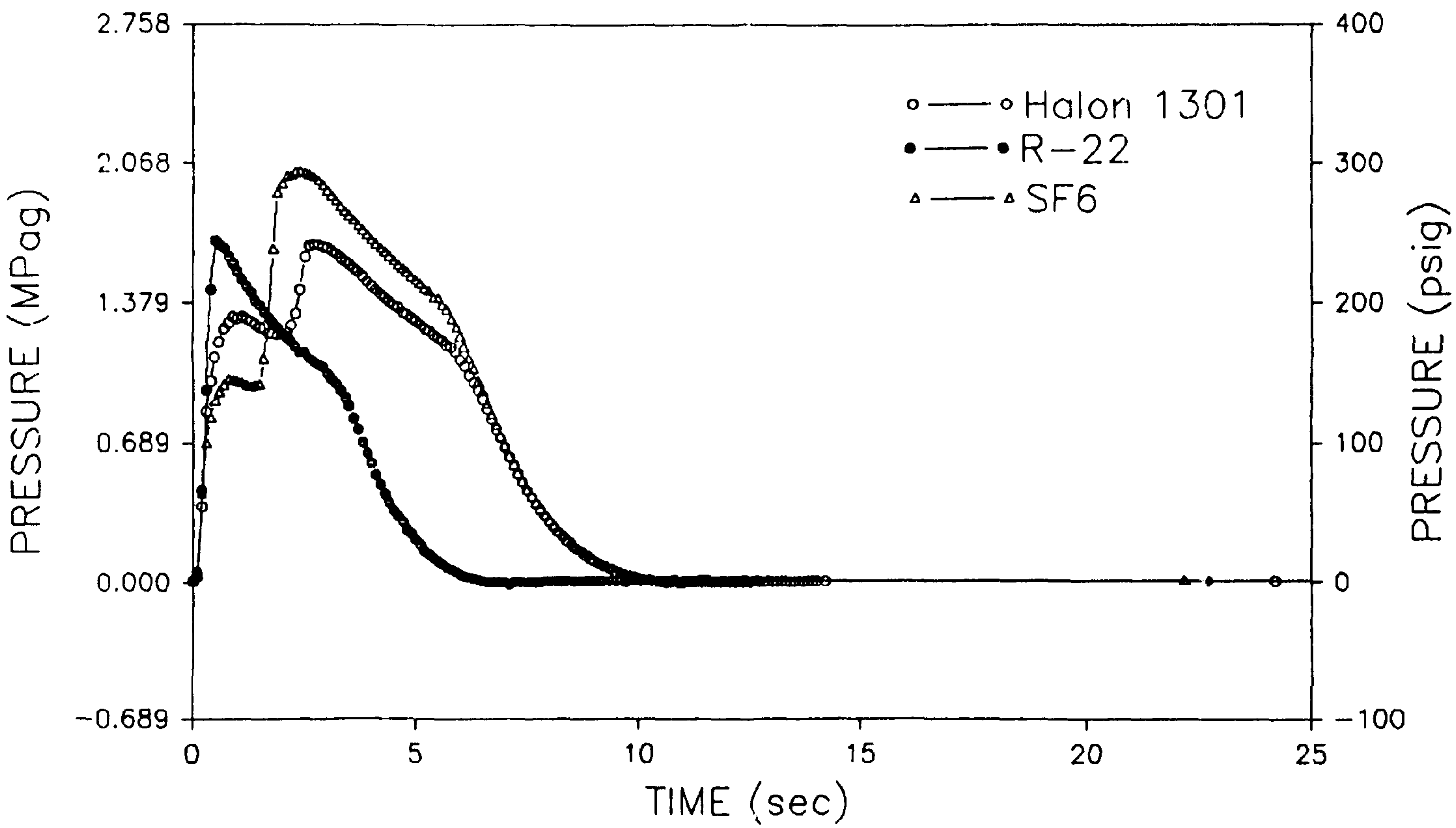


Fig. 4 – Nozzle pressure with fill density of 1100 kg/m3 (70 lb/ft3)

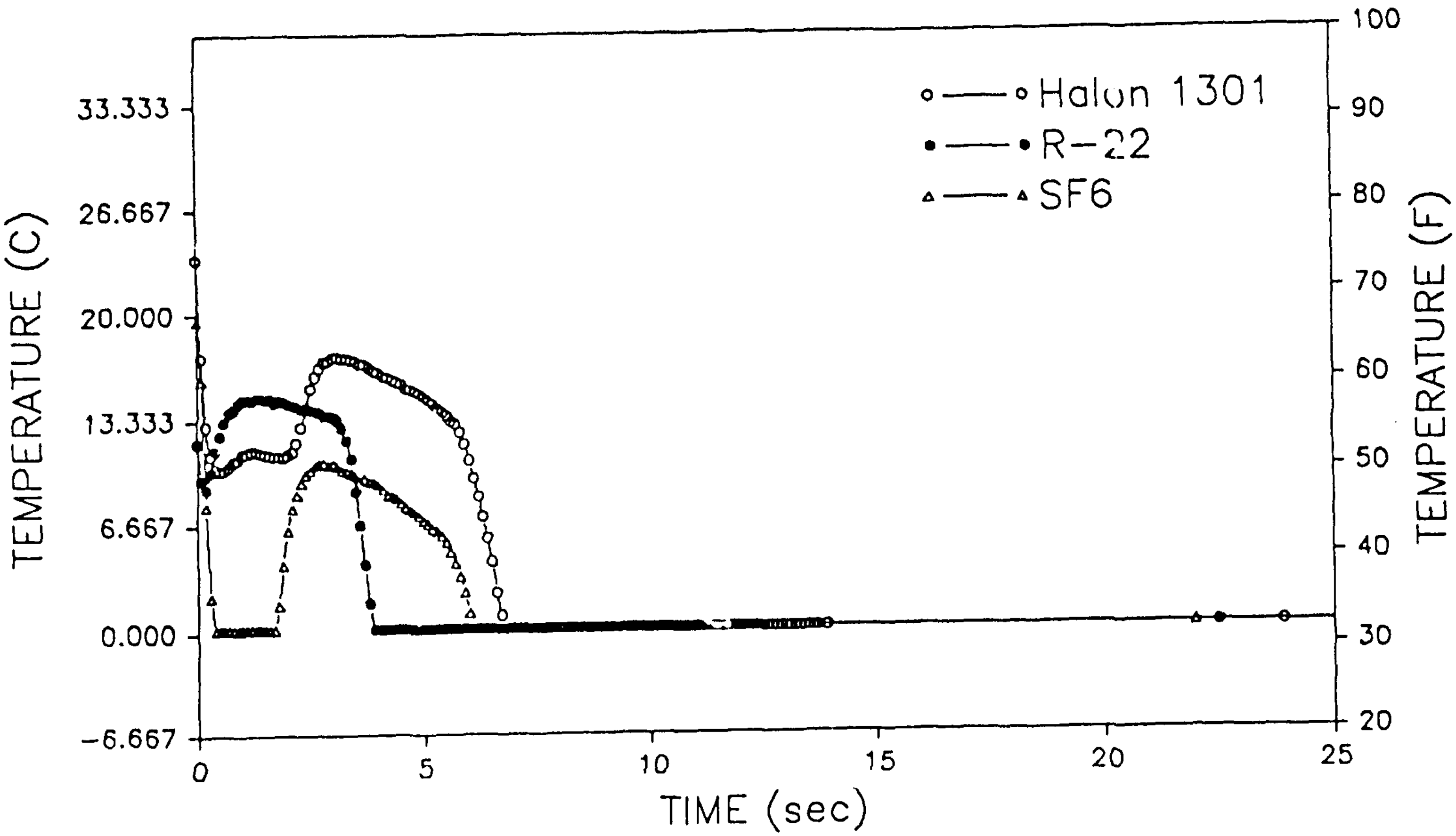


Fig. 5 – Nozzle temperature with fill density of 1100 kg/m3 (70 lb/ft3)

Table 2 - Modular System with 800 $kg/m^3$ (50 $lb/ft^3$) Fill Density

| Test Gas | Halon 1301 | $SF_6$ | R-22 |
|---|---|---|---|
| | | Peak Pressures | |
| Nozzle | 1.39 MPag (202 psig) | 1.94 MPag (282 psig) | 1.75 MPag (254 psig) |
| | | Discharge Times [seconds] | |
| Pressure Inflexion | 4.7 | 4.5 | 2.5 |
| Temperature Method | 4.7 | 4.3 | 2.5 |
| 345 kPa (50 psig) Pressure | 7.0 | 6.6 | 4.0 |

Table 3 - Modular System with 1100 kg/$m^3$ (70 lb/$ft^3$) Fill Density

| Test Gas | Halon 1301 | $SF_6$ | R-22 |
|---|---|---|---|
| | | Peak Pressures | |
| Nozzle | 1.67 MPag (242 psig) | 2.03 MPag (294 psig) | 1.69 MPag (245 psig) |
| | | Discharge Times [seconds] | |
| Pressure Inflexion | 5.8 | 5.5 | 3.5 |
| Temperature Method | 5.7 | 5.5 | 3. |
| 345 kPag (50 psig) Pressure | 7.9 | 7.9 | 4.6 |

As can be seen from these results, sulfur hexafluoride ($SF_6$) discharges at a similar rate to that of Halon 1301. The maximum difference in discharge time between $SF_6$ and Halon 1301 is 0.4 seconds which is a relative difference of approximately 8%. On the other hand chlorodifluoromethane (R-22) discharges at a faster rate than Halon 1301. R-22 takes as much as 3 seconds less time to discharge than Halon 1301 which is a relative difference of approximately 40%.

## 5.0 BANKED SYSTEM TESTS

### 5.1 Test Facilities

These tests were also conducted at the Chesapeake Bay Detachment (CBD), of the Naval Research Laboratory, using the same test enclosure that was used in the modular system tests.

Two additional enclosures were constructed for these tests with nominal inside dimensions of 2.4 m x 2.4 m x 2.4 m (8 ft x 8 ft x 8 ft), each providing a floodable volume of approximately 14.5 $m^3$ (512 $ft^3$). They are similar in construction to the larger enclosure except that only one layer of gypsum wallboard was attached and hollow prehung wood doors were used. These enclosures were not fitted with observation windows.

### 5.2 Halon 1301 Total Flooding Systems

Six different systems were tested. All used a 4.1 mPag (600 psig) Navy standard discharge cylinder rated for 56.7 kg (125 lb) of Halon 1301 [Ansul Part No. 52705N]. This cylinder has an internal volume of .0506 $m^3$ (1.7880 $ft^3$), an empty or tare weight of 70.3 kg (155 lb), and was pneumatically actuated using compressed nitrogen. The cylinder was connected to the piping network through an 3.81 cm (1.5 in.) NPS flex hose 0.91 m (3 ft) in length and a 3.81 cm (1.5 in.) NPS two part thread adaptor [4.76 cm (1.875 in.) 12-UN-2B to 3.81 cm (1.5 in.) NPT]. All networks were constructed with NPT threaded Schedule 80 steel pipe and fittings. The nozzles used were Navy Standard 360° four hole nozzles.

The six systems tested utilized four different pipe geometries and three different nozzle sizes. The first system was a two nozzle balanced network and is shown in Figure 6. One nozzle was inserted approximately 0.76 m (2.5 ft) into the large enclosure at a height of approximately 0.9 m (3 ft), while the other nozzle (nozzle 2) was unenclosed. Both nozzles had orifice areas of 3.24 $cm^2$ (0.503 $in^2$). The second system, which is shown in Figure 7, was the same as the first system except that the enclosed nozzle was switched to one with an orifice area of 1.27 $cm^2$ (0.196 $in.^2$). The third system was a four nozzle balanced network and is shown in Figure 8. Three of the nozzles were inserted approximately 0.76 m (2.5 ft) at a height of approximately 0.9 m (3 ft); one in each enclosure. All had an orifice area of 1.70 $cm^2$ (0.264 $in.^2$). The fourth network is shown in Figure 9 and was similar to a Navy Type II banked

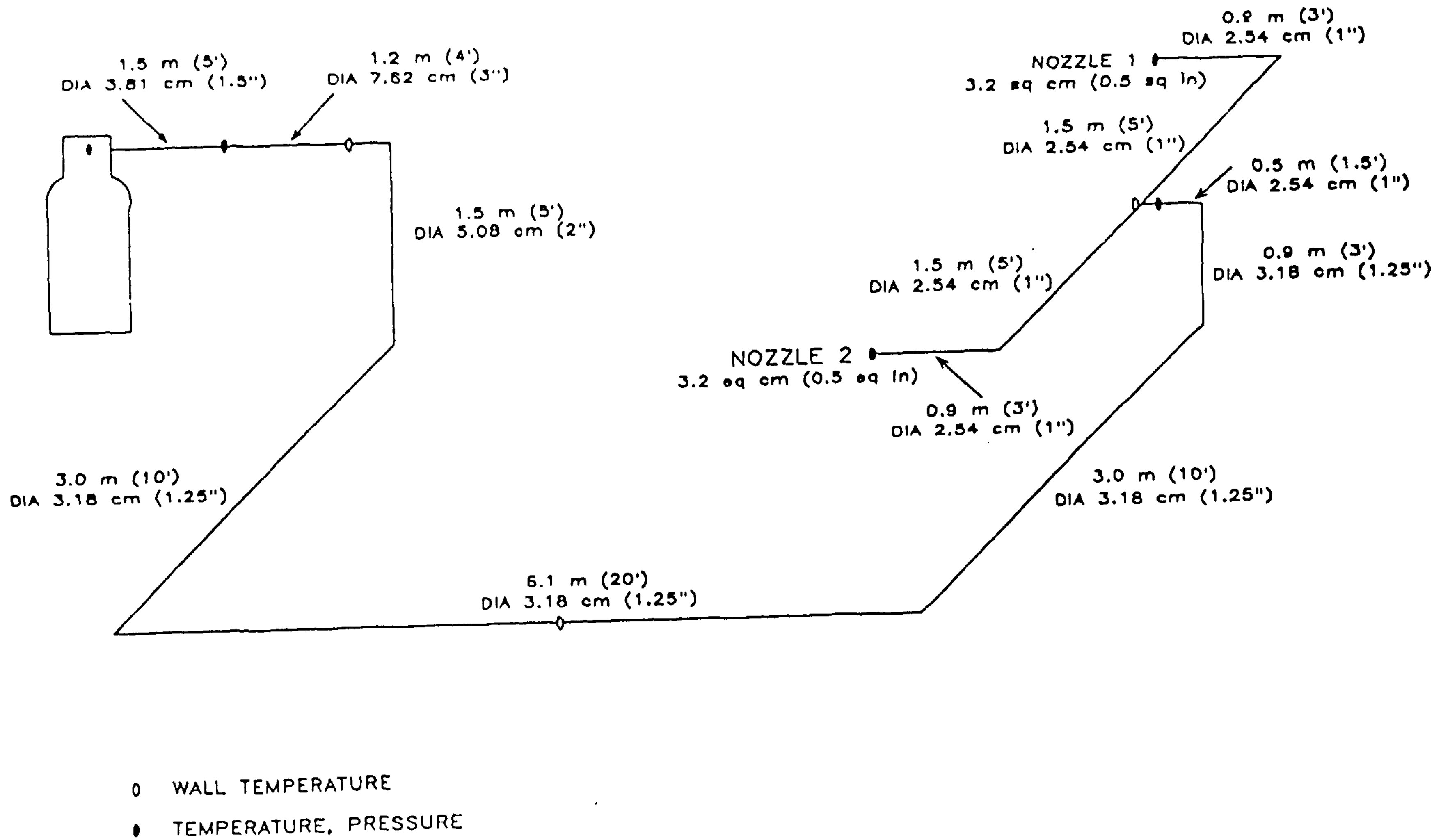


Fig. 6 – System 1: Two nozzle, balanced

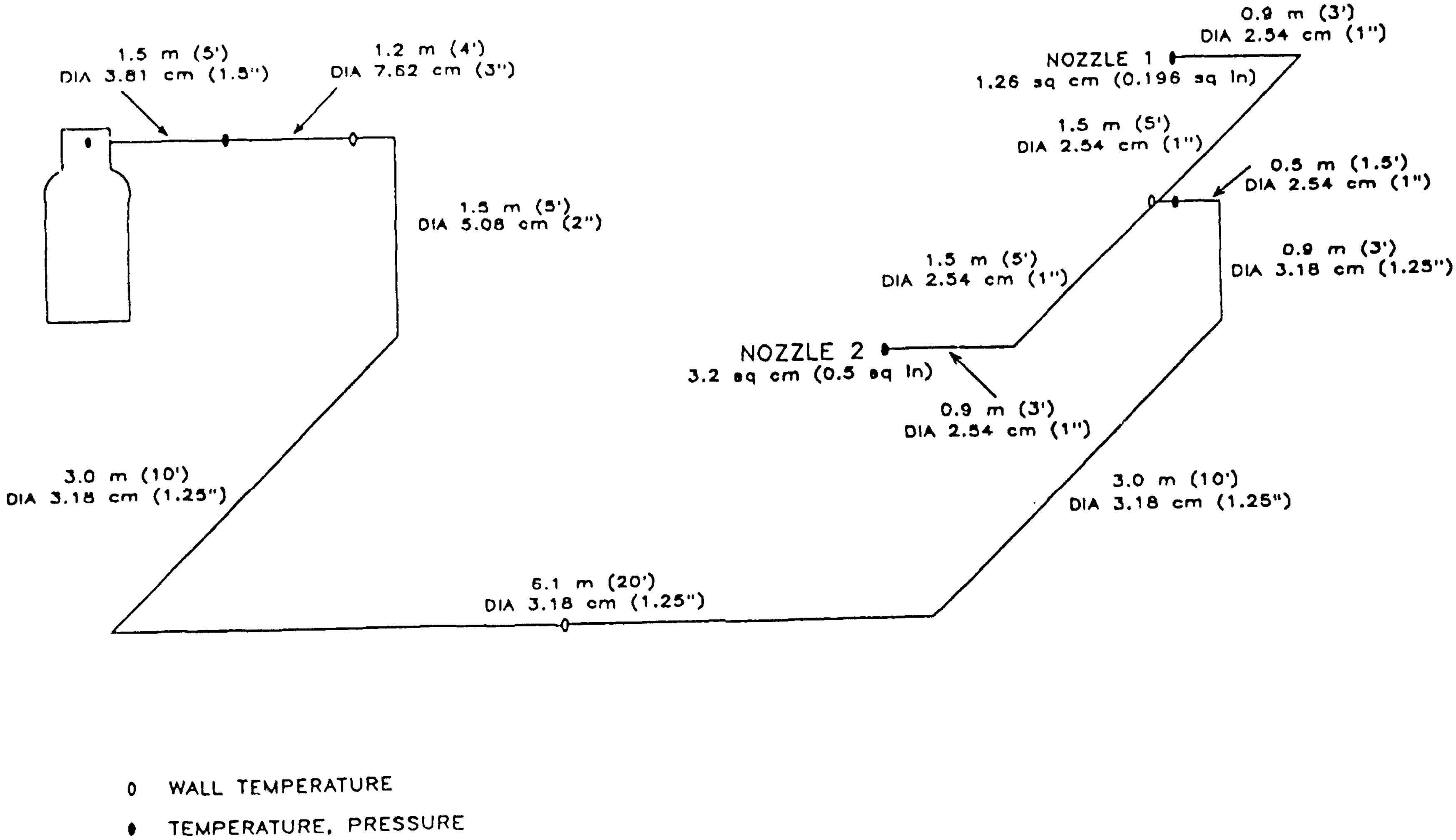


Fig. 7 — System 2: Two nozzle, unbalanced

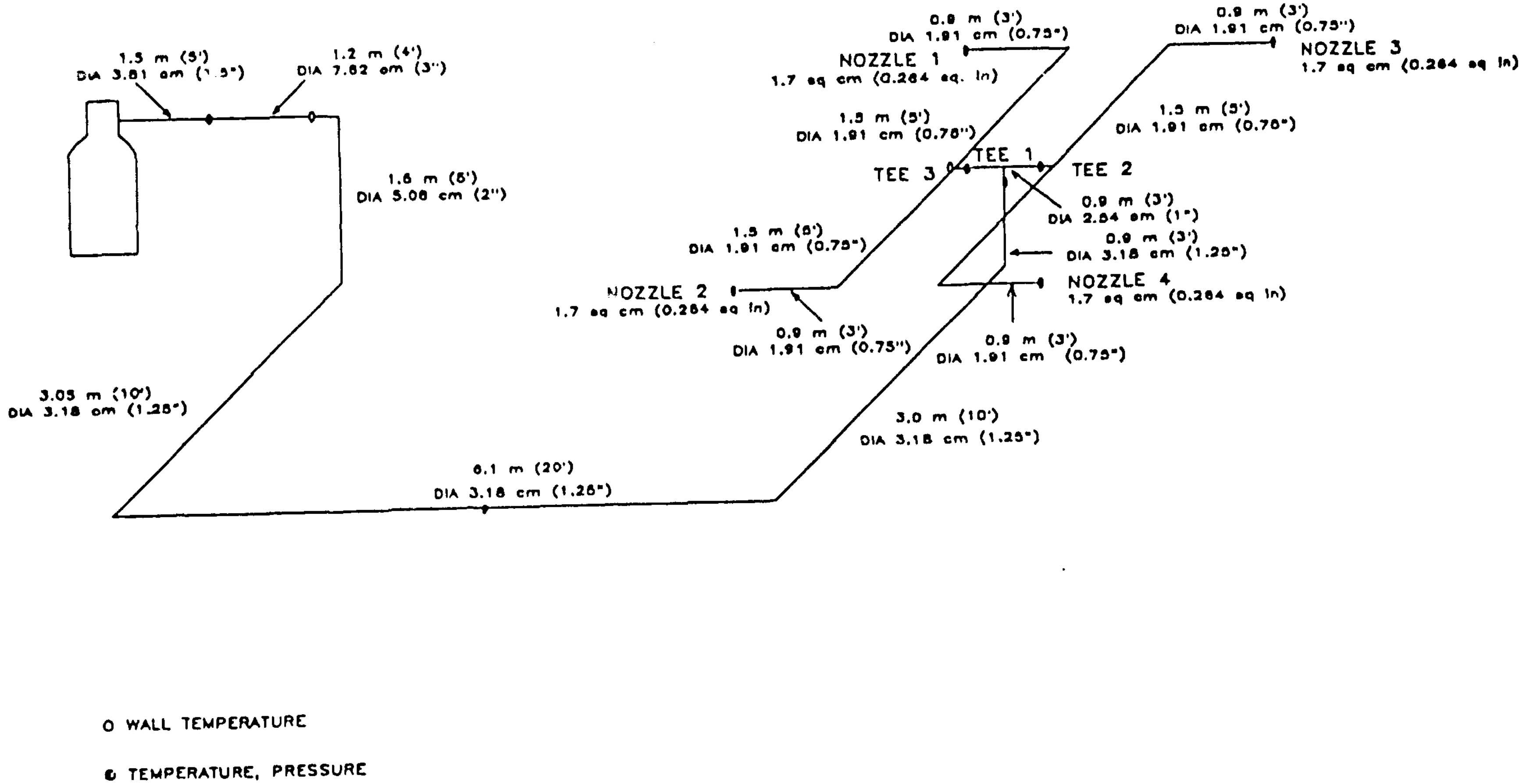


Fig. 8 — System 3: Four nozzle, balanced

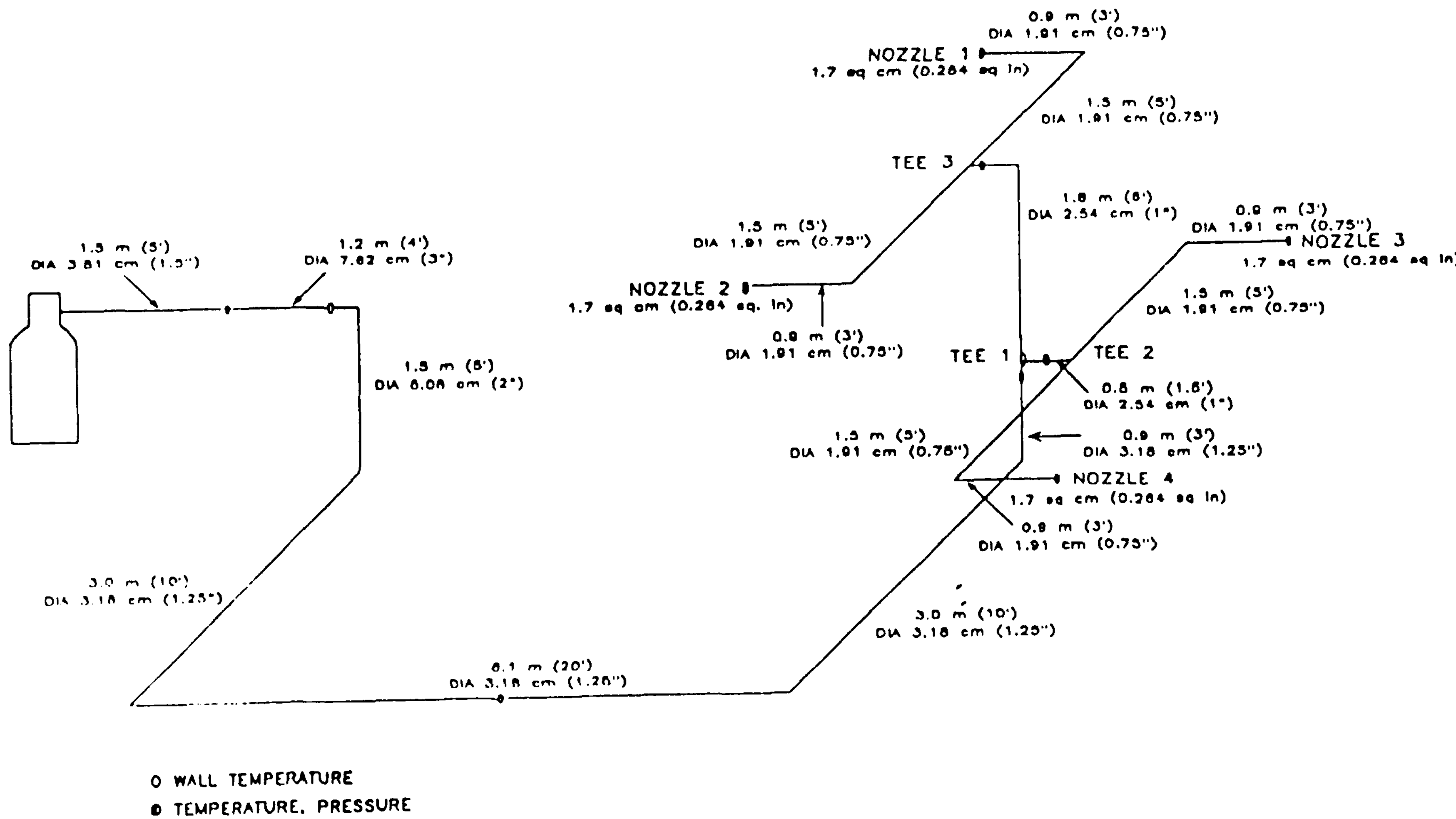


Fig. 9 — System 4: Four nozzle, unbalanced

system. It was the same as the third system except that nozzle 1 and nozzle 2 were raised approximately 1.8 m (6 ft) and are fed from a through tee. The fifth network was a four nozzle unbalanced network representing a Navy Type III system. It is shown in Figure 10. It was similar to the fourth network with nozzle 2 moved. The last system, shown in Figure 11, was the same as the fifth system except that nozzles 1 and 4 were changed to 3.24 $cm^2$ (0.503 $in.^2$) nozzles.

All systems used parameters (based on Halon 1301 flow) that are typical of Navy systems. Standard fill densities of 1100 $kg/m^3$ (70 $lb/ft^3$) were used. The percent of agent in piping was approximately 40% and the pressure drop in the networks was estimated at 760 kPa (110 psi). Actual parameters of the six systems are given in Table 4.

### 5.3 Procedure

Three tests are run for each system, one for each candidate simulant and Halon 1301. The same targeted percent by volume concentration was used in all tests.

#### 5.3.1 Test Sequence

A. Cylinder was filled with desired agent and super pressurized to 4.1 MPag (600 psig) with nitrogen.

B. Data logging was initiated.

C. Discharge was actuated.

D. Test was ended after the concentration profiles have remained stable for five minutes.

E. Enclosures were purged.

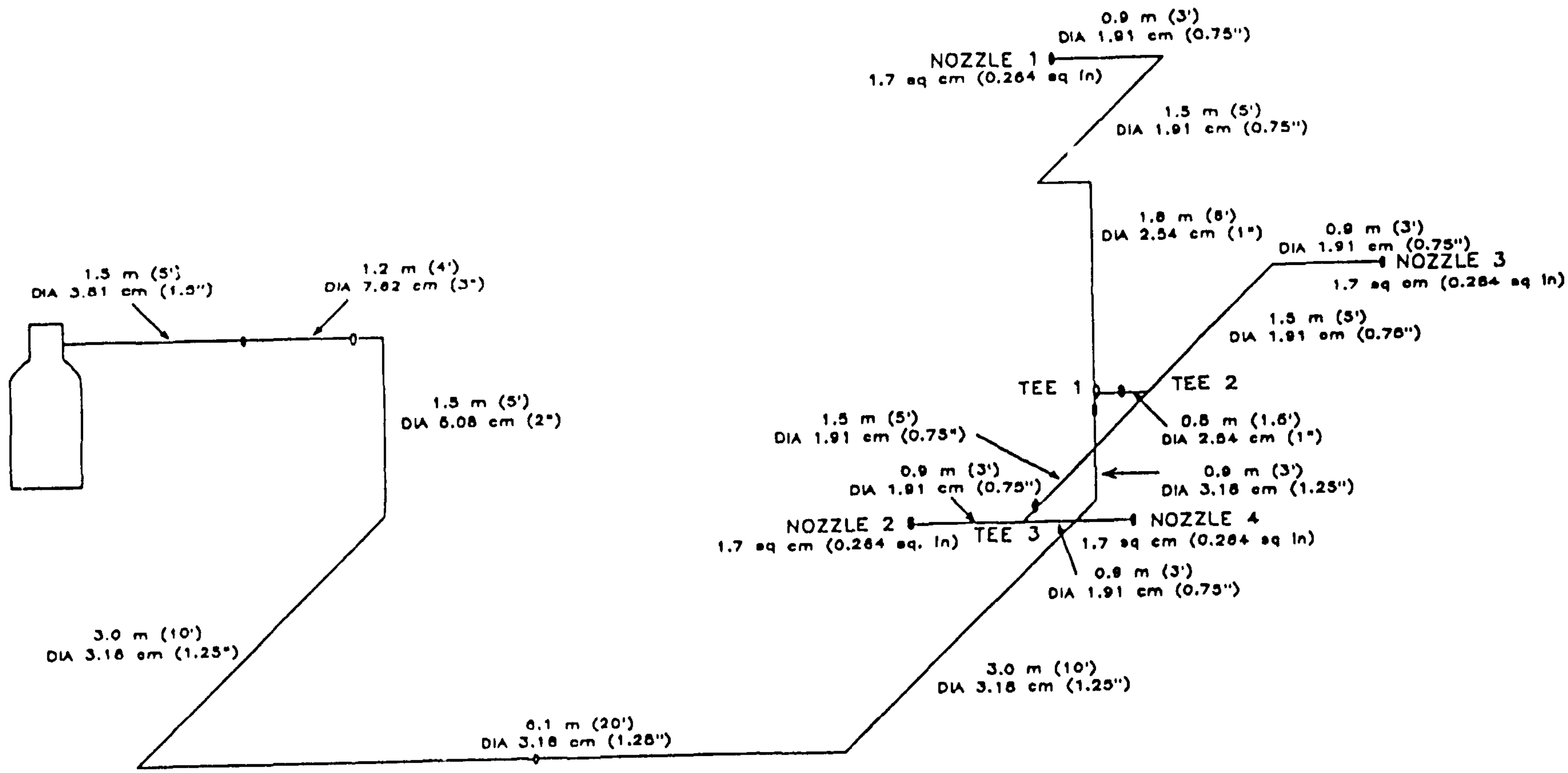


O WALL TEMPERATURE
◐ TEMPERATURE, PRESSURE

Fig. 10 — System 5: Four nozzle, unbalanced

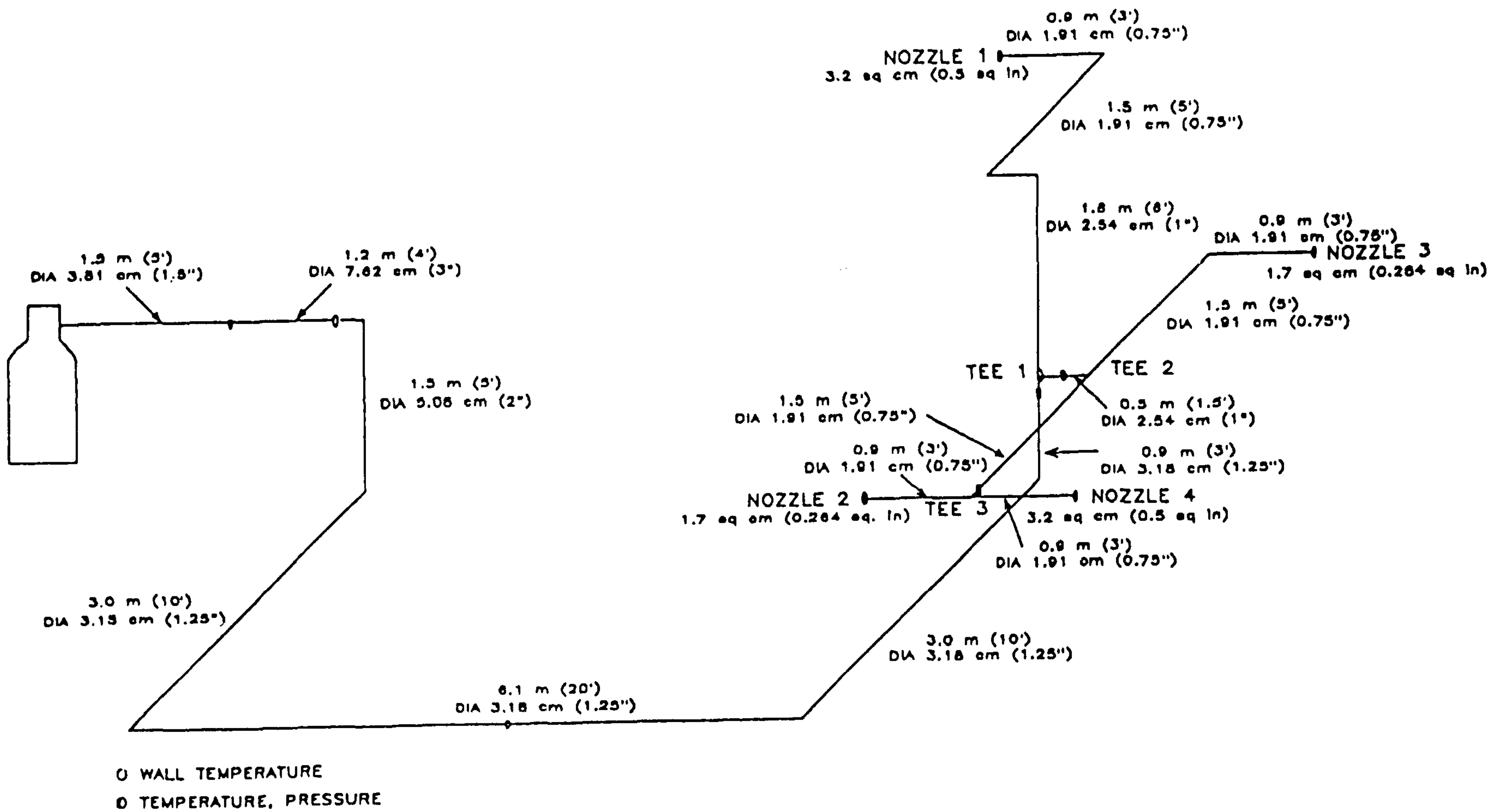


Fig. 11 — System 6: Four nozzle, unbalanced

Table 4 - System Parameters

| System | 1 | 2 | 3 | 4 | 5 | 6 |
|---|---|---|---|---|---|---|
| Initial Pressure MPag (psig) | 4.1 (600) | 4.1 (600) | 4.1 (600) | 4.1 (600) | 4.1 (600) | 4.1 (600) |
| Fill Density kg/$m^3$ (lb/$ft^3$) | 1100 (70) | 1100 (70) | 1100 (70) | 1100 (70) | 1100 (70) | 1100 (70) |
| Pipe Volume $m^3$ ($ft^3$) | .023 (.82) | .023 (.82) | .024 (.84) | .025 (.87) | .025 (.87) | .025 (.87) |
| Percent agent in piping* | 41 % | | 41.9% | 42.6% | 42.4% | |
| Pressure Drop* | | | | | | |
| kPag (psig) to: | | | | | | |
| Tee 1 | 596 (86.5) | | 447. (64.8) | 453. (65.7) | 452. (65.5) | |
| Tee 2 | | | 499. (72.4) | 505. (73.3) | 581. (84.3) | |
| Tee 3 | | | 499. (72.4) | 575. (83.3) | 670. (97.2) | |
| Nozzle 1 | 758 (110) | | 616. (89.4) | 704. (102.1) | 620. (90.0) | |
| Nozzle 2 | 758 (110) | | 616. (89.4) | 704. (102.1) | 752. (109.1) | |
| Nozzle 3 | | | 616. (89.4) | 625. (90.7) | 711. (103.2) | |
| Nozzle 4 | | | 616. (89.4) | 625. (90.7) | 752. (109.1) | |
| Orifice Area $cm^2$ ($in.^2$) | | | | | | |
| Calculated* | | | | | | |
| Nozzle 1 | 4.01 (.622) | | 1.68 (.261) | 1.92 (.298) | 1.71 (.265) | |
| Nozzle 2 | 4.01 (.622) | | 1.68 (.261) | 1.92 (.298) | 2.05 (.318) | |
| Nozzle 3 | | | 1.68 (.261) | 1.73 (.268) | 1.94 (.300) | |
| Nozzle 4 | | | 1.68 (.261) | 1.73 (.268) | 2.05 (.318) | |
| Used | | | | | | |
| Nozzle 1 | 3.25 (.503) | 1.26 (.196) | 1.70 (.264) | 1.70 (.264) | 1.70 (.264) | 3.25 (.503) |
| Nozzle 2 | 3.25 (.503) | 3.25 (.503) | 1.70 (.264) | 1.70 (.264) | 1.70 (.264) | 1.70 (.264) |
| Nozzle 3 | | | 1.70 (.264) | 1.70 (.264) | 1.70 (.264) | 1.70 (.264) |
| Nozzle 4 | | | 1.70 (.264) | 1.70 (.264) | 1.70 (.264) | 3.25 (.503) |

* Based on 10 second discharge, equal flow from each nozzle, and 1987 NFPA 12-A method (see Appendix A)

## 5.4 Instrumentation

The location of the instrumentation is shown in Figures 6 through 11.

### 5.4.1 Halon 1301 Analyzers

Halon 1301 concentrations, as well as simulant concentrations, were monitored by three TUURE Halon Analyzers. Each of these provide three sampling points for a total of nine. All analyzers were located outside of the space and connected to the desired sampling points via .16 cm (.25 in.) Tygon tubing. While testing a two nozzle system, all nine points were located inside the large enclosure as follows:

- Seven were located on a vertical tier with .6 m (2 ft) intervals except near the ceiling where the first two intervals were .3 m (1 ft).
- One located in the center of the room .6 m (2 ft) from the ceiling.
- One located on the ceiling across the room from the vertical tier.

When testing a four nozzle system, the nine sampling points were split among the three enclosures, three to each. They were located on a vertical tier in each enclosure as follows:

- One on the ceiling [moved .3 m (1 ft) down in small enclosures before system 5 was tested].
- One midway down the tier.

- One .6 m (2 ft) above the floor.

5.4.2 Temperature

The temperature of the flowing fluid was monitored at four locations for a two nozzle system and at eight locations for a four nozzle system. Inconel sheathed thermocouples were used to accomplish this. For all systems the thermocouples were distributed as follows:

- One located just after the thread adaptor on the flex hose.
- One before each tee
- One before each nozzle.

In addition, three Inconel sheathed thermocouples were used to monitor the pipe wall temperatures.

5.4.3 Pressure

The pressure was monitored at four locations for a two nozzle system and at eight locations for a four nozzle system. Six 0 to 6.9 MPag (0 to 1000 psig) range, Genisco Technology Corporation Model SP500 pressure transducers and two 0 to 5.2 MPag (0 to 750 psig) range, Viatran Corporation pressure transducers were used to accomplish this. For all systems they were distributed as follows:

- One located after the thread adaptor for the flex hose with the exception of the two nozzle systems where it was moved to the discharge cylinder.
- One before each tee.
- One before each nozzle.

#### 5.4.4 Cylinder Weight

The discharge cylinder weight was monitored using an Allegheny Technology Load Cell Model 301LC with a range of 0 to 4,450 N (0 to 1000 lb).

#### 5.4.5 Video Recording

The discharges of nozzle 1 were recorded for System 6.

### 5.5 Results

The mass distribution between nozzles was determined from the concentration in the enclosures as follows:

$$m = pV\ [C/(100-C)]$$

where m is the mass discharged from the nozzle, p is the vapor density of Halon 1301 or candidate simulant, V is the volume of the enclosure and C is the concentration in the enclosure in percent by volume [11]. The mass discharged from the unenclosed nozzle (nozzle 2) is found by difference.

The generated peak pressures and discharge times for each system are shown in Tables 5 through 10. Also, a series of figures for each system is presented. The first figure in the series shows the mass distribution between the nozzles as a percent of the mass discharged. The second shows the flow split at each tee in the system. The third shows the percent weight loss from the cylinder (percent outage). The next six figures show the generated pressures and temperature traces for Halon 1301 and the two candidate simulants. This series for System 1 is Figure 12 through 20. System 2 results are shown in Figures 21 through 29. System 3 results are shown in Figures 30 through 38. System 4 results are shown in Figures 39 through 47. System 5 results are shown in Figures 48 through 56. The results for System 6 are shown in Figures 57 through 65.

In addition, the Halon 1301 pressures are compared to those predicted by the method of NFPA Standard 12A in Appendix A.

As can be seen from these results, both candidate simulants distributed between the nozzles in a similar manner to Halon 1301. The maximum deviation in percent of mass discharged for either $SF_6$ or R-22 is less than 5%. The flow divisions for both candidate simulants are also similar to those of Halon 1301 with the maximum deviation being less than 6%.

$SF_6$ discharged at a similar rate to Halon 1301. The maximum difference in discharge time between $SF_6$ and Halon 1301 by any of the three methods used was 1.4 seconds which is a relative difference of approximately 11%.

R-22, on the other hand, discharged at a faster rate than Halon 1301. The discharge time for R-22 was as much as 4 seconds shorter than that for Halon 1301, which is a relative difference of 35%.

The relationships between the discharge times of the two candidate simulants and those of Halon 1301 are the consequence of their physical properties. The lower liquid densities of both simulants cause them to flow at a higher volumetric flow rate when they experience the same pressure change. The higher vapor pressure of $SF_6$ represents an increased pressure opposing the flow and reducing the flow rate (this pressure also depends on the temperature and composition of the flow). On the other hand, R-22 has a lower vapor pressure thus augmenting the flow rate. These effects can be seen from the pressure coefficient, Cp, which is used to characterize a high Reynolds flow [15]

$$Cp = P/(0.5pV^2)$$

where P is the pressure drop in the system, p is the fluid density, and V is the velocity. (Note that the Reynolds number is not used to characterize these flows, as the viscous forces are insignificant with respect to the magnitude of the inertial and pressure forces acting on the flow).

In addition to these effects, the vapor density of R-22 is much lower than that of Halon 1301 which means that a lower mass of R-22 is required to achieve the same percent by volume concentration in an enclosure. Therefore, a lower initial mass of R-22 was used, further reducing its discharge times. The vapor density of $SF_6$ is within 3% of that of Halon 1301, therefore nearly the same mass of $SF_6$ was used.

Table 5 - Banked System 1

| Test Gas | Halon 1301 | $SF_6$ | R-22 |
|---|---|---|---|
| | | Peak Pressure | |
| Bottle | | 4.32 MPag (627 psig) | 3.97 MPag (576 psig) |
| Manifold | 2.55 MPag (384 psig) | | |
| Tee | 1.63 MPag (237 psig) | 2.00 MPag (290 psig) | 1.22 MPag (177 psig) |
| Nozzle 1 | 1.35 MPag (196 psig) | 1.58 MPag (229 psig) | 0.97 MPag (140 psig) |
| Nozzle 2 | 1.37 MPag (198 psig) | 1.62 MPag (235 psig) | 0.98 MPag (142 psig) |
| | | Discharge Times [seconds] | |
| Pressure Inflexion | 10.7 | 10.2 | 7.2 |
| Temperature Method | 10.6 | 10.2 | 7.1 |
| 345 kPag (50 psig) Pressure | | | |
| Nozzle 1 | 13.8 | 13.8 | 9.3 |
| Nozzle 2 | 13.8 | 13.7 | 9.3 |

Table 6 - Banked System 2

| Test Gas | Halon 1301 | $SF_6$ | R-22 |
|---|---|---|---|
| **Peak Pressures** | | | |
| Bottle | 4.05 MPag (587 psig) | | 4.03 MPag (584 psig) |
| Tee | 1.84 MPag (267 psig) | 2.23 MPag (323 psig) | 1.42 MPag (206 psig) |
| Nozzle 1 | 1.73 MPag (251 psig) | 2.09 MPag (303 psig) | 1.33 MPag (193 psig) |
| Nozzle 2 | 1.45 MPag (210 psig) | 1.78 MPag (258 psig) | 1.11 MPag (161 psig) |
| **Discharge Times [seconds]** | | | |
| Pressure Inflexion | 11.8 | 11.2 | 8.2 |
| Temperature Method | 11.6 | 11. | 8.2 |
| 345 kPag (50 psig) Pressure | | | |
| Nozzle 1 | 17.1 | 17.1 | 12.1 |
| Nozzle 2 | 16.3 | 16.2 | 11.3 |

Table 7 - Banked System 3

| Test Gas | Halon 1301 | $SF_6$ | R-22 |
|---|---|---|---|
| | | **Peak Pressure** | |
| Manifold | 2.30 MPag (334 psig) | 2.56 MPag (372 psig) | 1.81 MPag (262 psig) |
| Tee 1 | 1.70 MPag (247 psig) | 2.08 MPag (302 psig) | 1.25 MPag (181 psig) |
| Tee 2 | 1.64 MPag (238 psig) | 1.99 MPag (288 psig) | 1.32 MPag (192 psig) |
| Tee 3 | 1.64 MPag (238 psig) | 2.05 MPag (298 psig) | 1.32 MPag (192 psig) |
| Nozzle 1 | 1.28 MPag (186 psig) | 1.61 MPag (233 psig) | 1.05 MPag (152 psig) |
| Nozzle 2 | 1.32 MPag (192 psig) | 1.70 MPag (246 psig) | 1.05 MPag (152 psig) |
| Nozzle 3 | 1.17 MPag (169 psig) | 1.46 MPag (212 psig) | 0.89 MPag (129 psig) |
| Nozzle 4 | 1.25 MPag (181 psig) | 1.63 MPag (236 psig) | 1.01 MPag (147 psig) |
| | | **Discharge Times [seconds]** | |
| Pressure Inflexion | 10.7 | 10.5 | 7.5 |
| Temperature Method | 10.7 | 10.2 | 7.3 |
| 345 kPag (50 psig) Pressure | | | |
| Nozzle 1 | 14.6 | 14.6 | 10.4 |
| Nozzle 2 | 13.8 | 13.8 | 9.8 |
| Nozzle 3 | 13.2 | 13.0 | 9.2 |
| Nozzle 4 | 13.8 | 13.8 | 9.8 |

Table 8 - Banked System 4

| Test Gas | Halon 1301 | $SF_6$ | R-22 |
|---|---|---|---|
| **Peak Pressure** | | | |
| Manifold | 2.28 MPag (330 psig) | 2.89 MPag (419 psig) | 2.01 MPag (292 psig) |
| Tee 1 | 1.63 MPag (236 psig) | 2.05 MPag (298 psig) | 1.34 MPag (195 psig) |
| Tee 2 | 1.48 MPag (215 psig) | 1.89 MPag (274 psig) | 1.22 MPag (177 psig) |
| Tee 3 | 1.56 MPag (226 psig) | 2.03 MPag (295 psig) | 1.31 MPag (190 psig) |
| Nozzle 1 | 1.17 MPag (170 psig) | 1.58 MPag (229 psig) | 0.98 MPag (142 psig) |
| Nozzle 2 | 1.23 MPag (178 psig) | 1.66 MPag (241 psig) | 1.02 MPag (148 psig) |
| Nozzle 3 | 1.14 MPag (165 psig) | 1.48 MPag (215 psig) | 0.94 MPag (136 psig) |
| Nozzle 4 | 1.12 MPag (162 psig) | 1.55 MPag (225 psig) | 0.93 MPag (135 psig) |
| **Discharge Time [seconds]** | | | |
| Pressure Inflexion | 11.3 | 10.5 | 7.5 |
| Temperature Method | 11.2 | 10.3 | 7.3 |
| 345 kPag (50 psig) Pressure | | | |
| Nozzle 1 | 14.0 | 13.6 | 9.8 |
| Nozzle 2 | 14.2 | 13.9 | 9.9 |
| Nozzle 3 | 14.5 | 13.3 | 9.5 |
| Nozzle 4 | 13.5 | 13.3 | 9.5 |

Table 9 - Banked System 5

| Test Gas | Halon 1301 | $SF_6$ | R-22 |
|---|---|---|---|
| **Peak Pressure** | | | |
| Manifold | 2.04 MPag (296 psig) | 2.80 MPag (406 psig) | 1.95 MPag (283 psig) |
| Tee 1 | 1.59 MPag (231 psig) | 2.13 MPag (309 psig) | 1.42 MPag (206 psig) |
| Tee 2 | 1.44 MPag (209 psig) | 1.99 MPag (288 psig) | 1.30 MPag (188 psig) |
| Tee 3 | 1.05 MPag (153 psig) | 1.54 MPag (223 psig) | 0.93 MPag (135 psig) |
| Nozzle 1 | 1.32 MPag (192 psig) | 1.85 MPag (269 psig) | 1.17 MPag (170 psig) |
| Nozzle 2 | 0.84 MPag (122 psig) | 1.27 MPag (184 psig) | 0.74 MPag (107 psig) |
| Nozzle 3 | 0.99 MPag (144 psig) | 1.43 MPag (208 psig) | 0.89 MPag (129 psig) |
| Nozzle 4 | 0.83 MPag (120 psig) | 1.28 MPag (185 psig) | 0.74 MPag (107 psig) |
| **Discharge Times [seconds]** | | | |
| Pressure Inflexion | 12.5 | 11.5 | 7.8 |
| Temperature Method | 12.4 | 11.0 | 7.6 |
| 345 kPag (50 psig) Pressure | | | |
| Nozzle 1 | 16.5 | 15.3 | 11.0 |
| Nozzle 2 | 14.4 | 13.6 | 9.9 |
| Nozzle 3 | 14.6 | 14.1 | 10.1 |
| Nozzle 4 | 14.3 | 13.5 | 9.8 |

Table 10 - Banked System 6

| Test Gas | Halon 1301 | $SF_6$ | R-22 |
|---|---|---|---|
| | | **Peak Pressure** | |
| Manifold | 2.10 MPag (305 psig) | 2.73 MPag (396 psig) | 1.98 MPag (287 psig) |
| Tee 1 | 1.57 MPag (228 psig) | 2.03 MPag (294 psig) | 1.37 MPag (198 psig) |
| Tee 2 | 1.42 MPag (206 psig) | 1.88 MPag (273 psig) | 1.19 MPag (172 psig) |
| Tee 3 | 0.95 MPag (138 psig) | 1.37 MPag (198 psig) | 0.85 MPag (123 psig) |
| Nozzle 1 | 0.90 MPag (130 psig) | 1.24 MPag (180 psig) | 0.79 MPag (114 psig) |
| Nozzle 2 | 0.72 MPag (105 psig) | 1.08 MPag (156 psig) | 0.64 MPag ( 93 psig) |
| Nozzle 3 | 0.94 MPag (136 psig) | 1.34 MPag (195 psig) | 0.82 MPag (119 psig) |
| Nozzle 4 | 0.55 MPag ( 80 psig) | 0.83 MPag (120 psig) | 0.48 MPag ( 69 psig) |
| | | **Discharge Times [seconds]** | |
| Pressure Inflexion | 11.5 | 11. | 7.5 |
| Temperature Method | 11.3 | 10.5 | 7.5 |
| 345 kPag (50 psig) Pressure | | | |
| Nozzle 1 | 13.3 | 13.0 | 9.3 |
| Nozzle 2 | 13.0 | 12.3 | 9.1 |
| Nozzle 3 | 13.4 | 13.2 | 9.4 |
| Nozzle 4 | 11.8 | 11.4 | 7.8 |

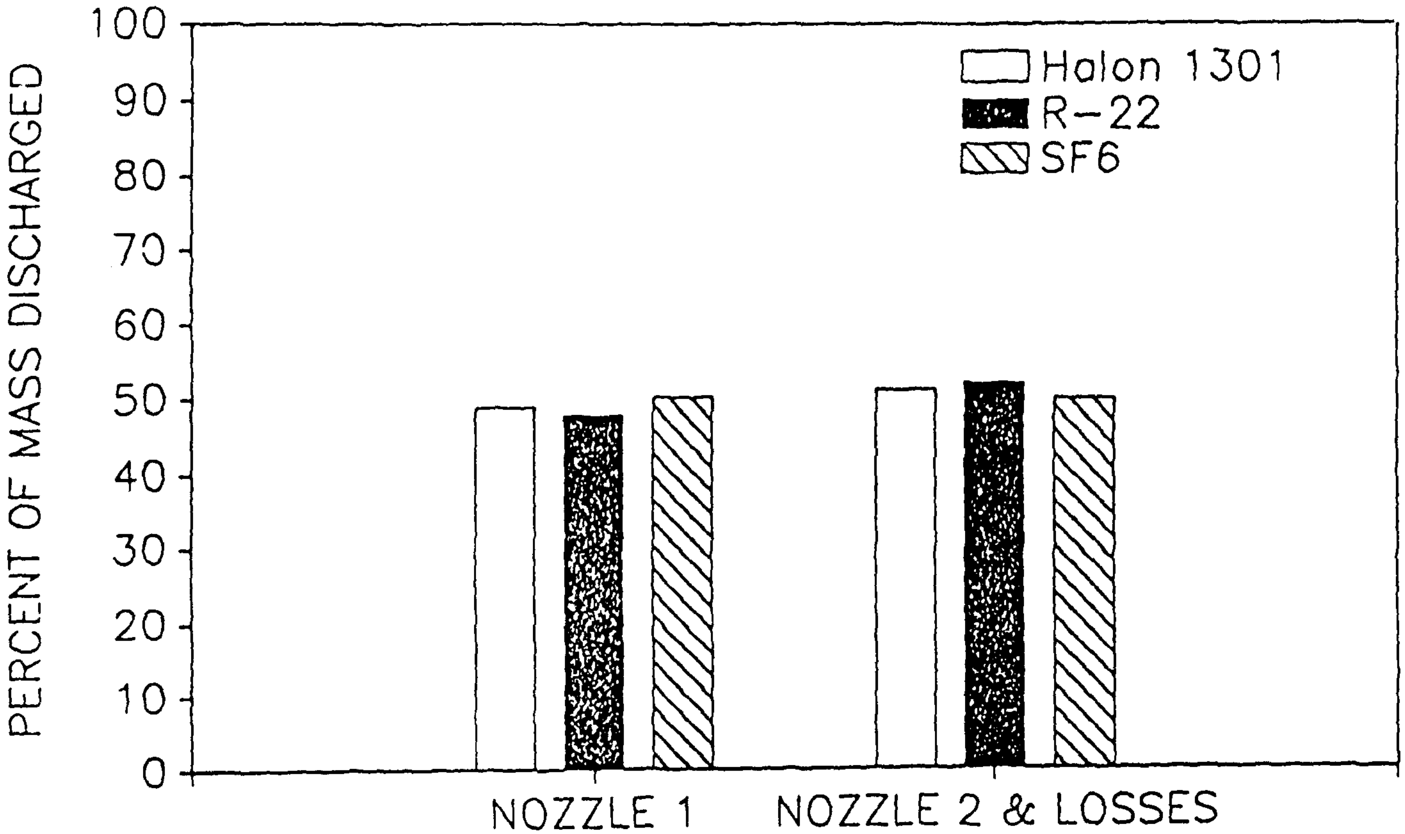


Fig. 12 – Mass distribution for system 1

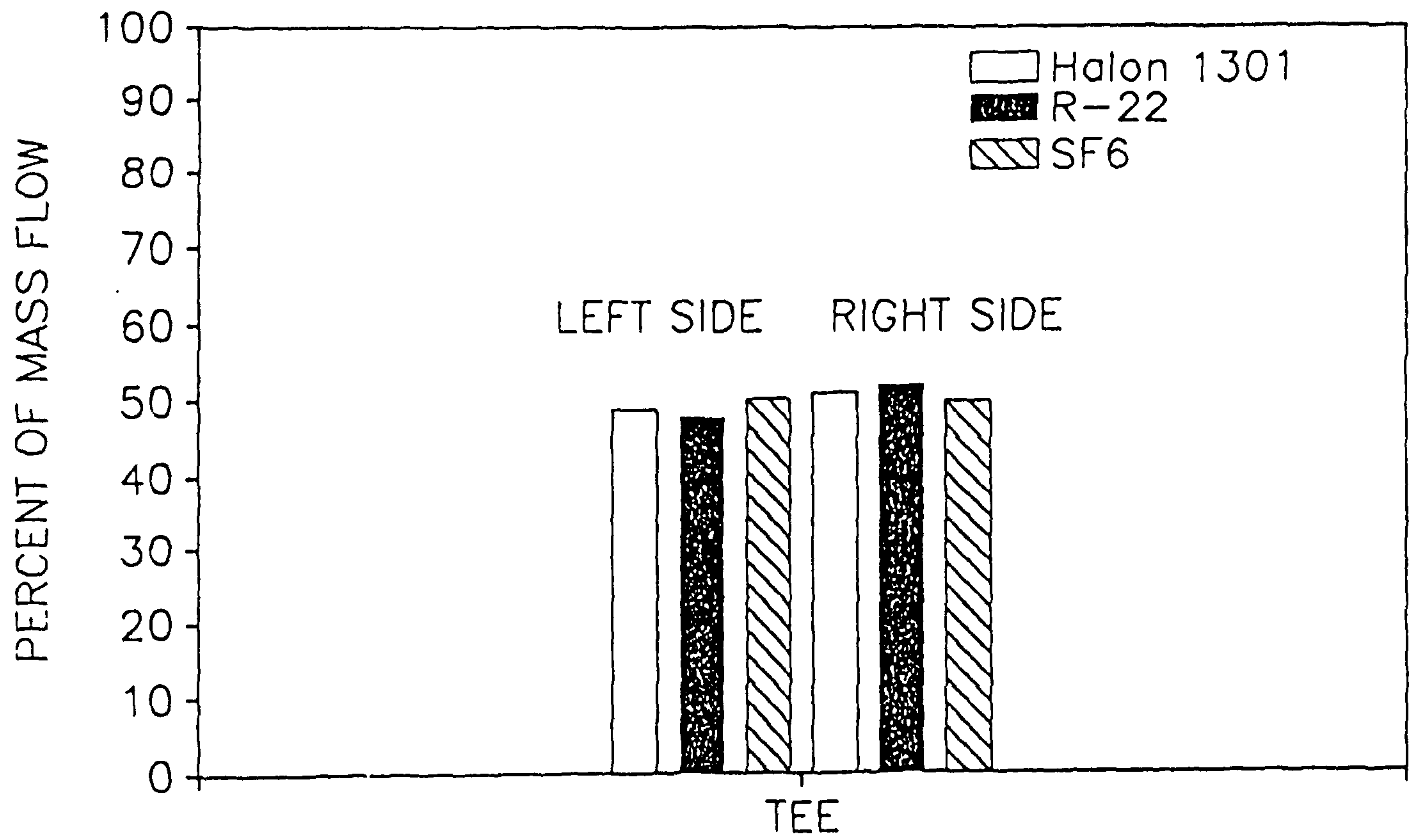


Fig. 13 – Mass flow distribution for system 1

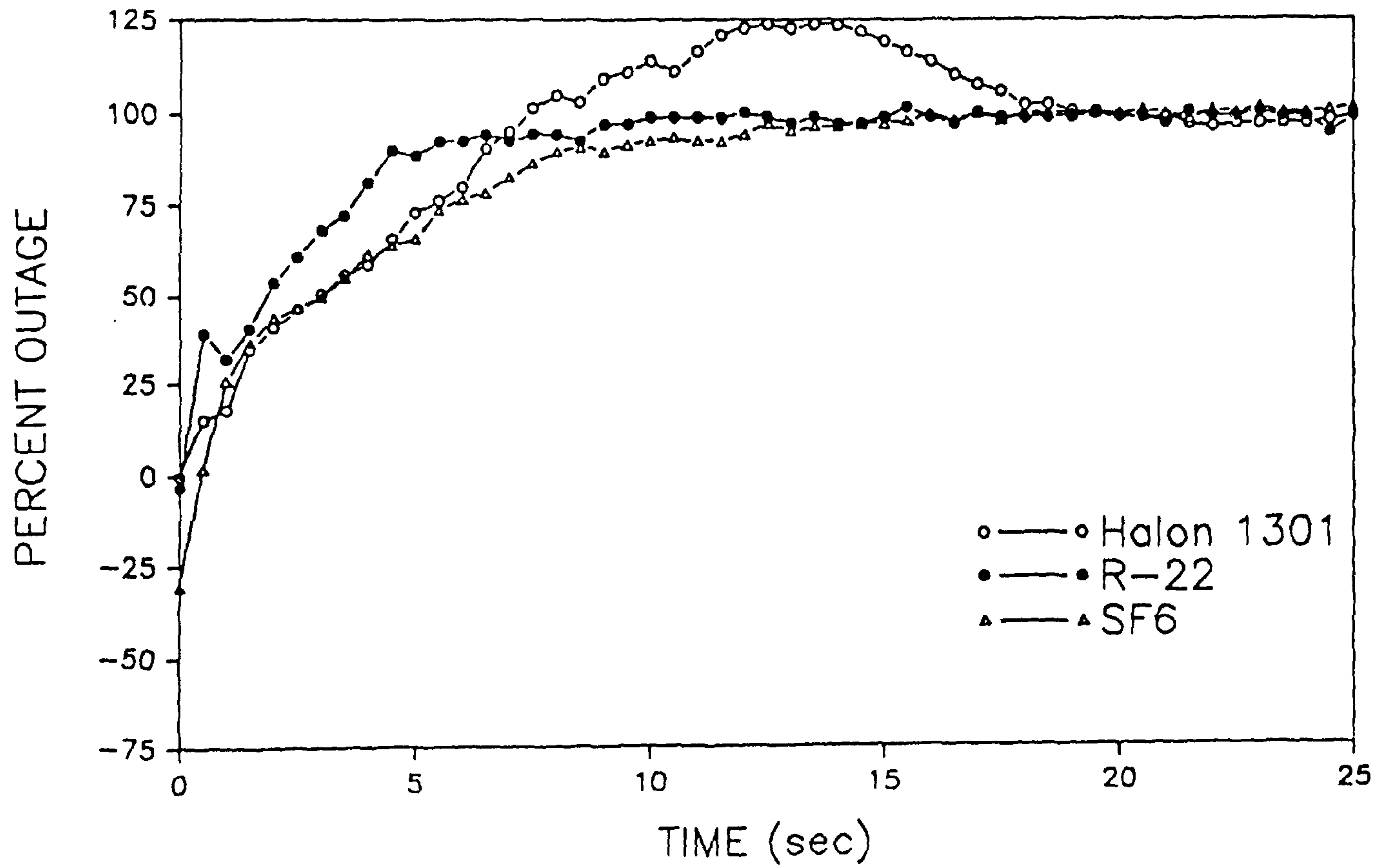


Fig. 14 — Percent outage for system 1

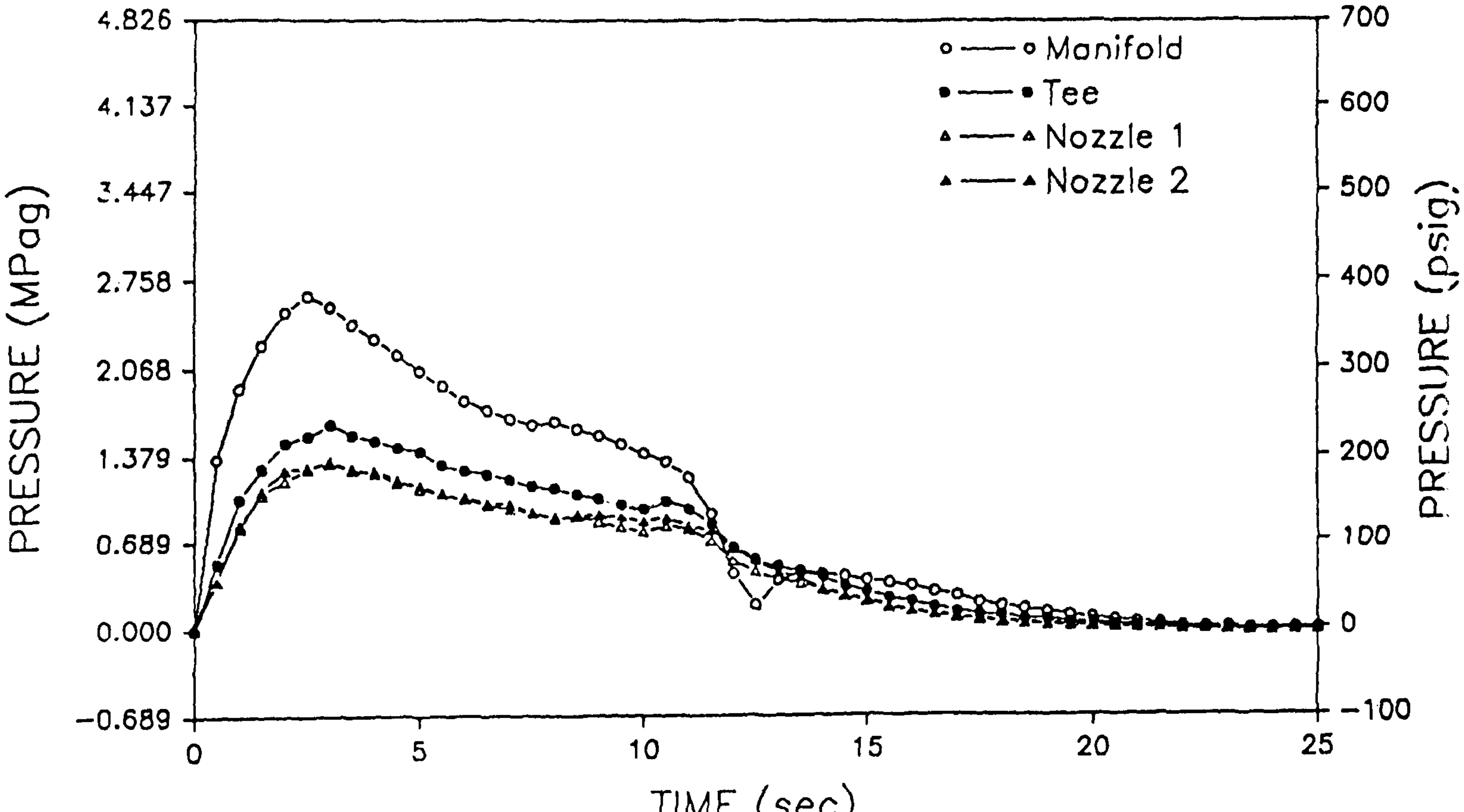


Fig. 15 – Pressure traces for system 1 with Halon 1301

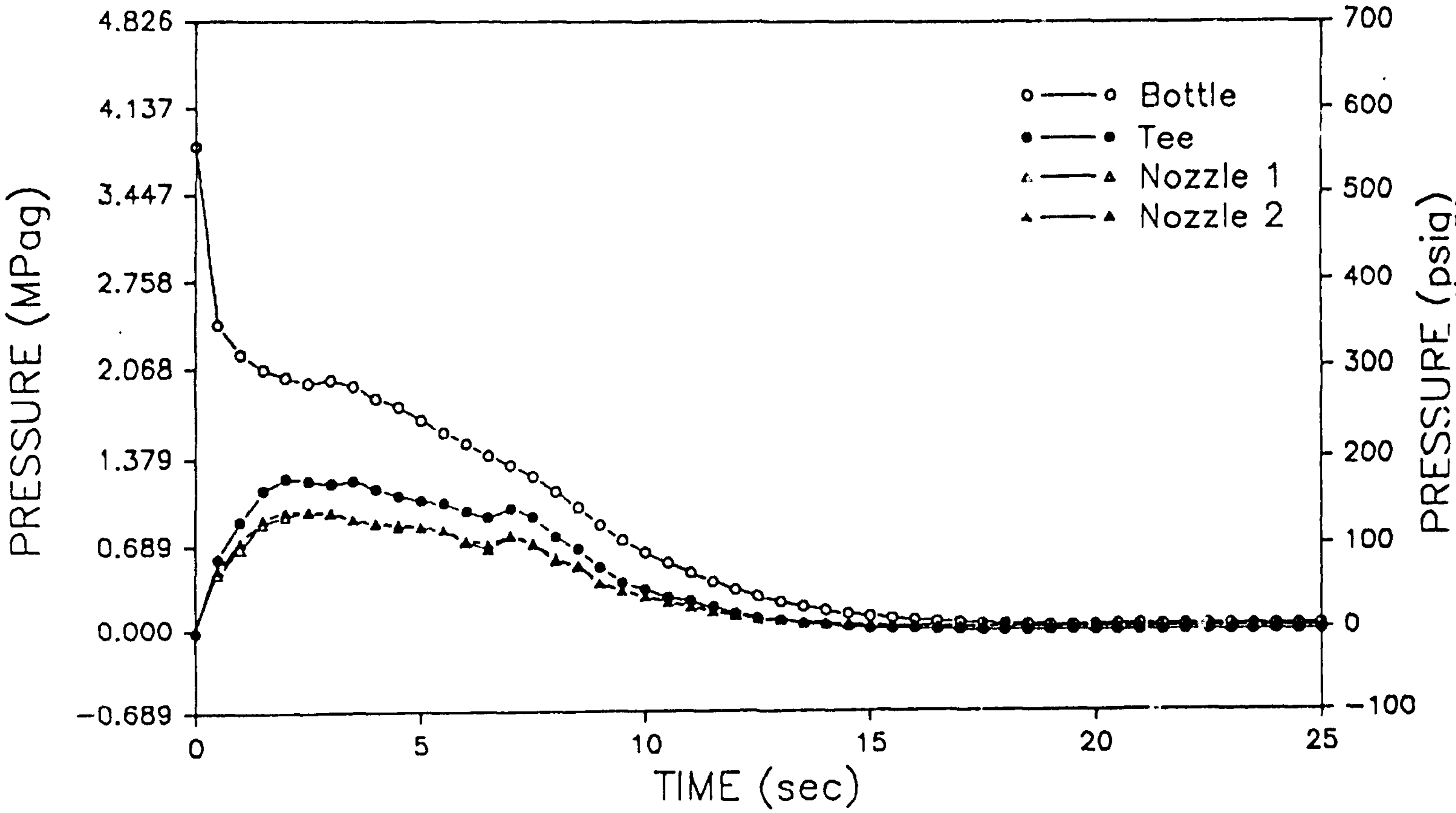


Fig. 16 – Pressure traces for system 1 with R–22

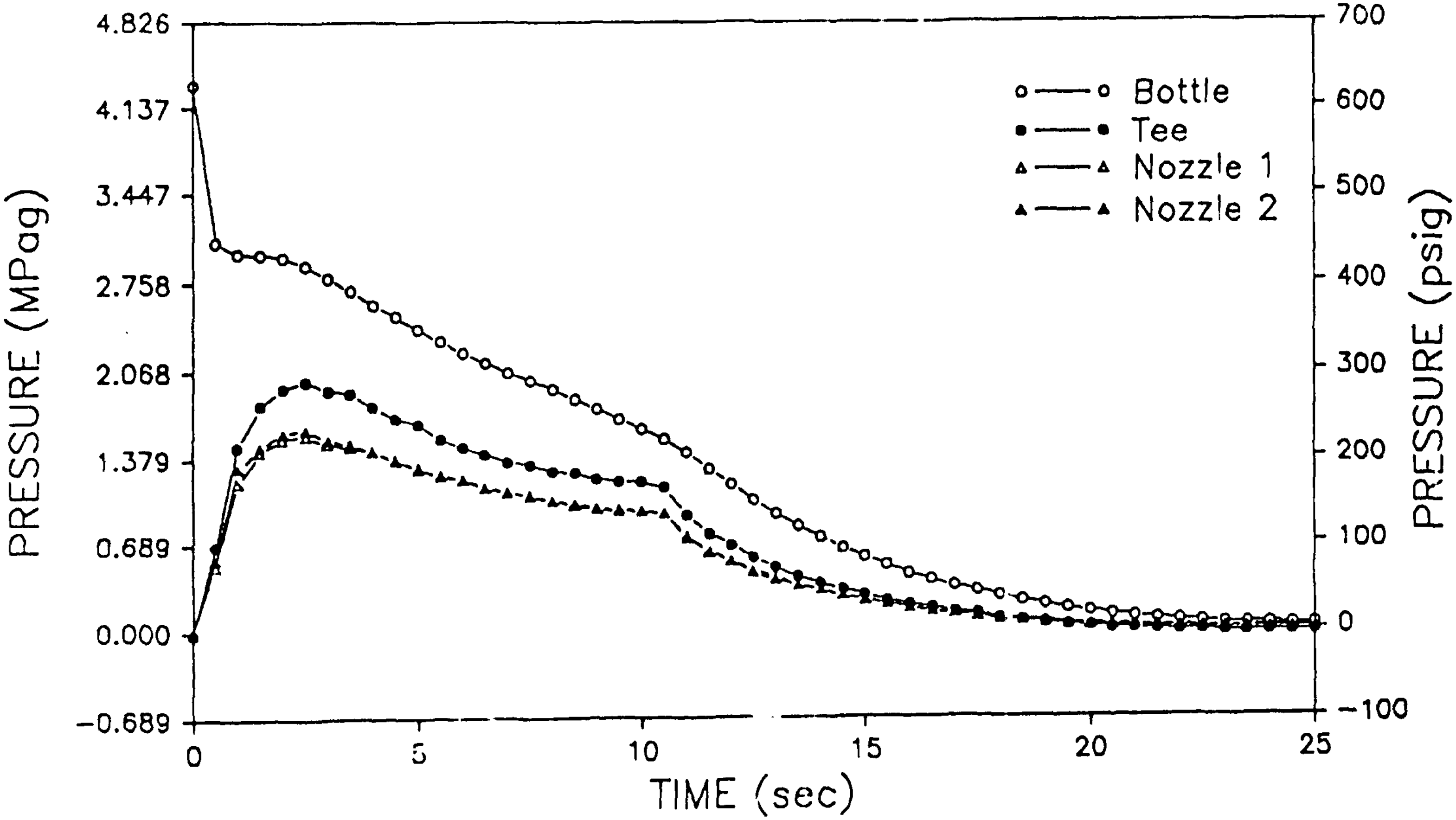


Fig. 17 — Pressure traces for system 1 with SF6

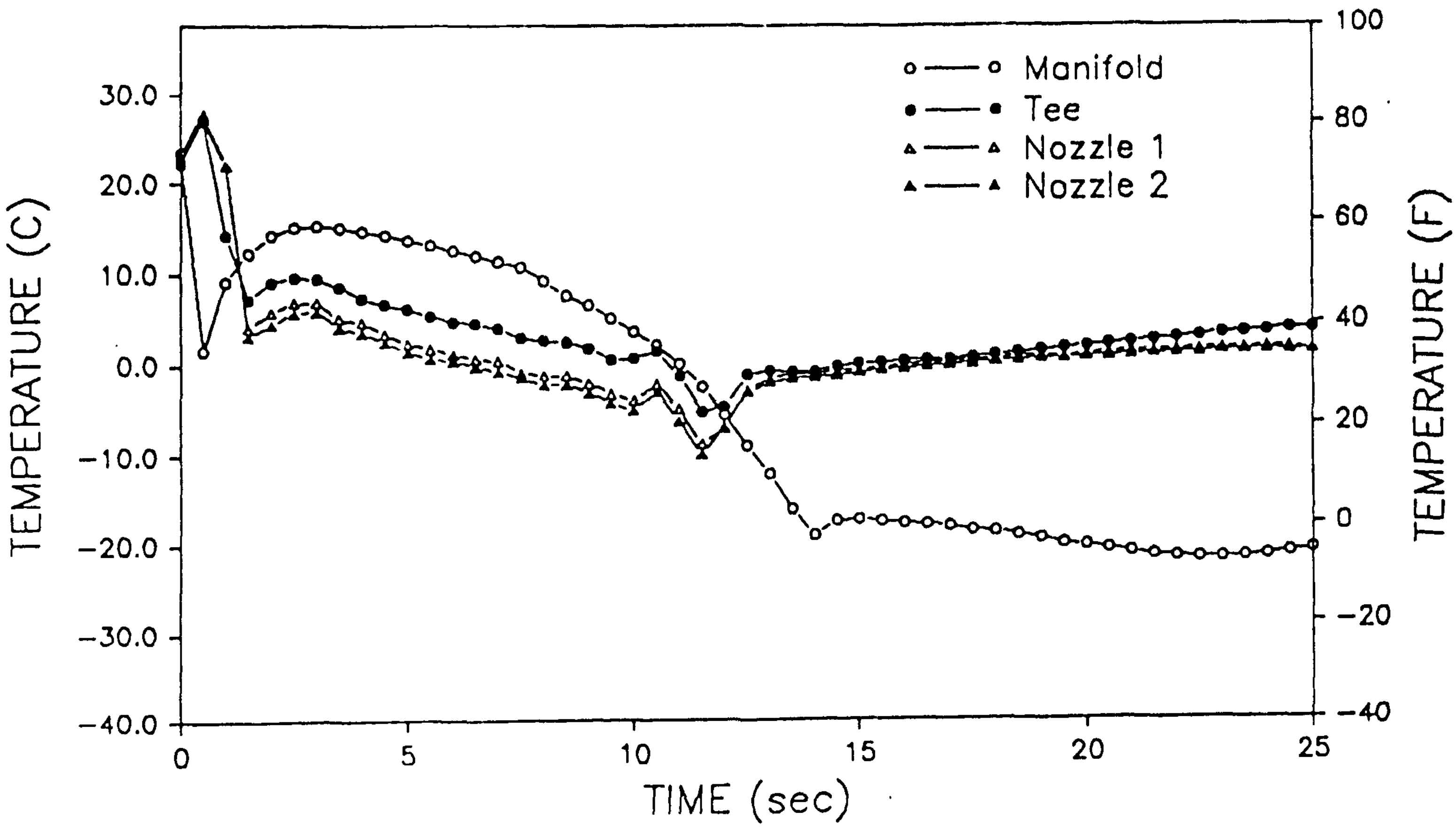


Fig. 18 – Temperature traces for system 1 with Halon 1301

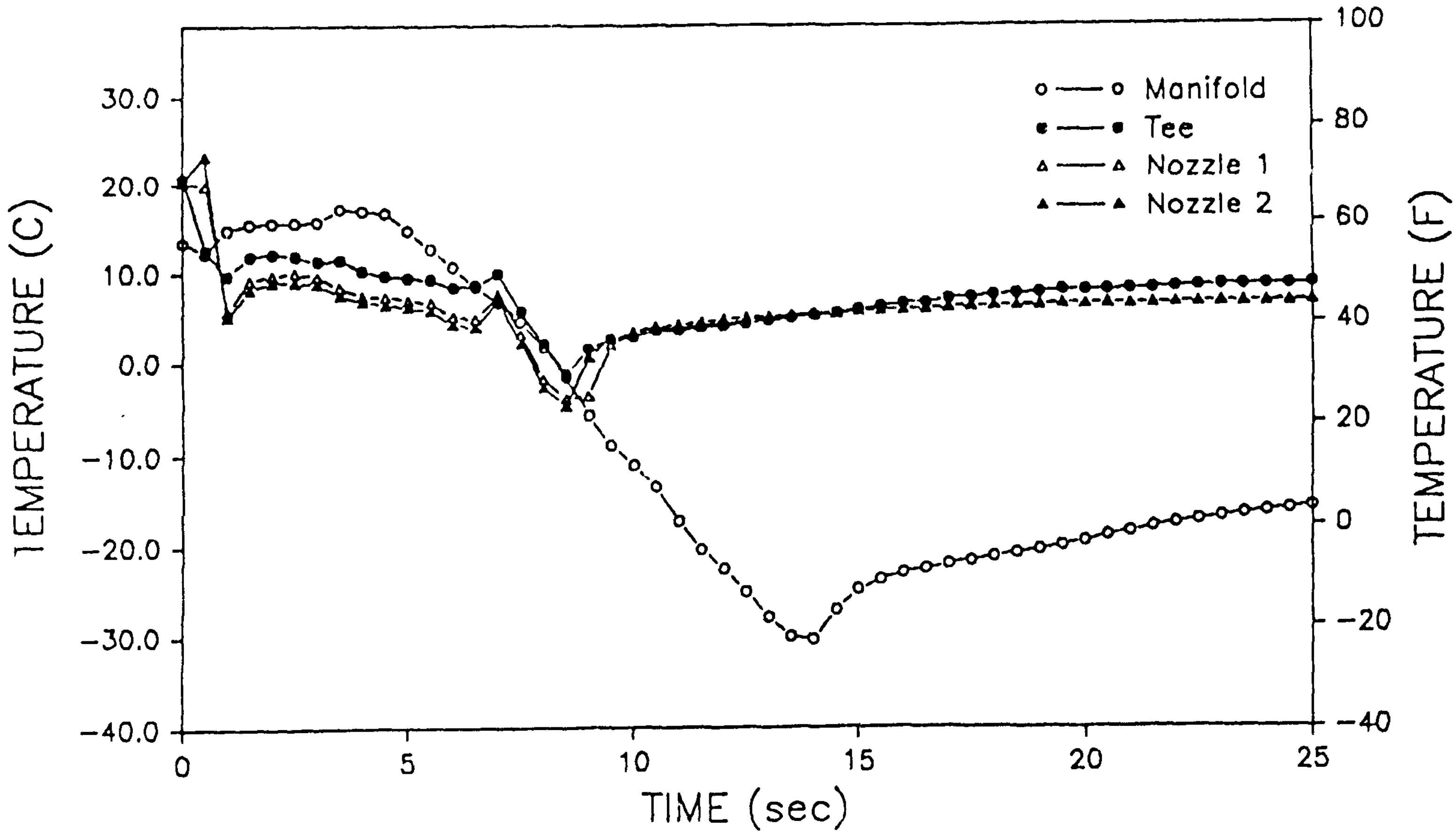


Fig. 19 – Temperature traces for system 1 with R–22

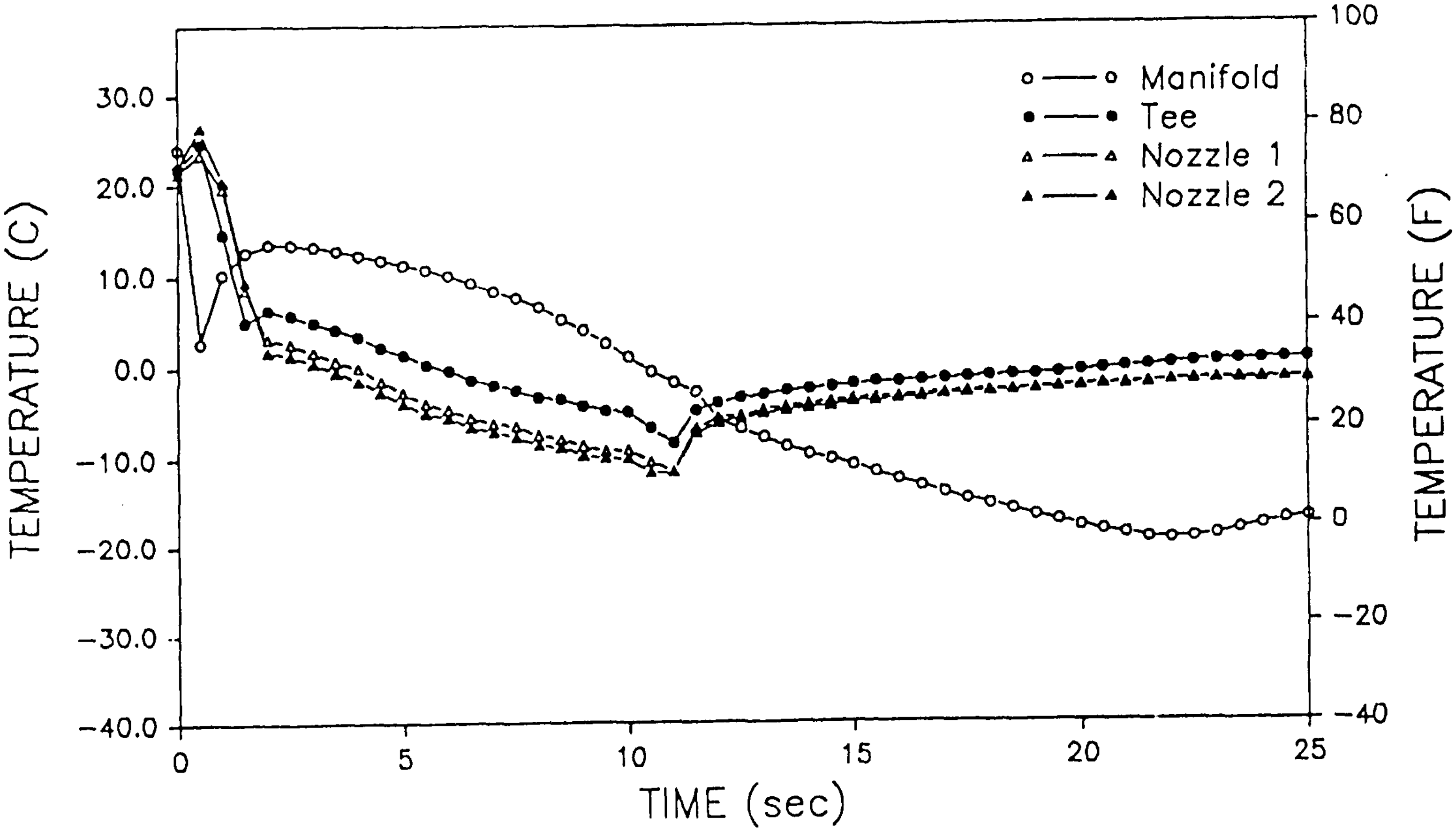


Fig. 20 — Temperature traces for system 1 with SF6

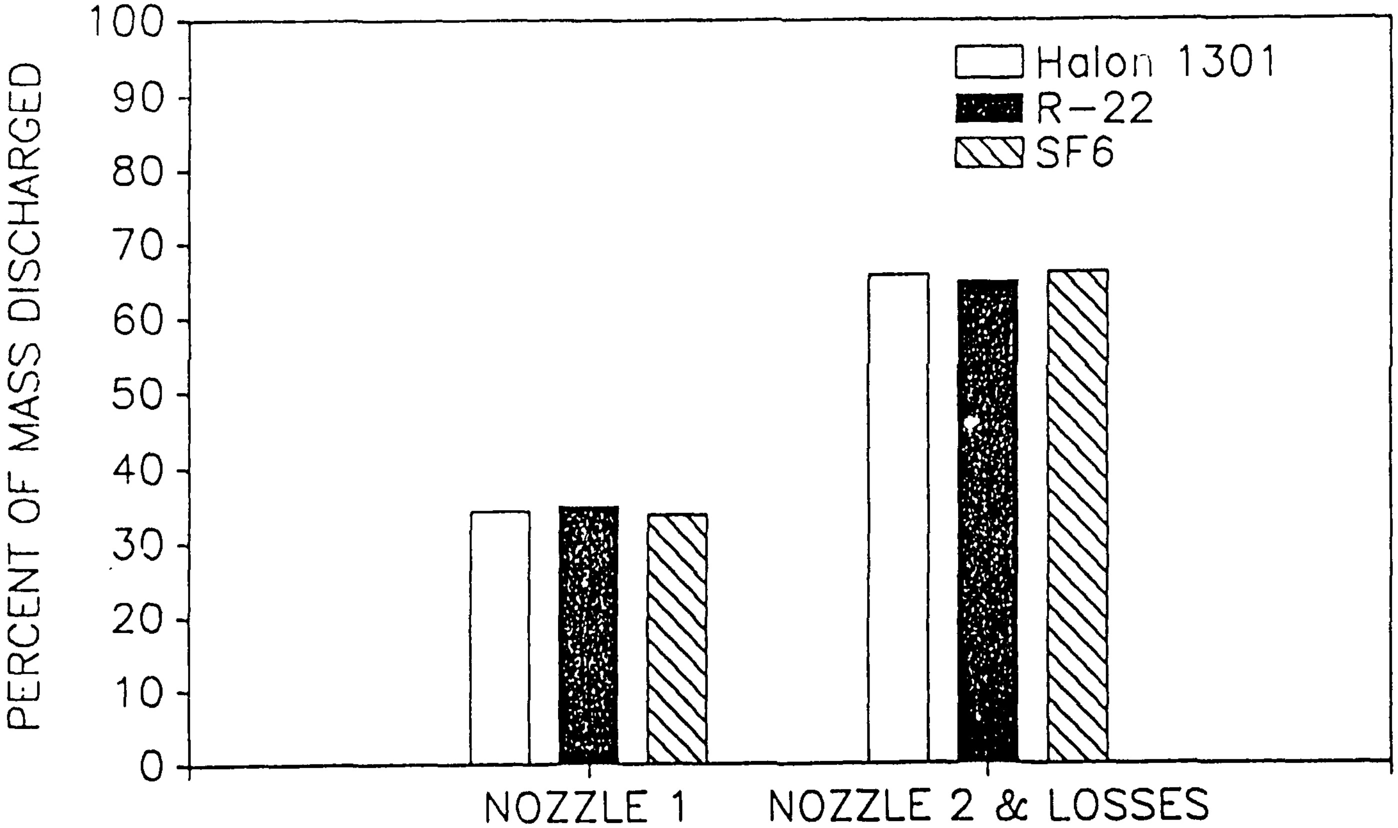


Fig. 21 -- Mass distribution for system 2

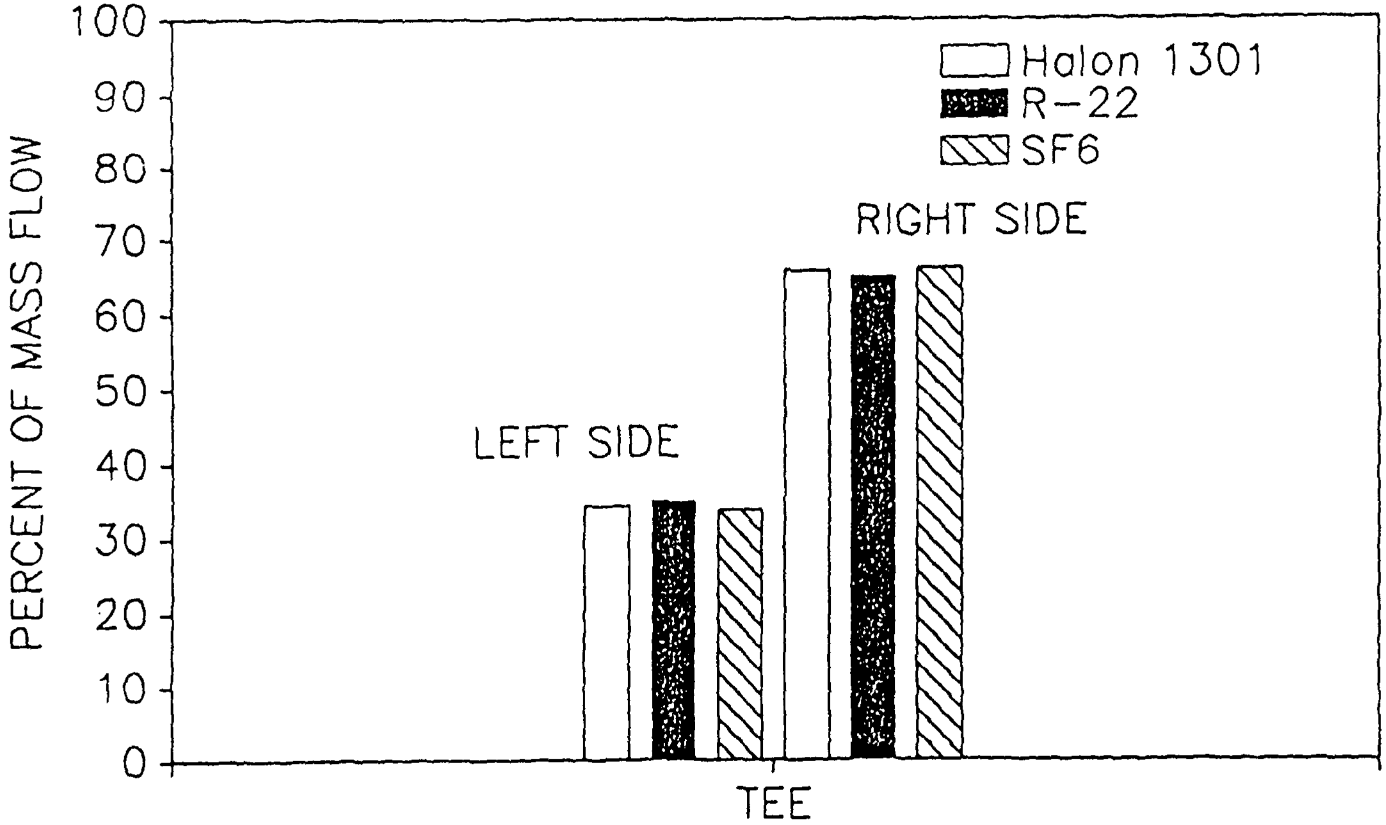


Fig. 22 — Mass flow distribution for system 2

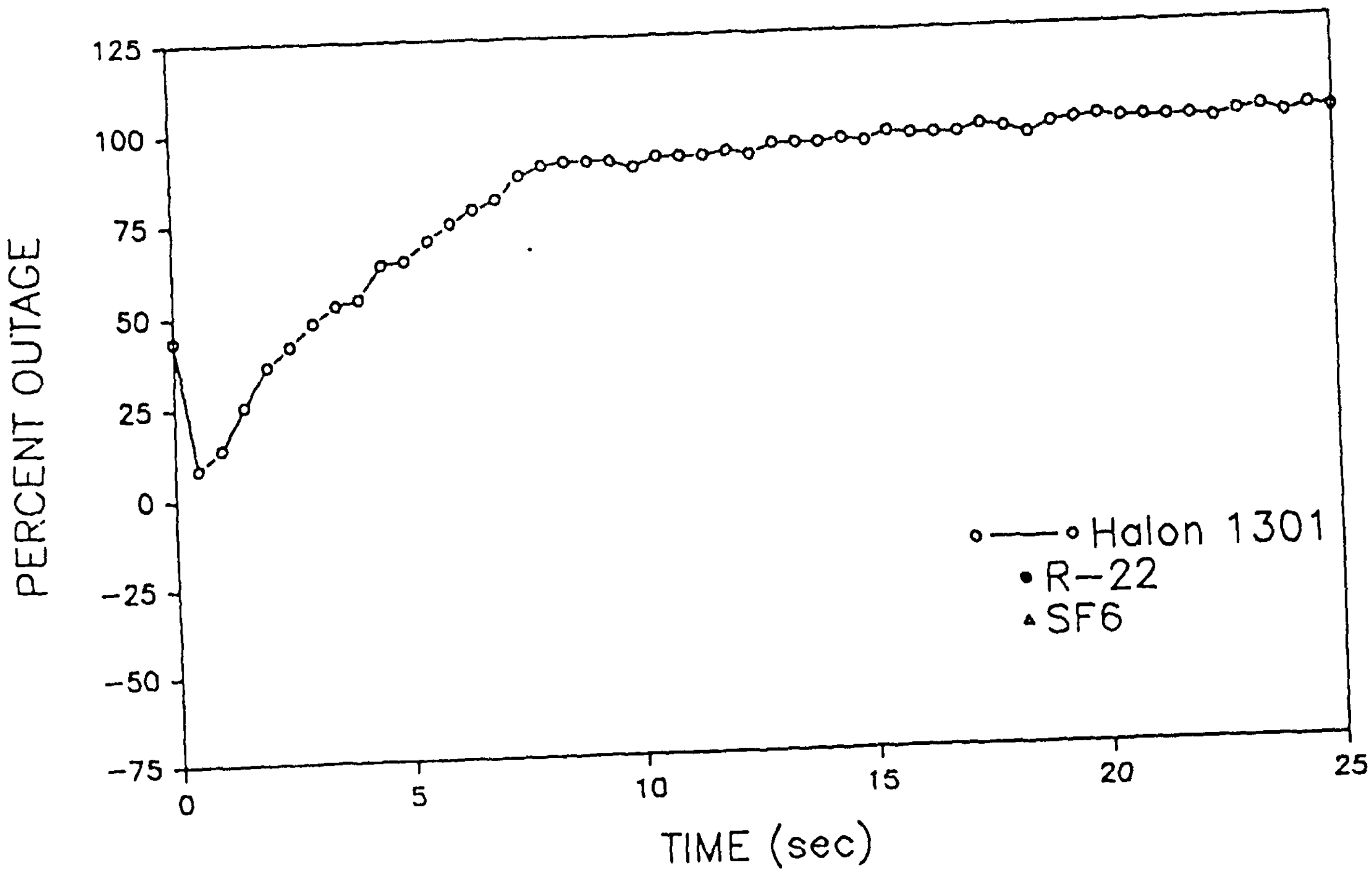


Fig. 23 – Percent outage for system 2

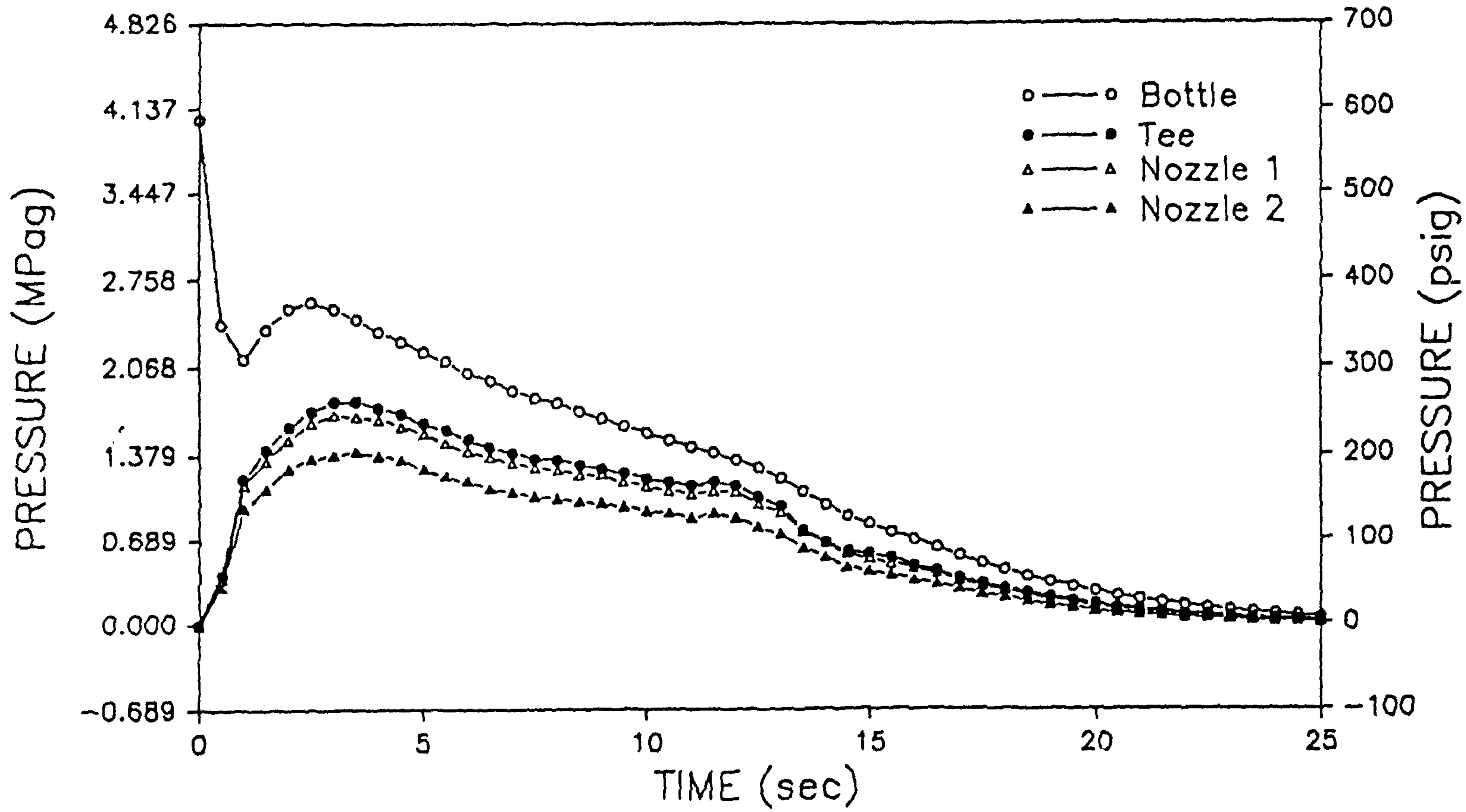


Fig. 24 – Pressure traces for system 2 with Halon 1301

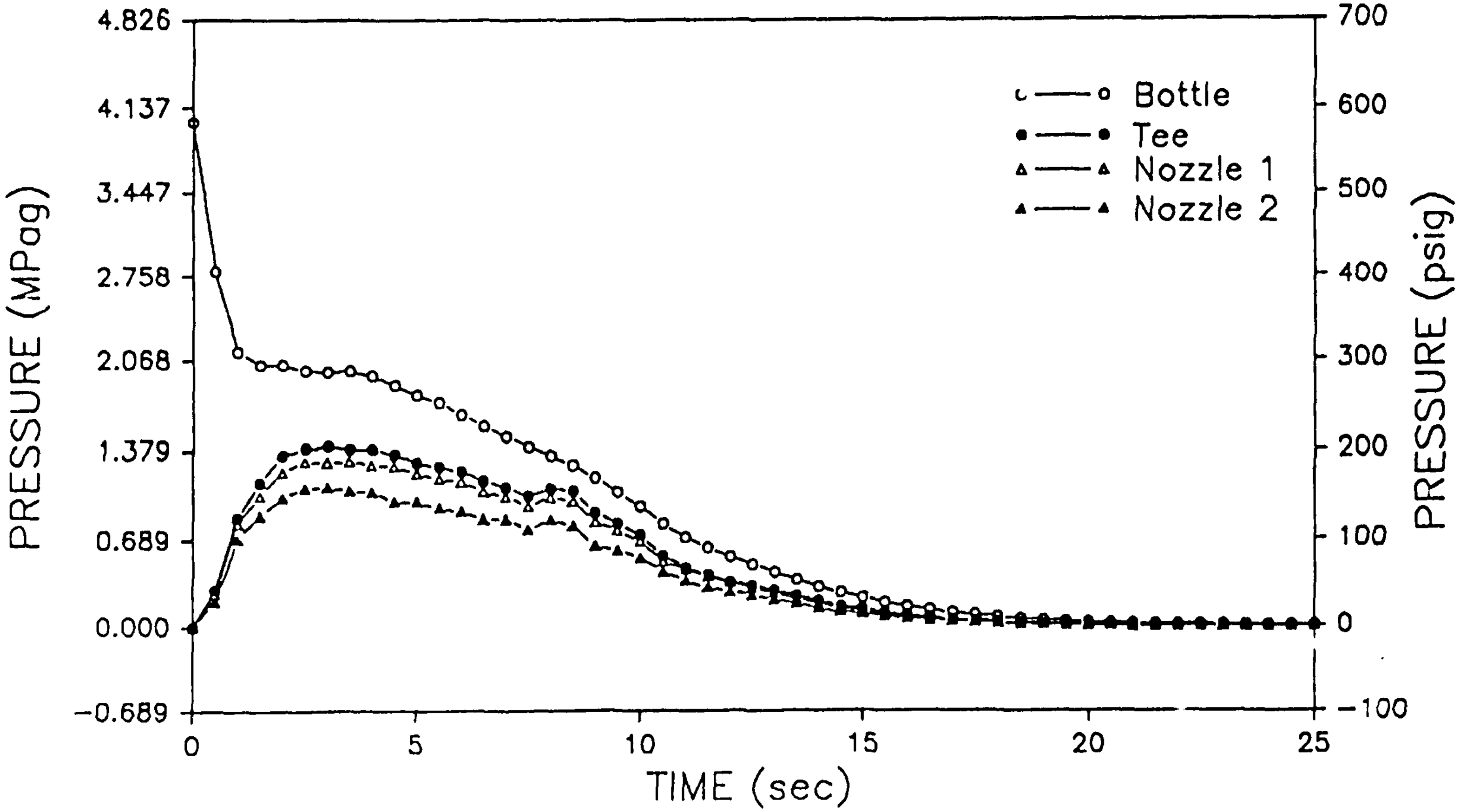


Fig. 25 – Pressure traces for system 2 with R–22

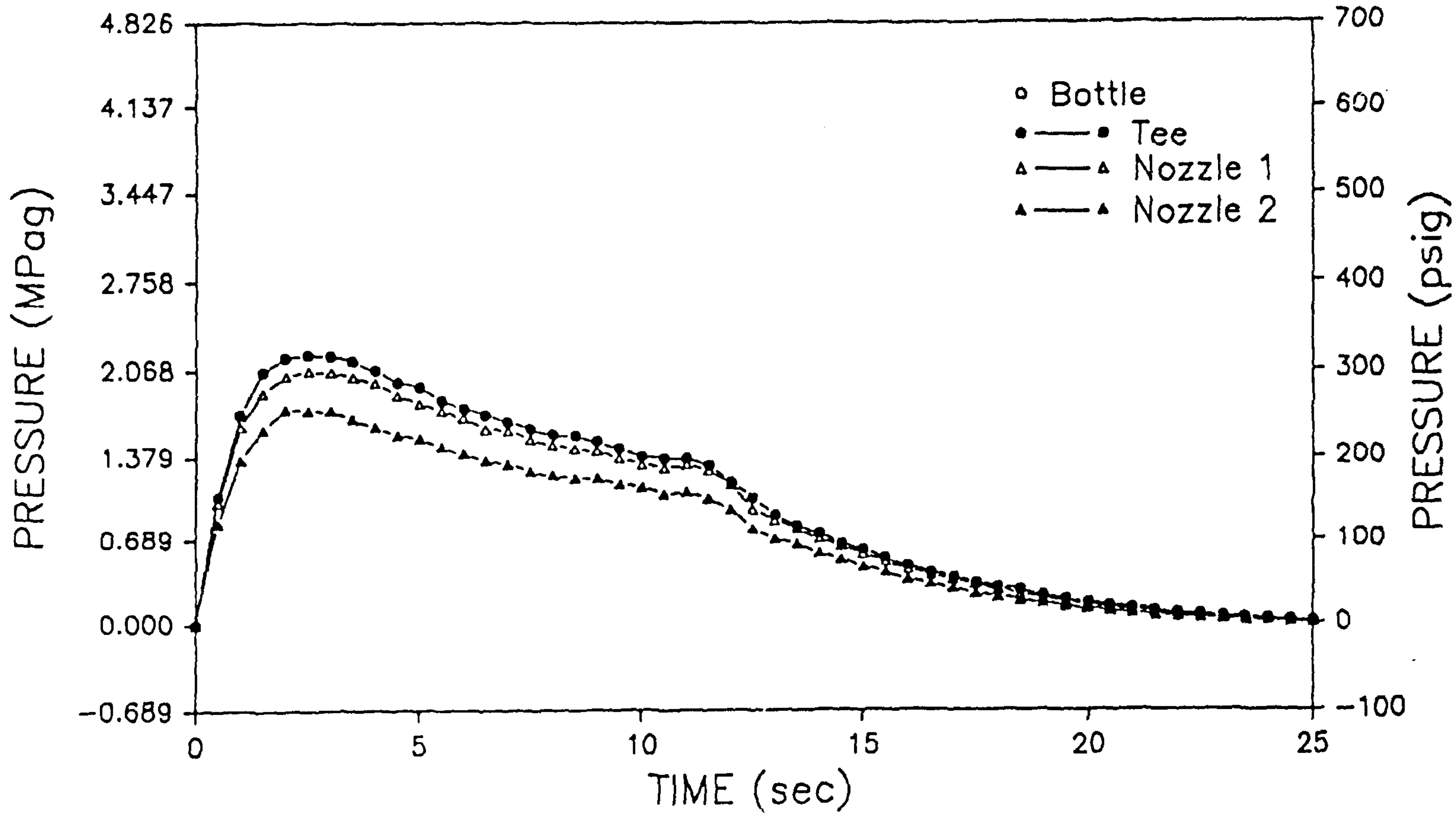


Fig. 26 – Pressure traces for system 2 with SF6

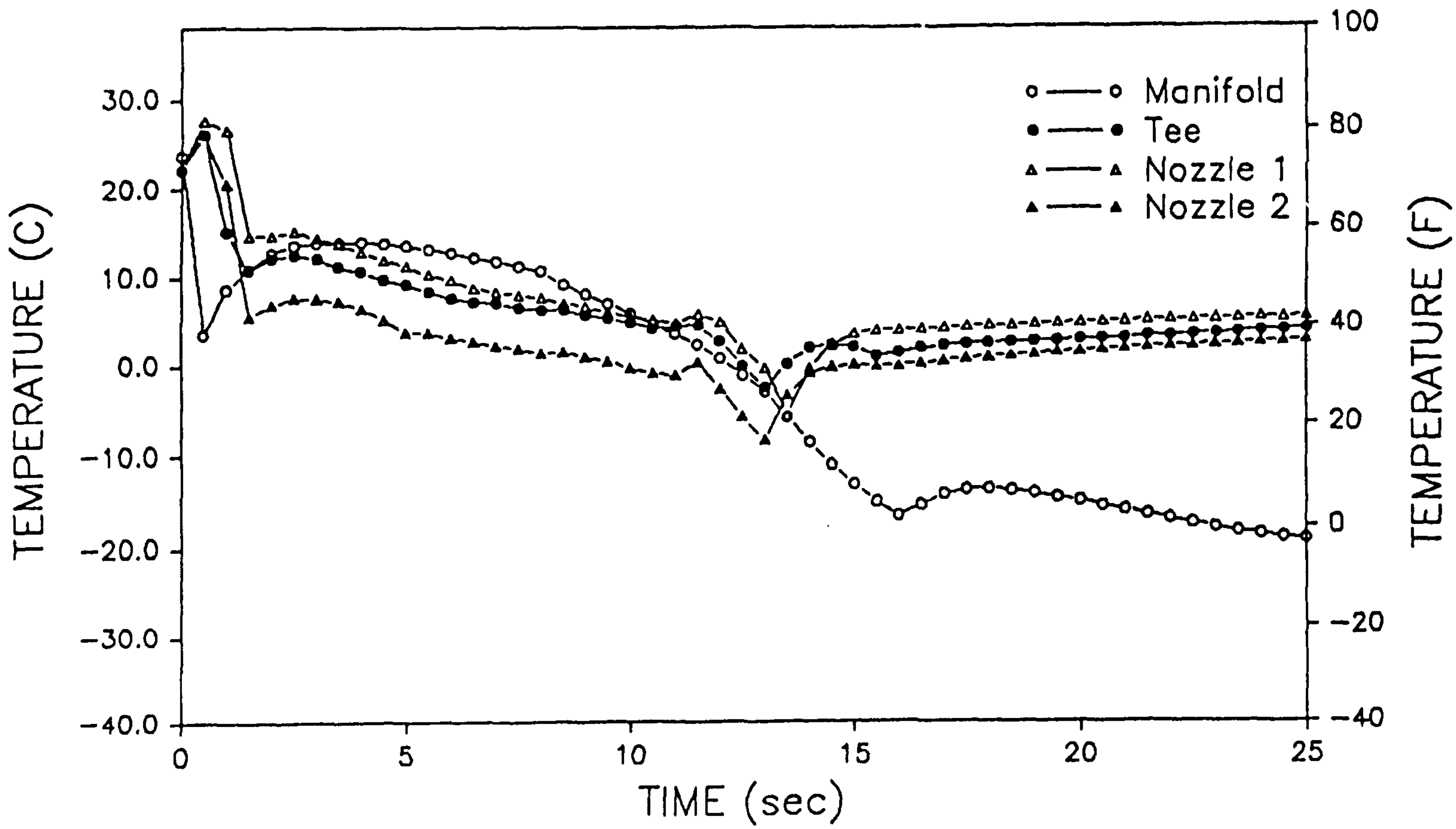


Fig. 27 – Temperature traces for system 2 with Halon 1301

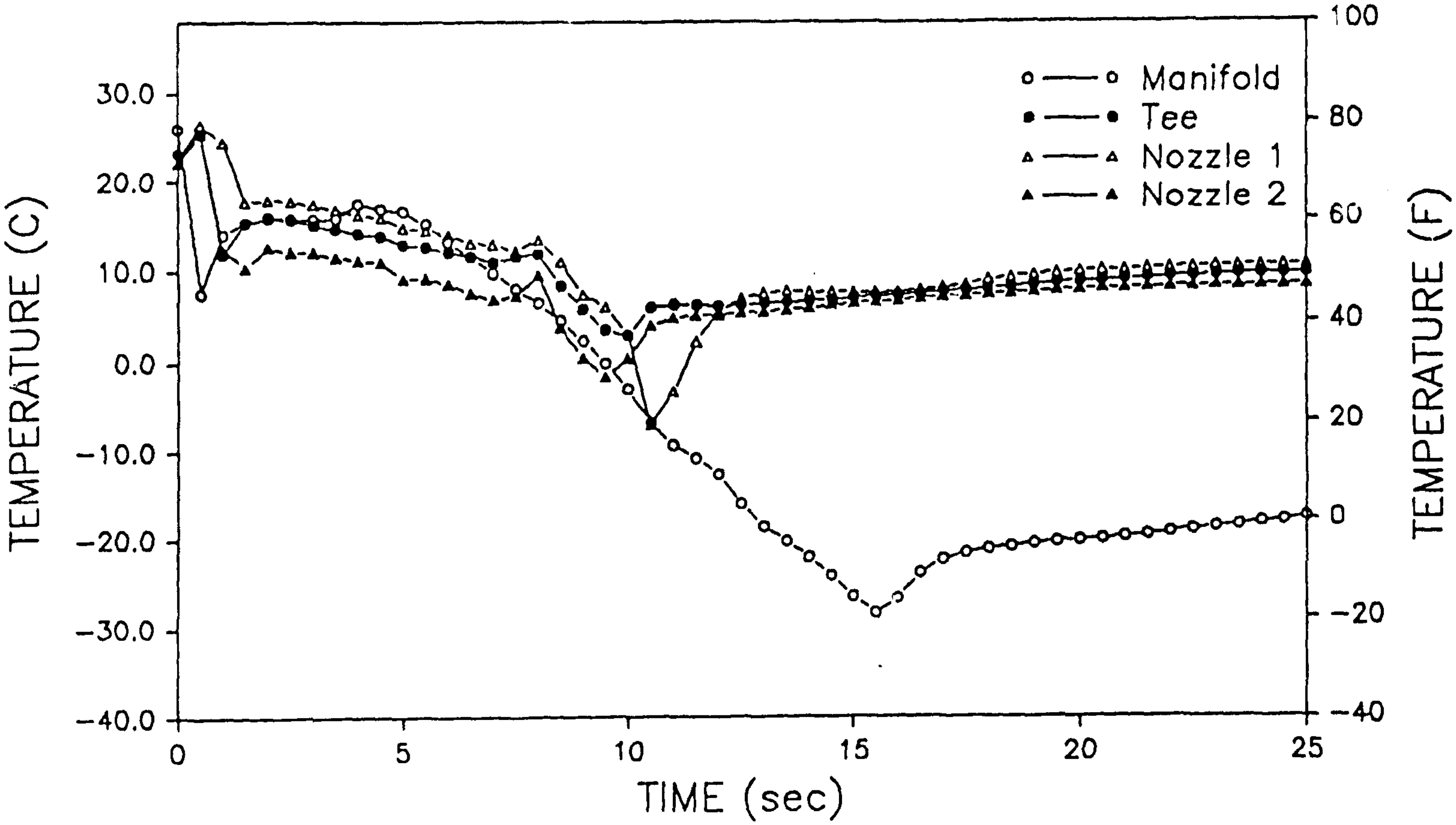


Fig. 28 — Temperature traces for system 2 with R−22

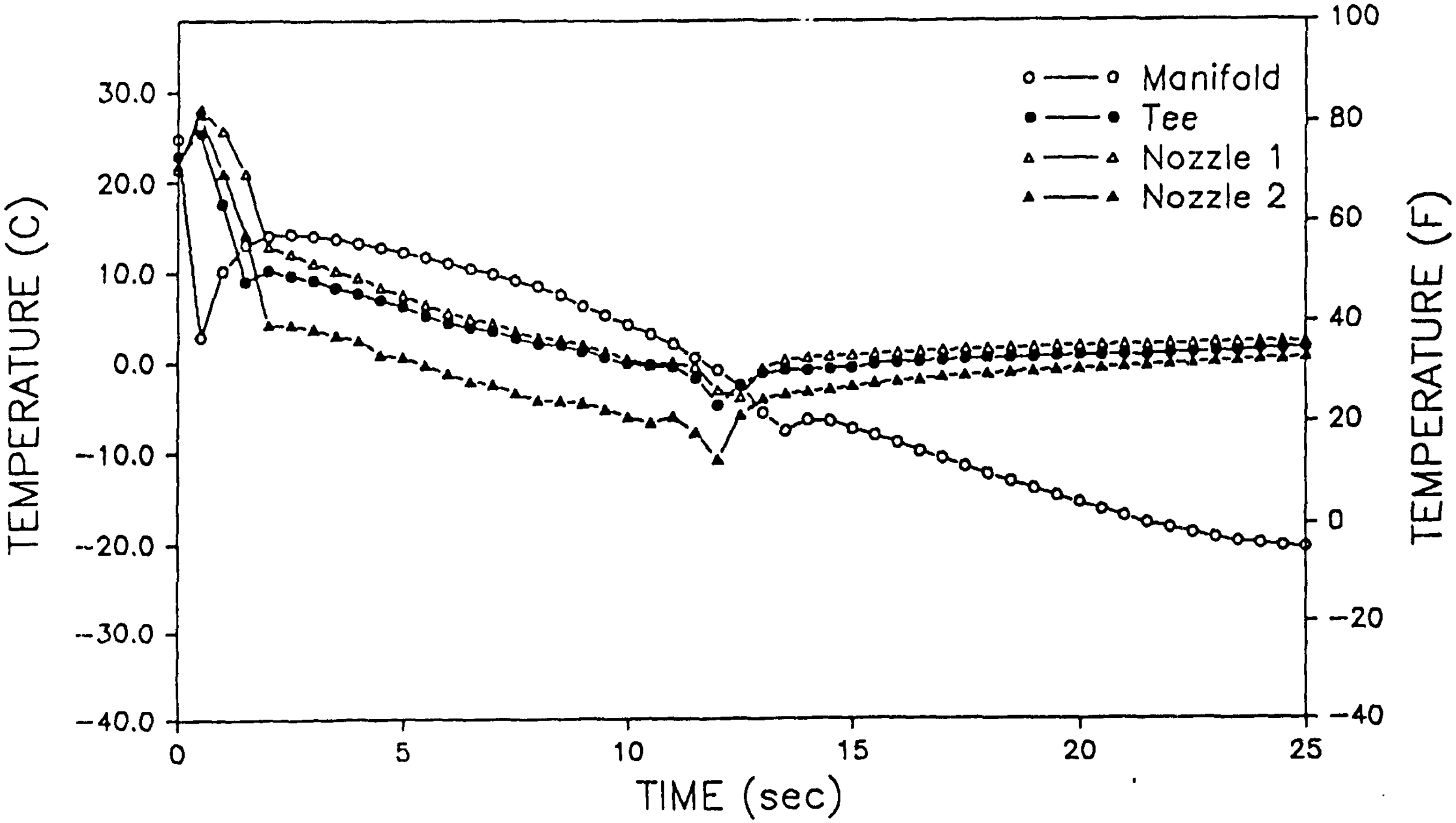


Fig. 29 — Temperature traces for system 2 with SF6

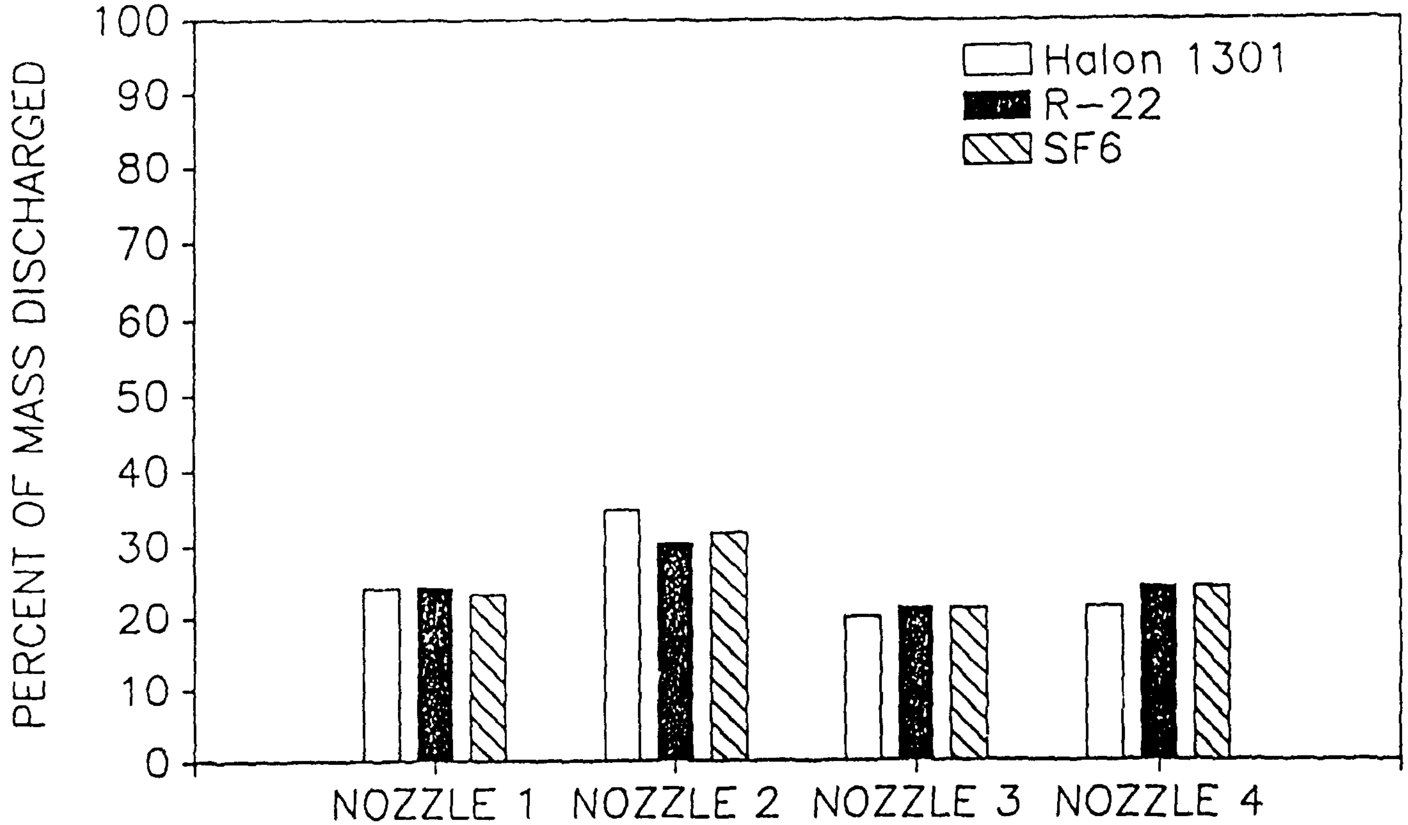


Fig. 30 – Mass distribution for system 3

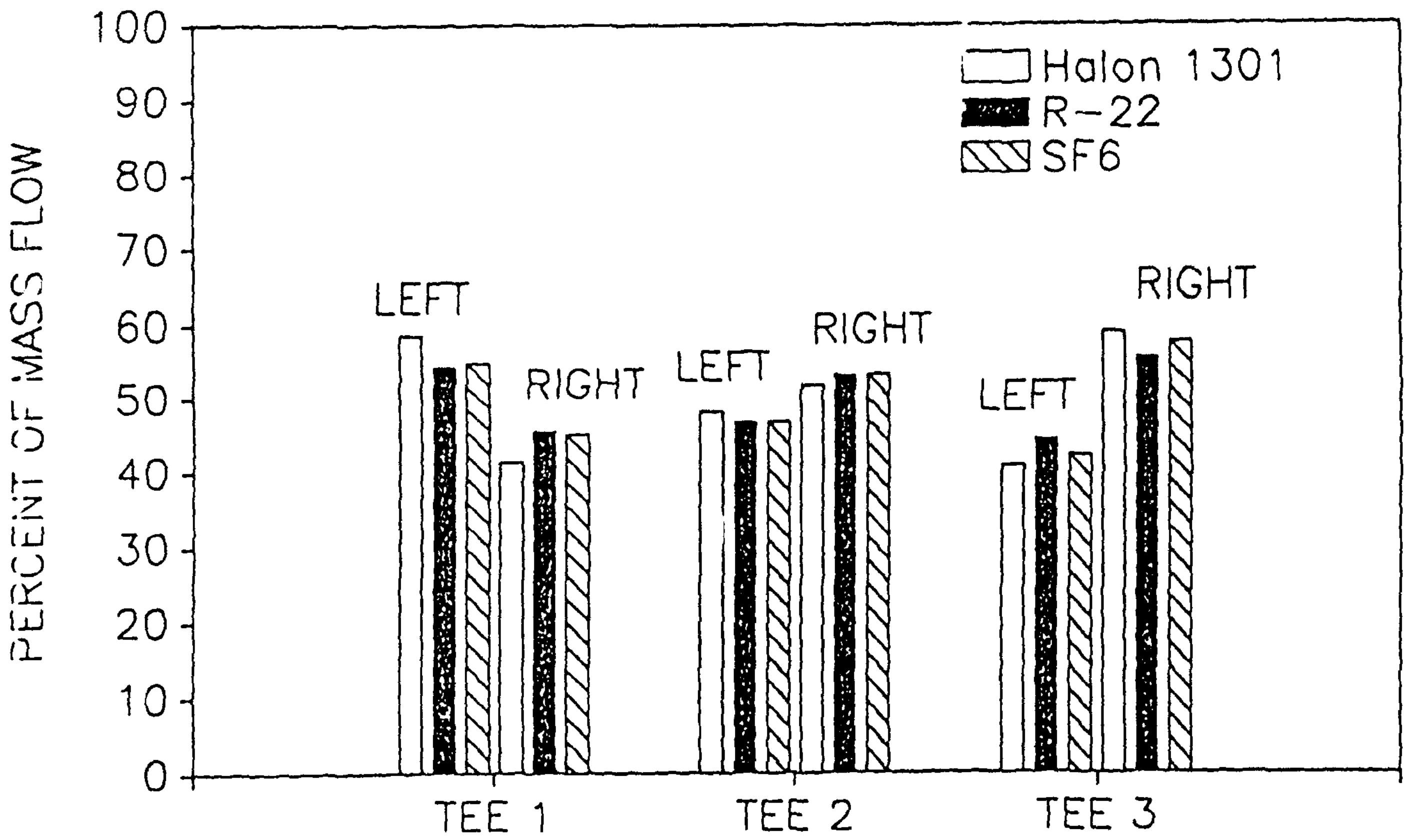


Fig. 31 — Mass flow distribution for system 3

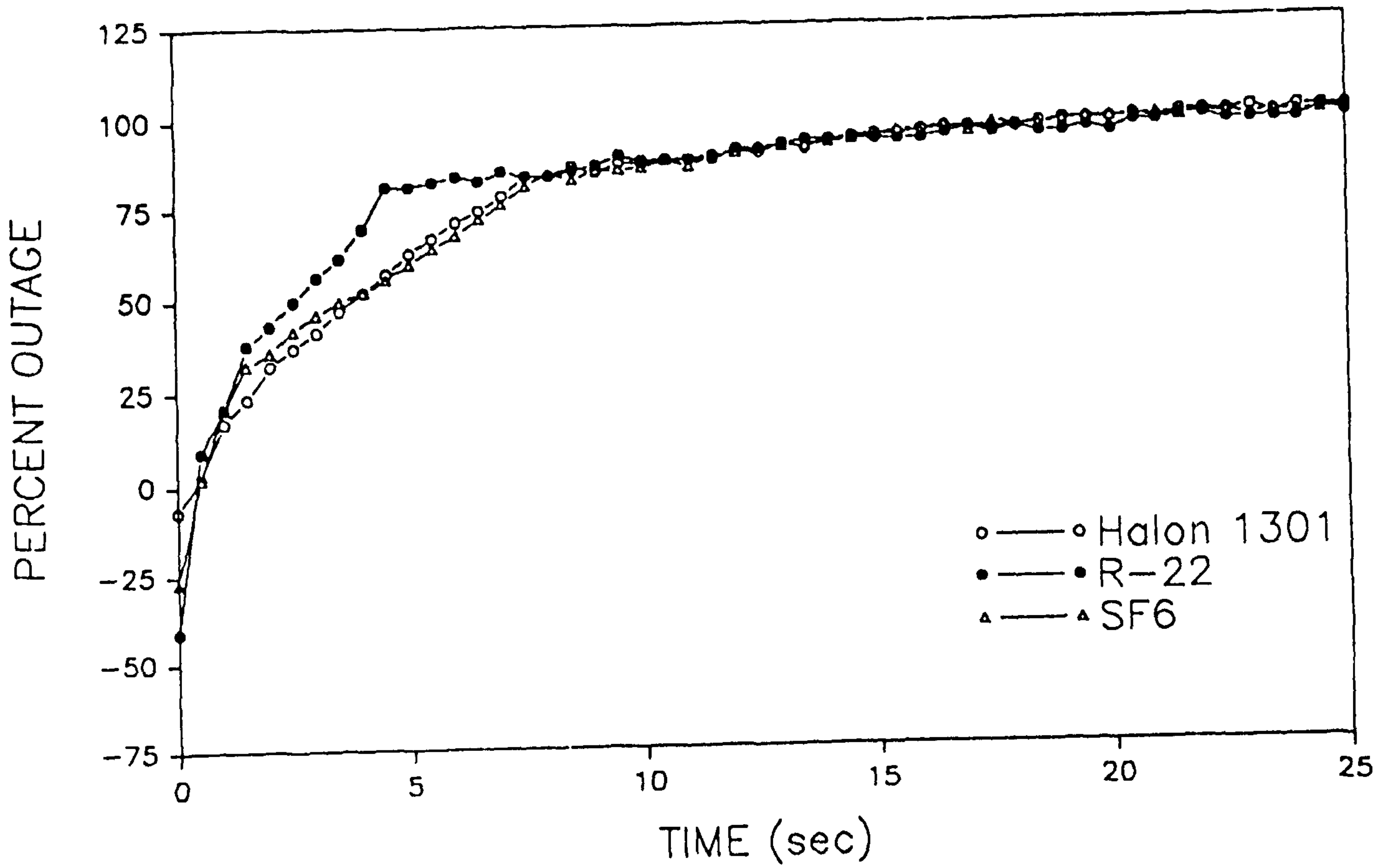


Fig. 32 − Percent outage for system 3

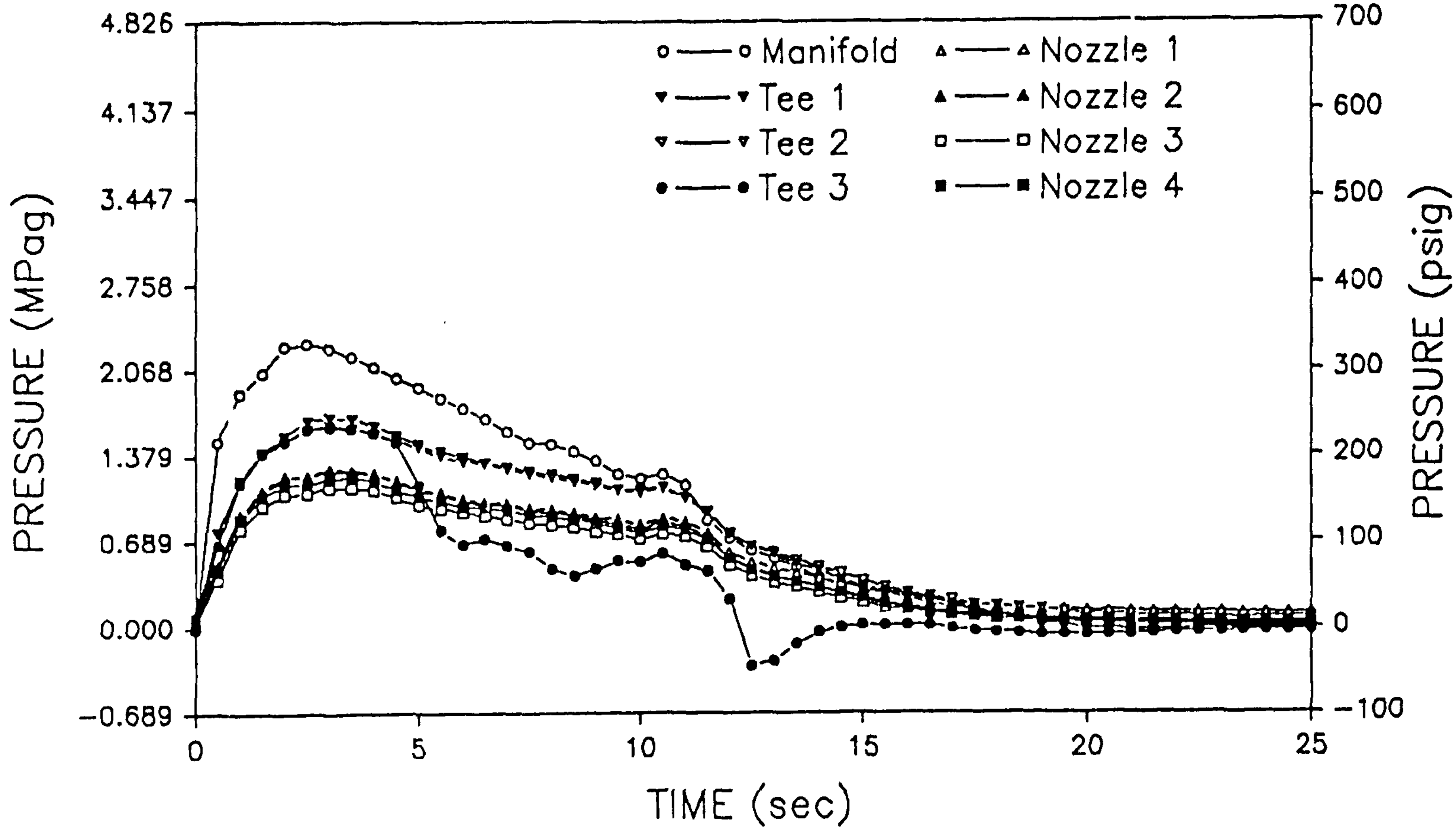


Fig. 33 – Pressure traces for system 3 with Halon 1301

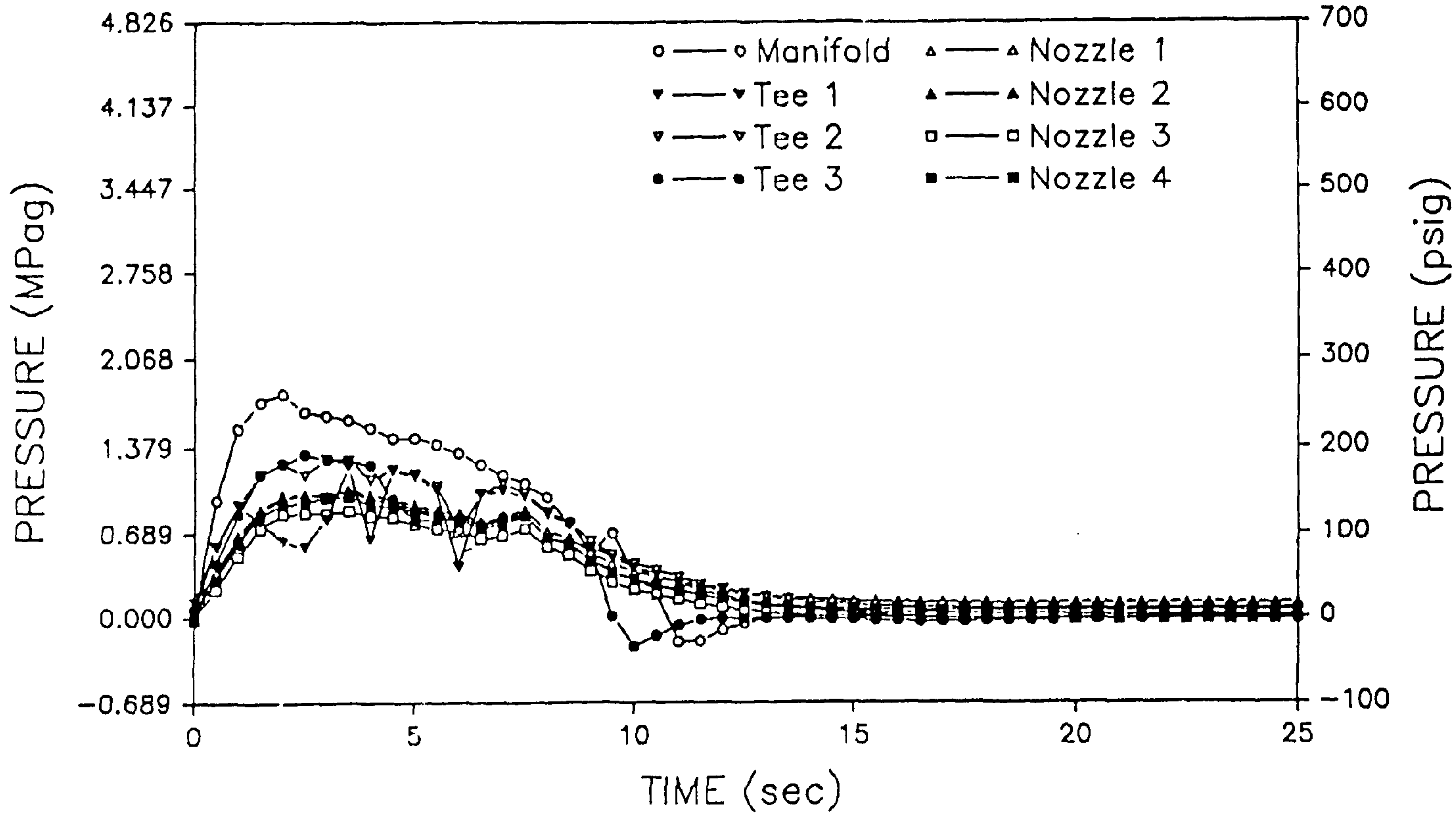


Fig. 34 – Pressure traces for system 5 with R–22

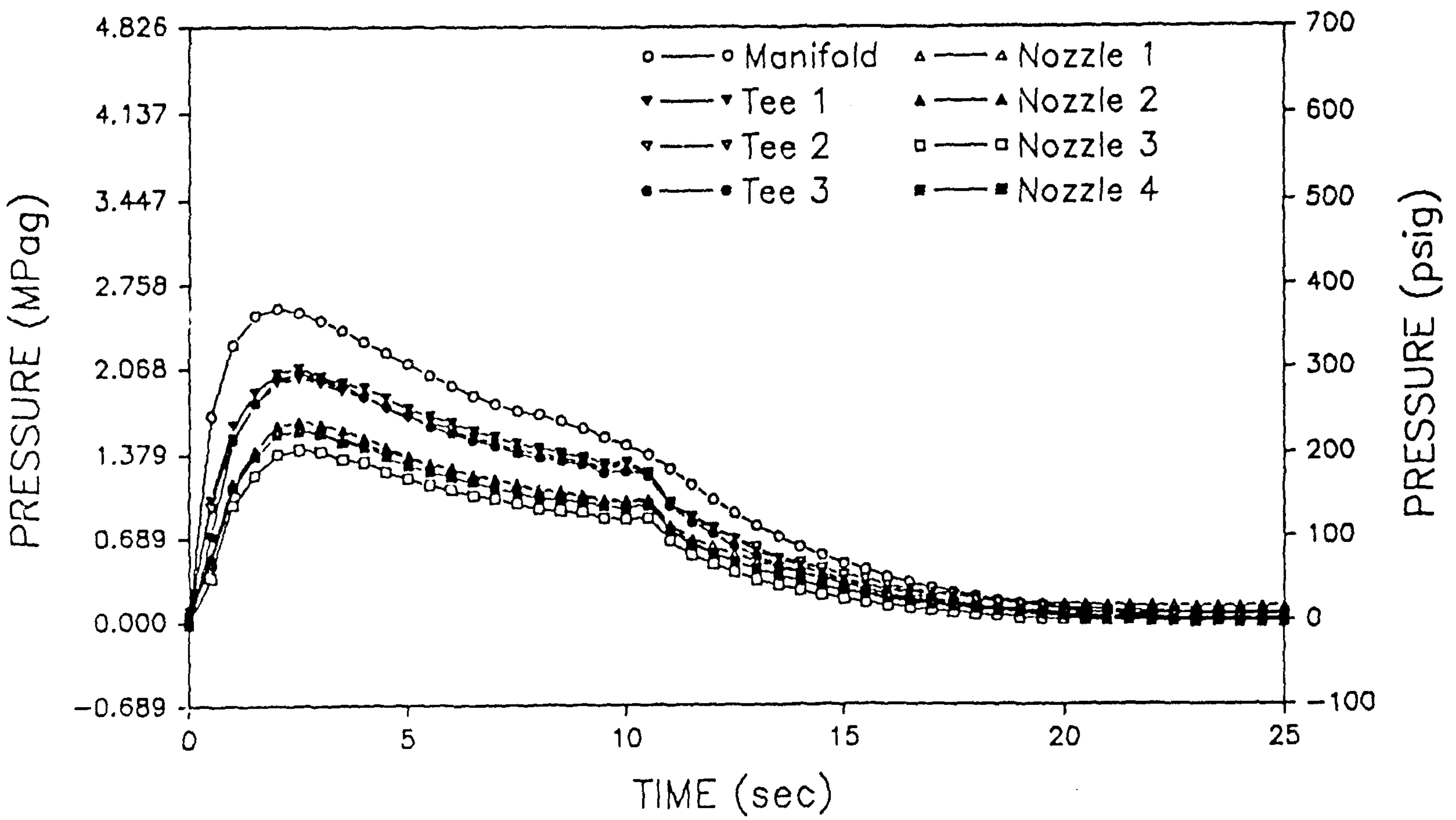


Fig. 35 – Pressure traces for system 3 with SF6

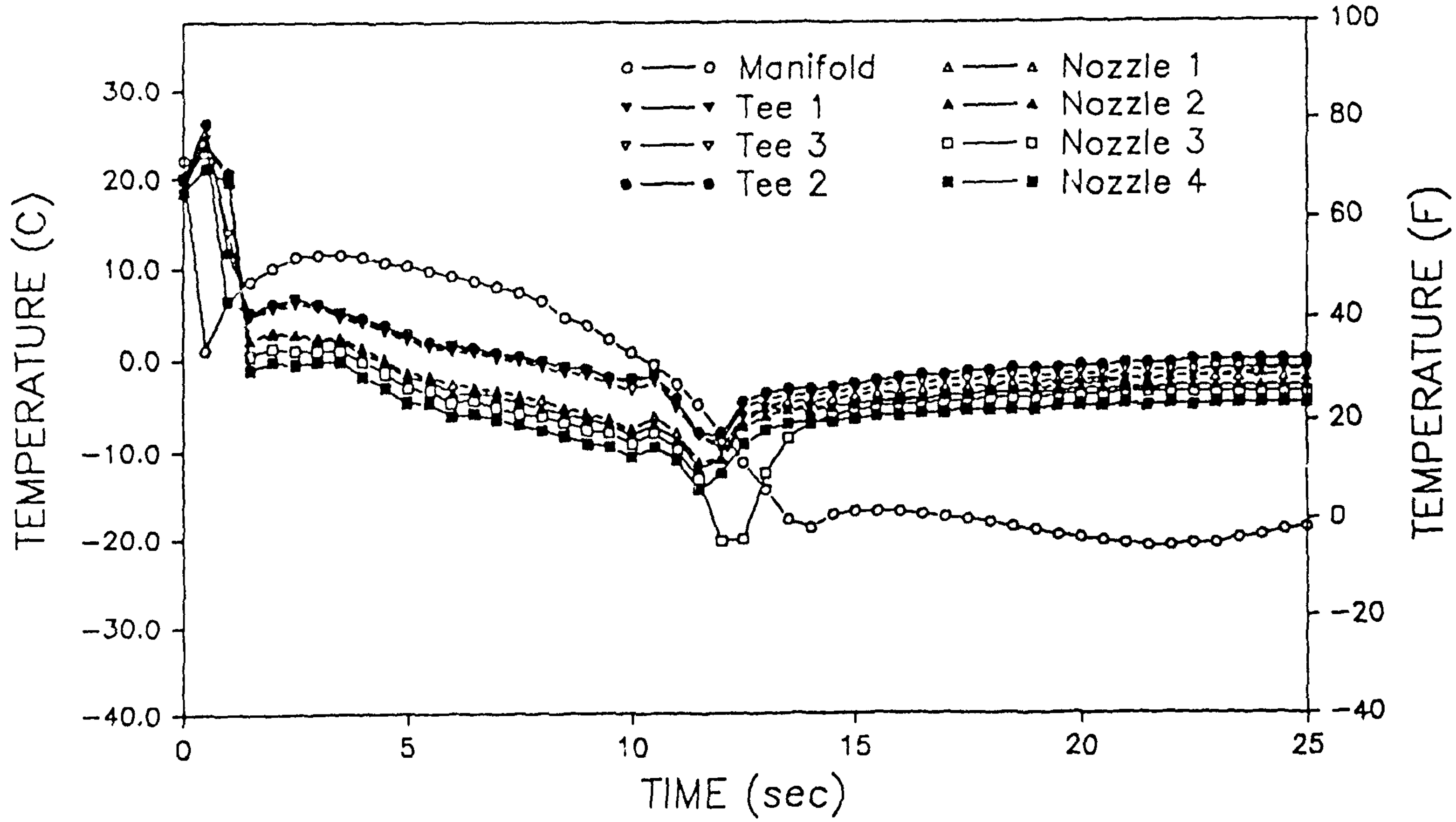


Fig. 36 – Temperature traces for system 3 with Halon 1301

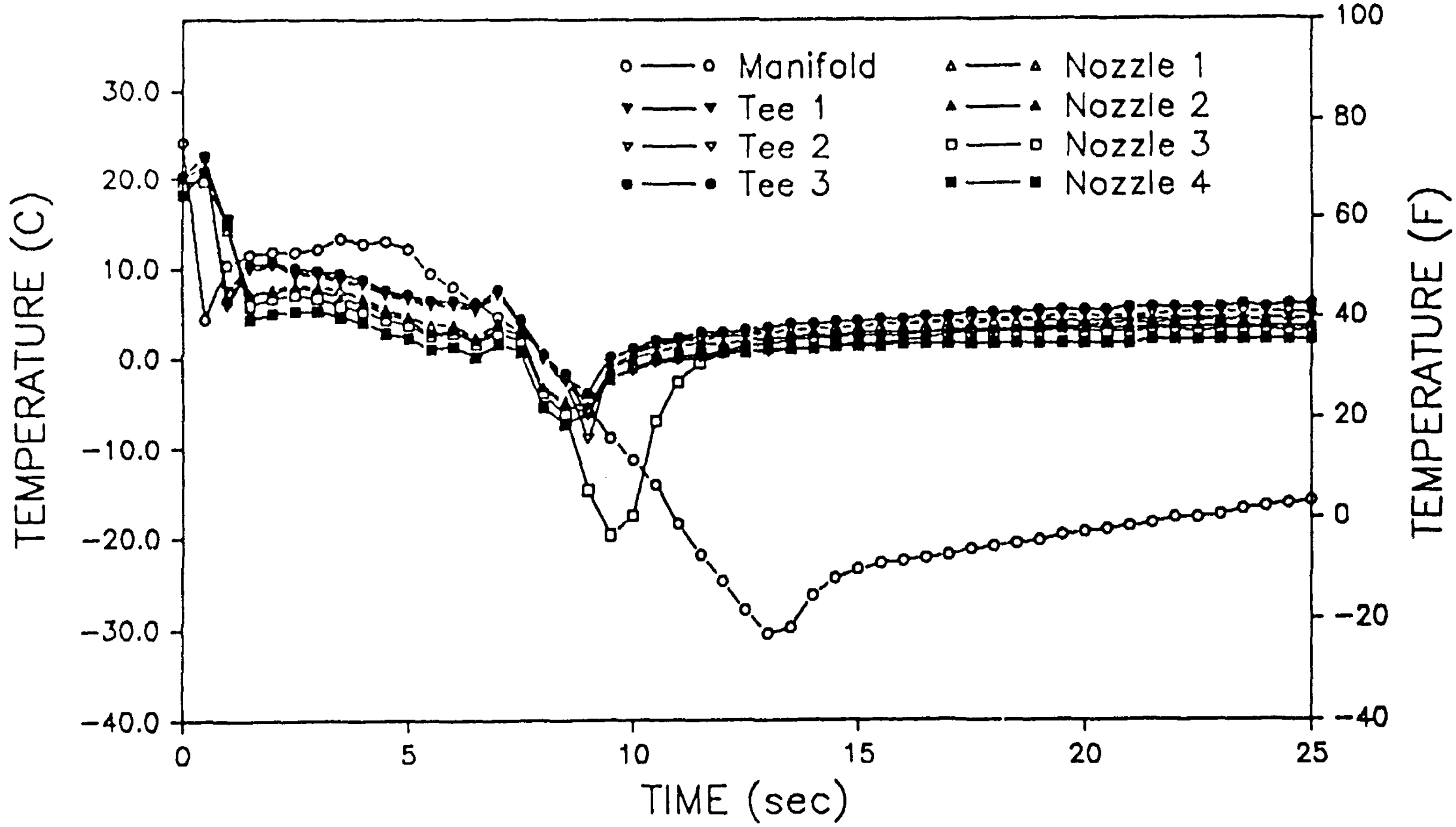


Fig. 37 – Temperature traces for system 3 with R-22

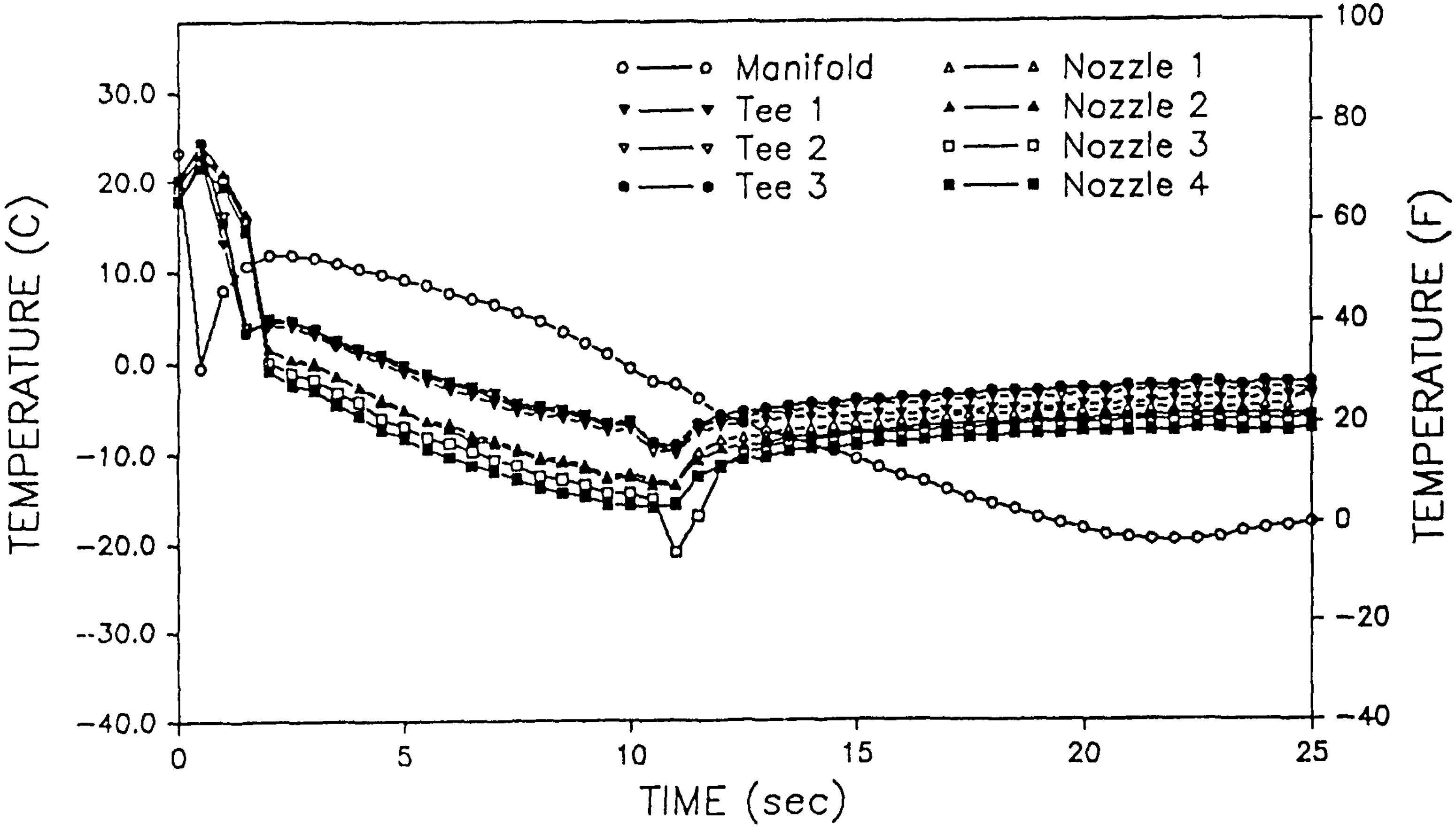


Fig. 38 – Temperature traces for system 3 with SF6

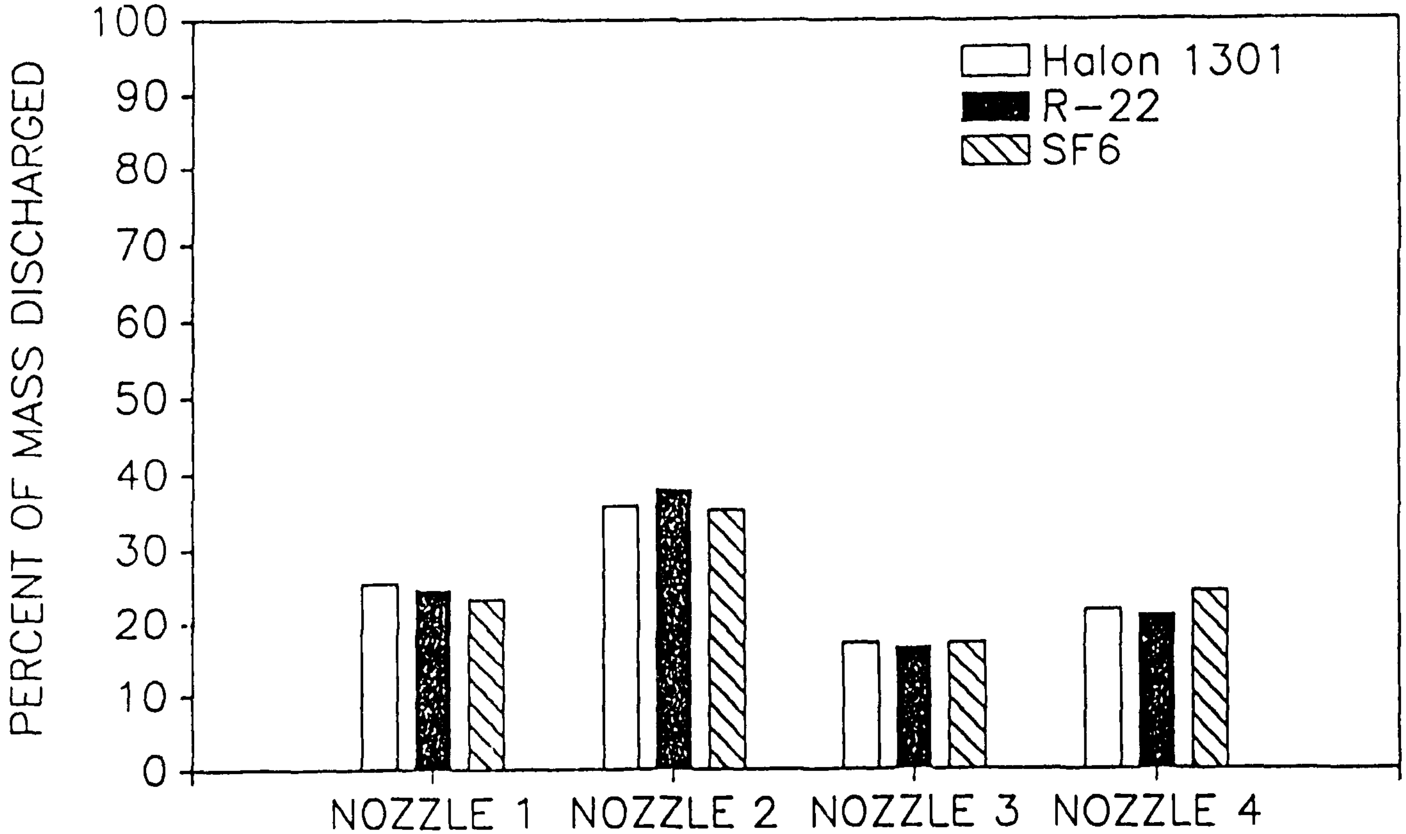


Fig. 39 – Mass distribution for system 4

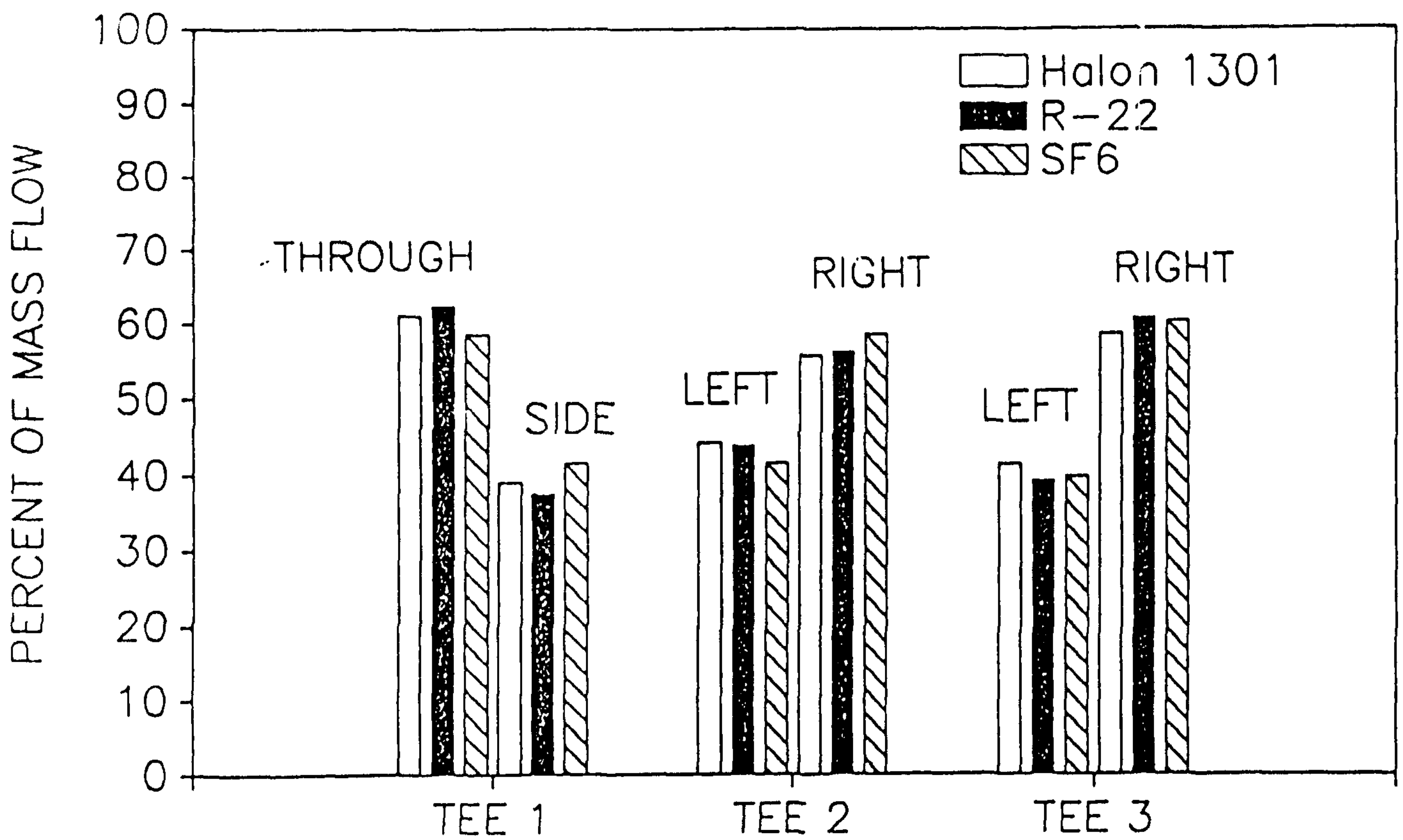


Fig. 40 – Mass flow distribution for system 4

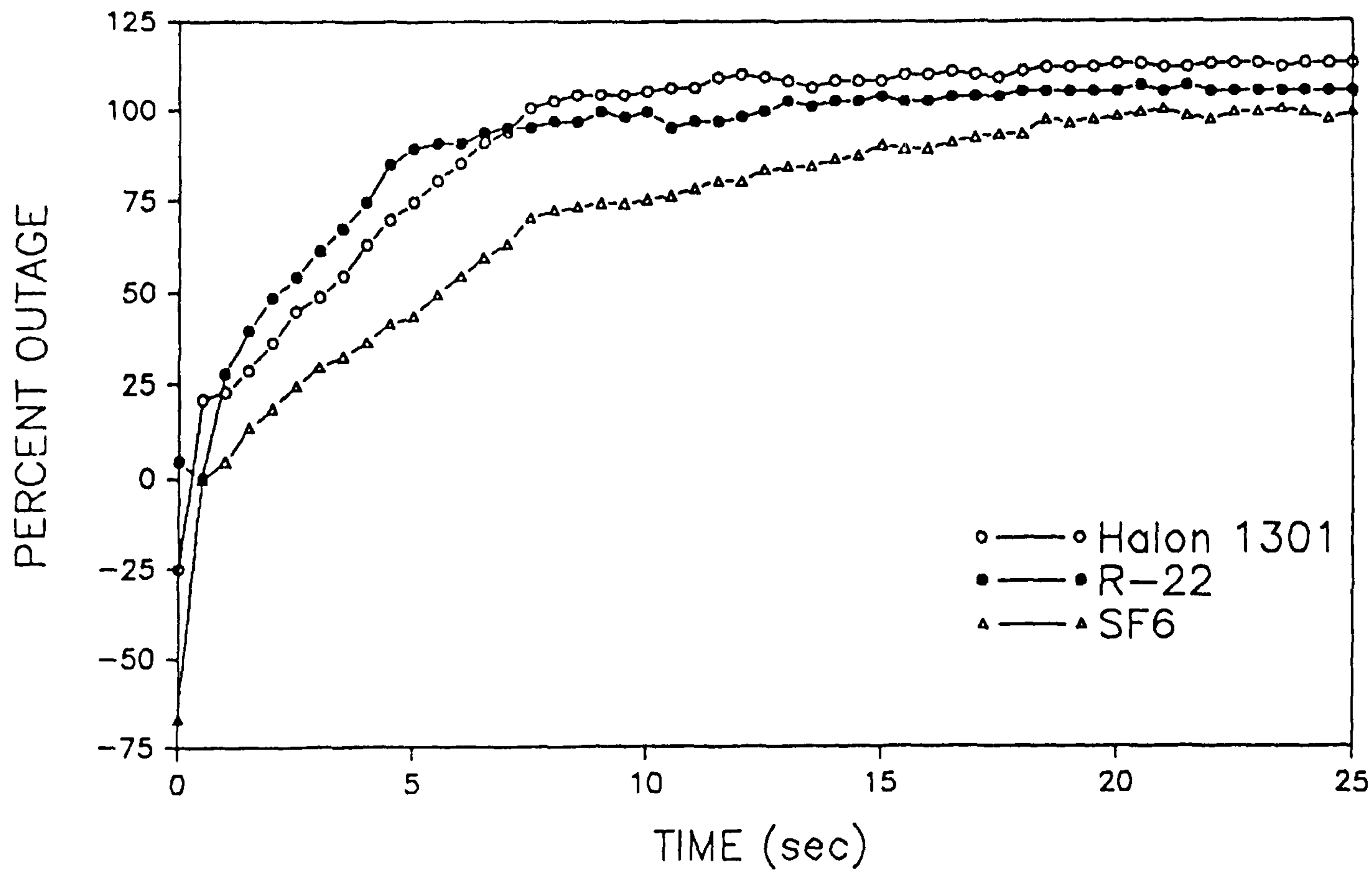


Fig. 41 – Percent outage for system 4

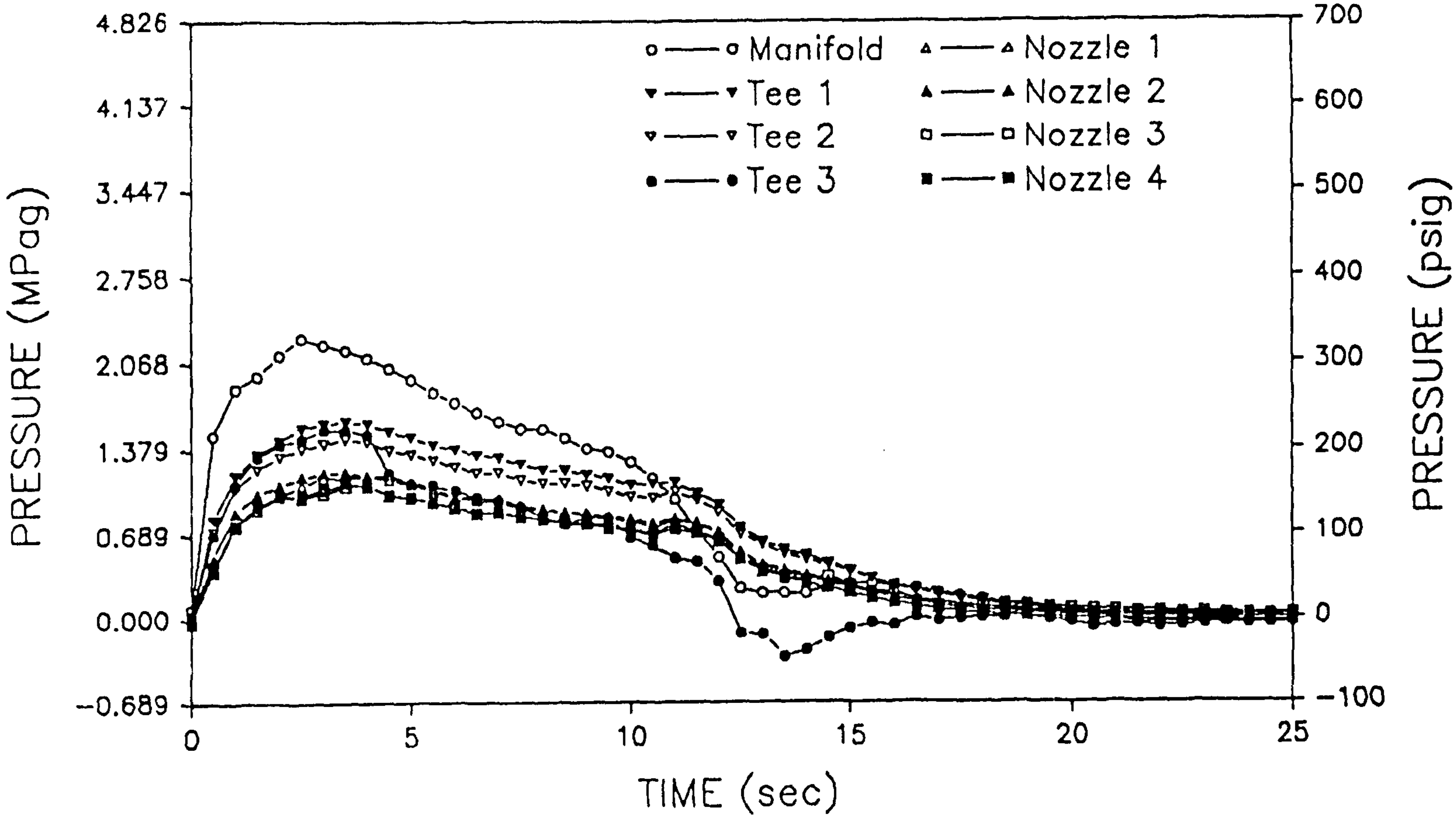


Fig. 42 – Pressure traces for system 4 with Halon 1301

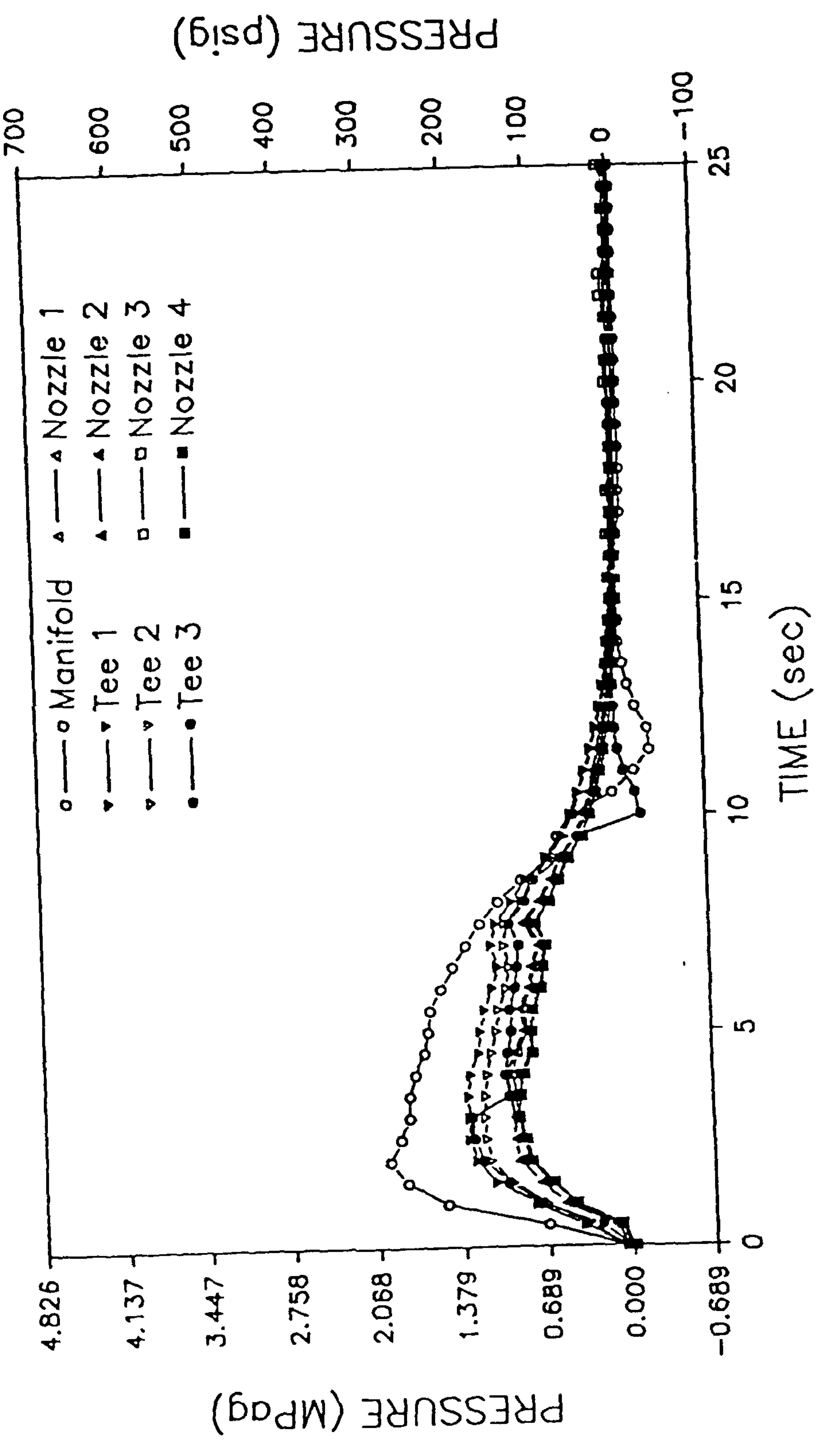


Fig. 43 — Pressure traces for system 4 with R−22

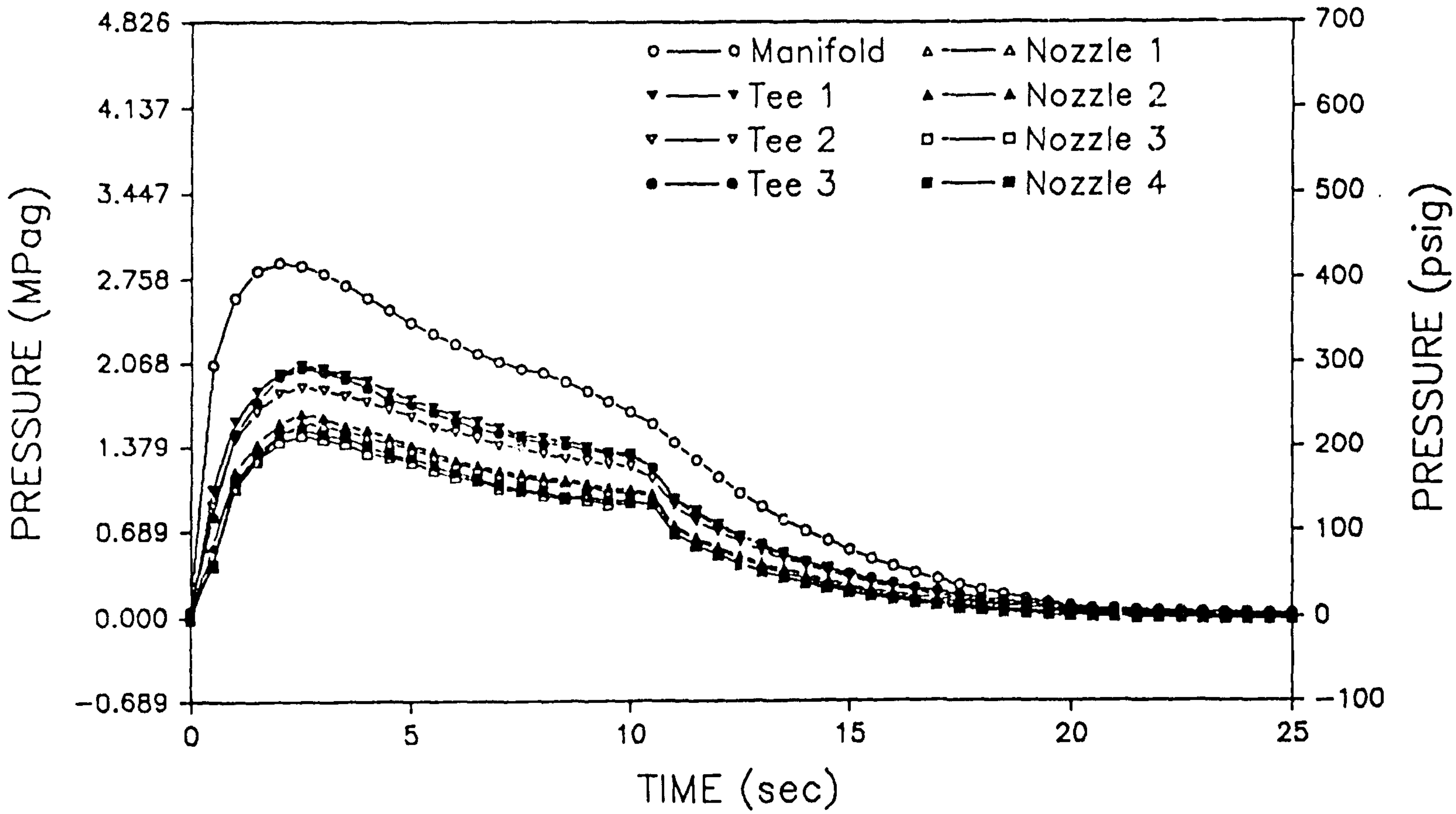


Fig. 44 — Pressure traces for system 4 with SF6

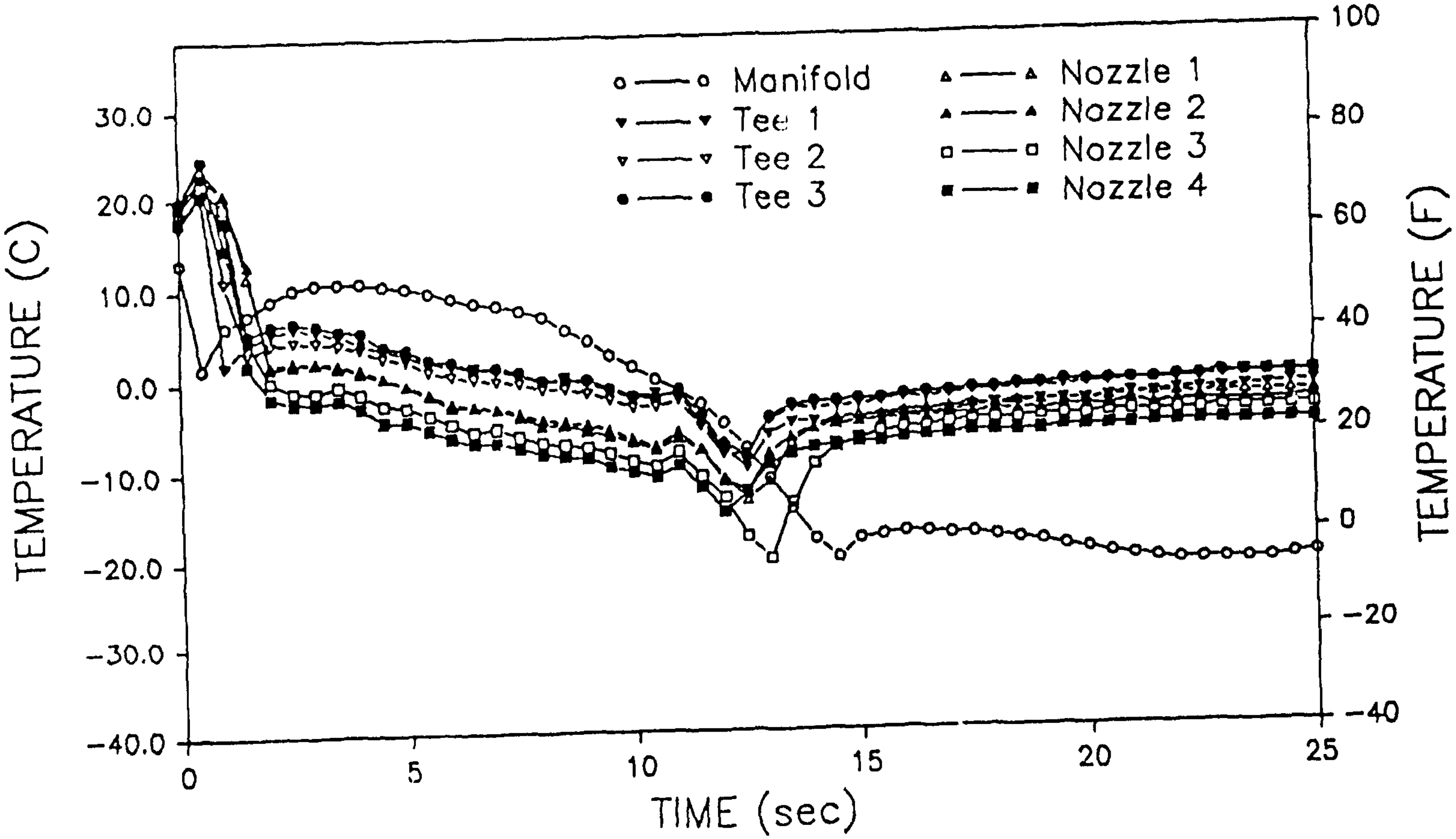


Fig. 45 – Temperature traces for system 4 with Halon 1301

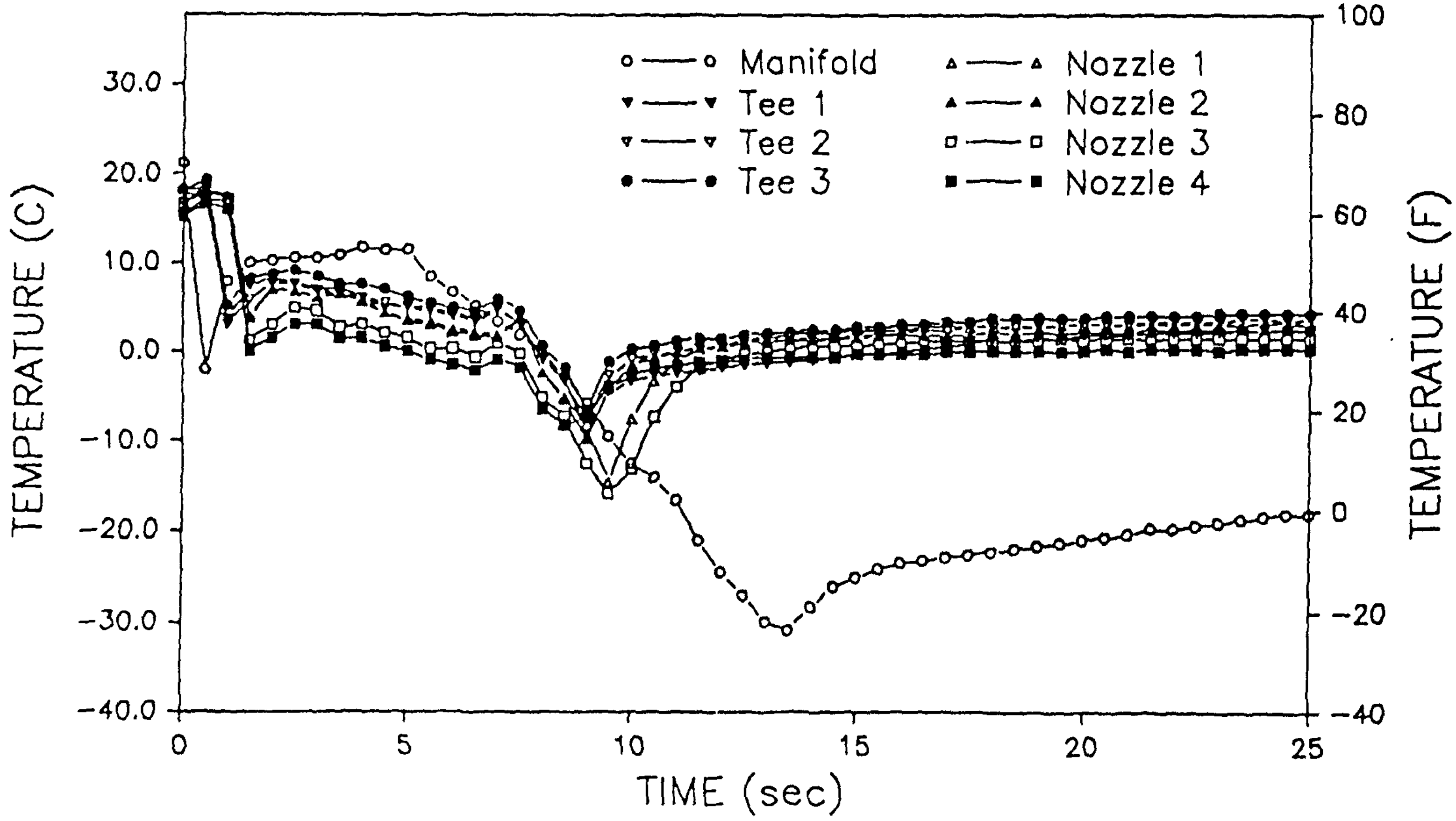


Fig. 46 – Temperature traces for system 4 with R–22

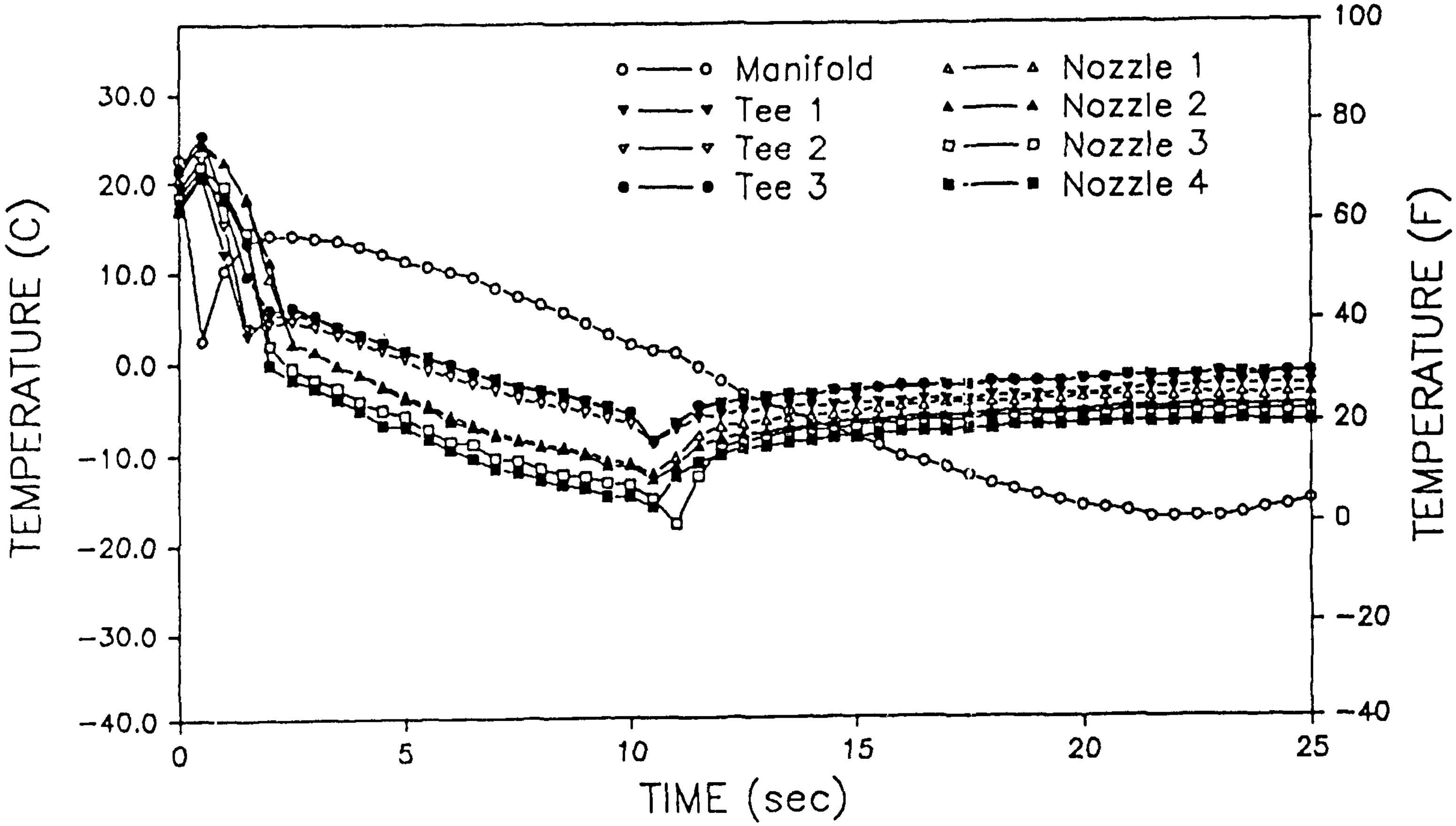


Fig. 47 – Temperature traces for system 4 with SF6

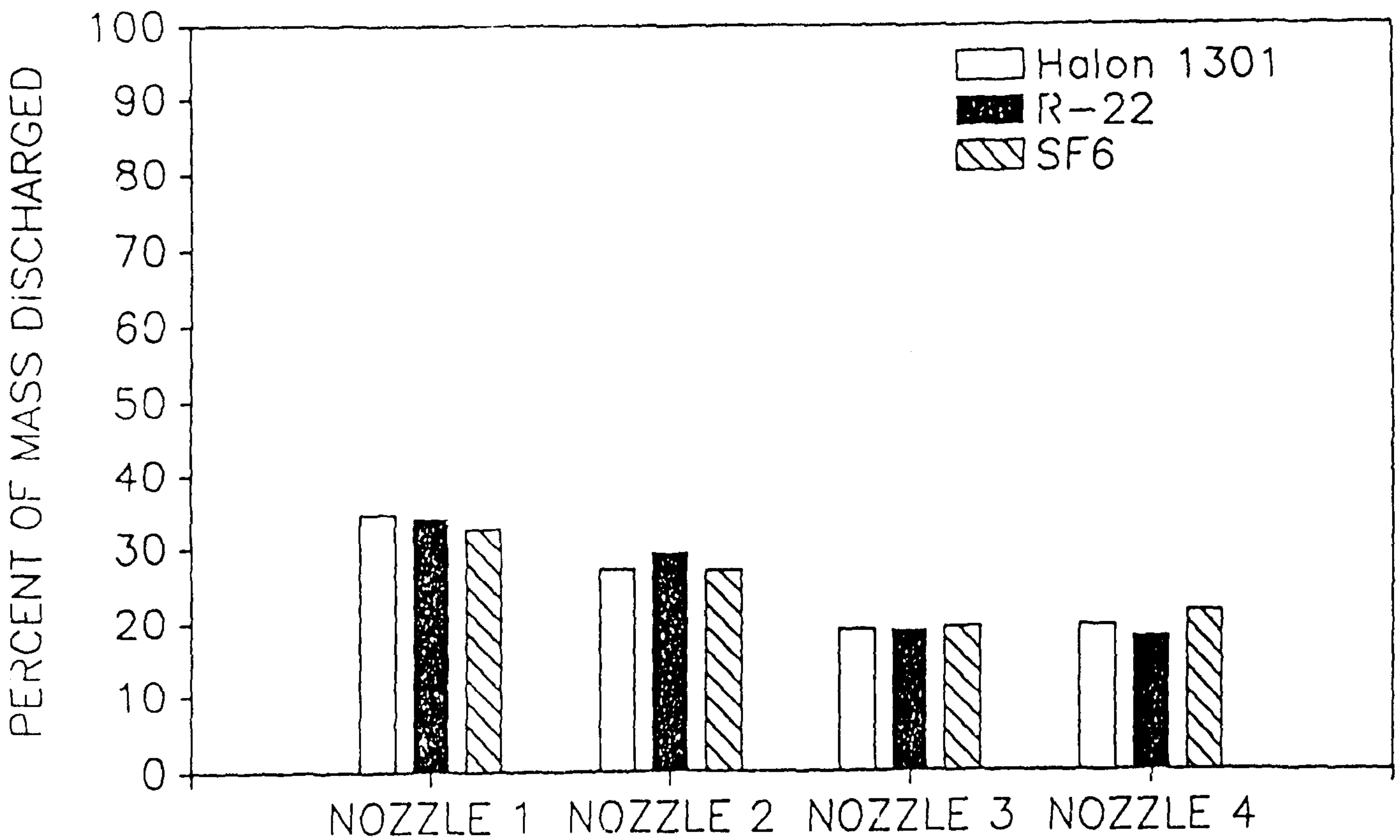


Fig. 48 — Mass distribution for system 5

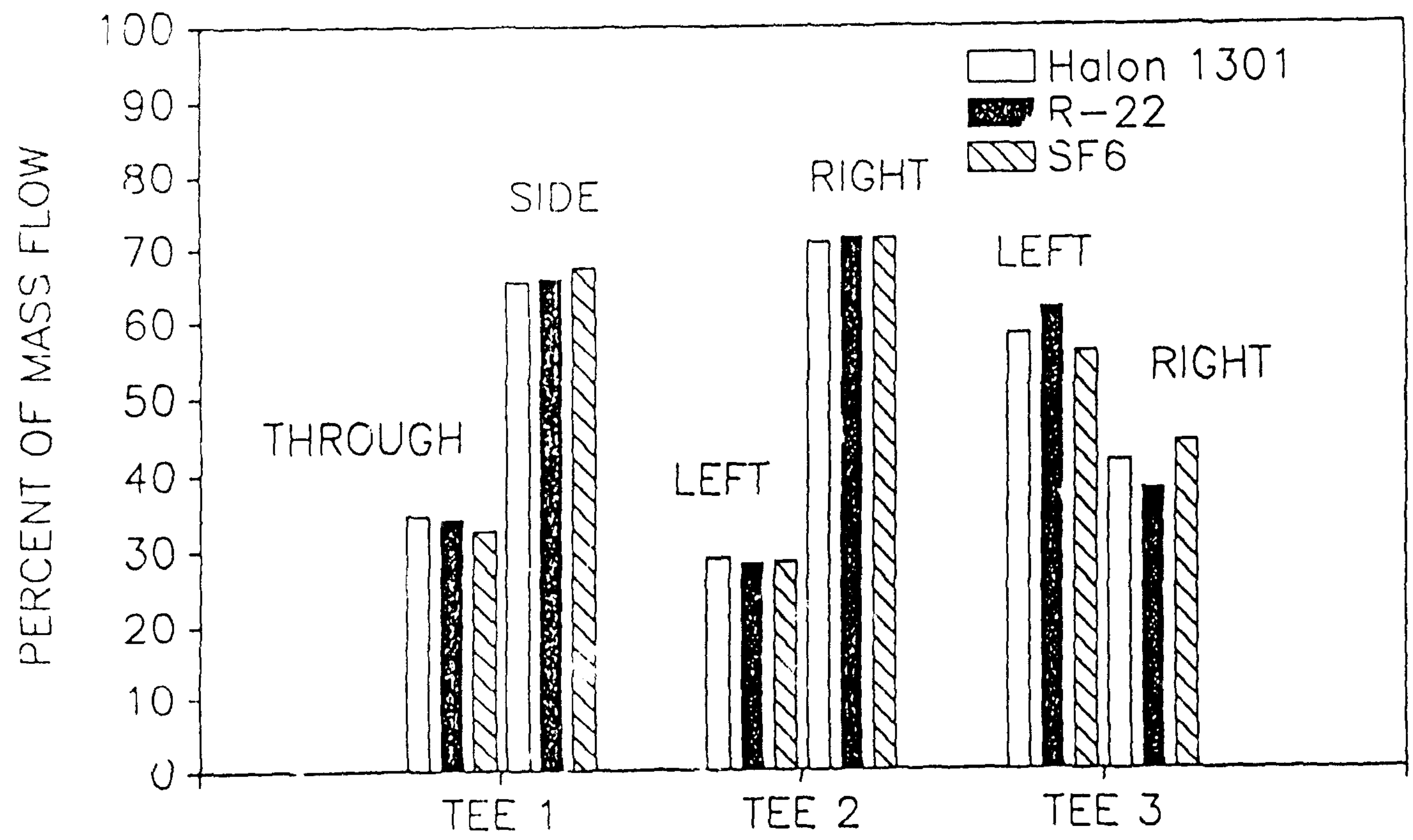


Fig. 49 – Mass flow distribution for system 5

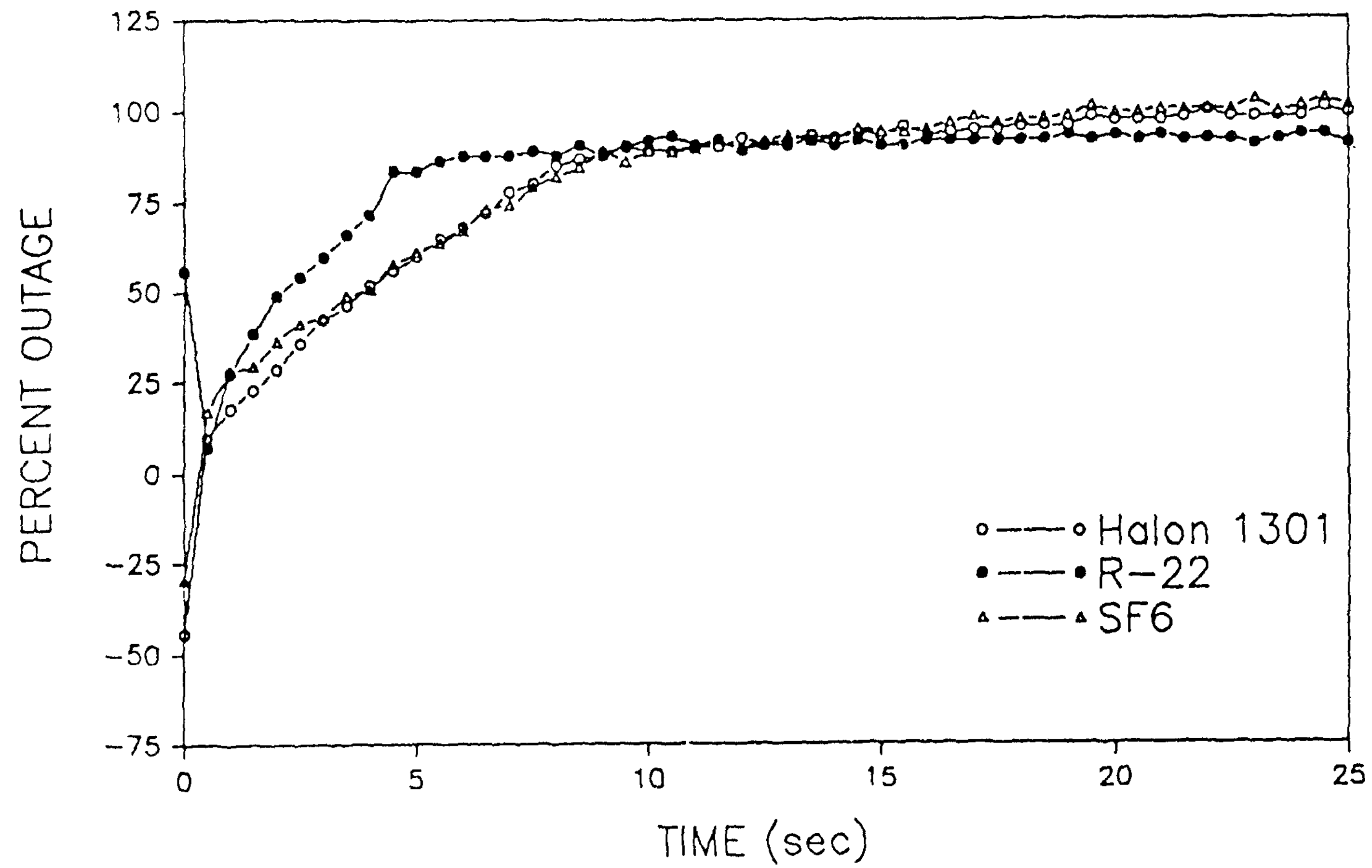


Fig. 50 – Percent outage for system 5

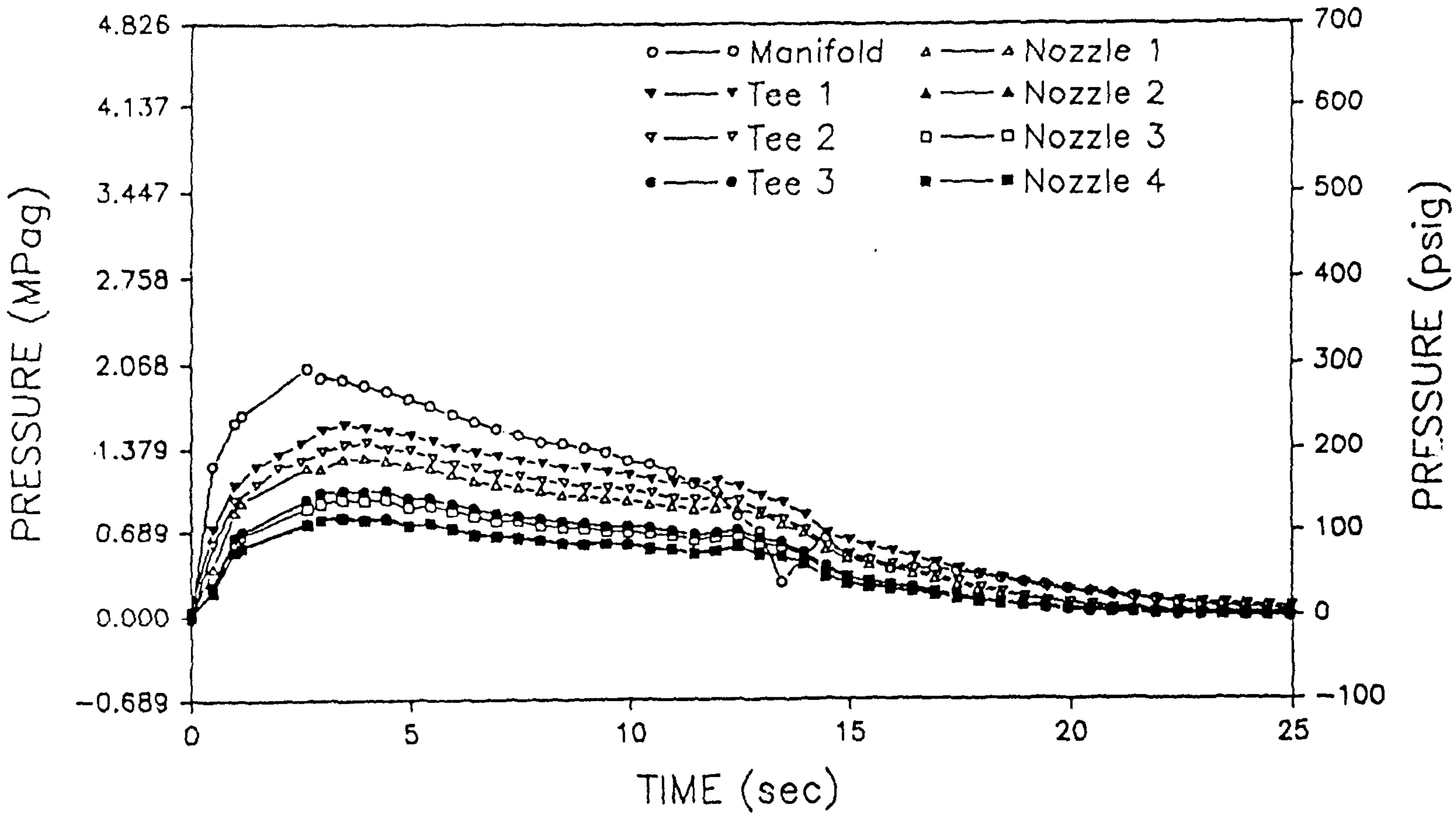


Fig. 51 – Pressure traces for system 5 with Halon 1301

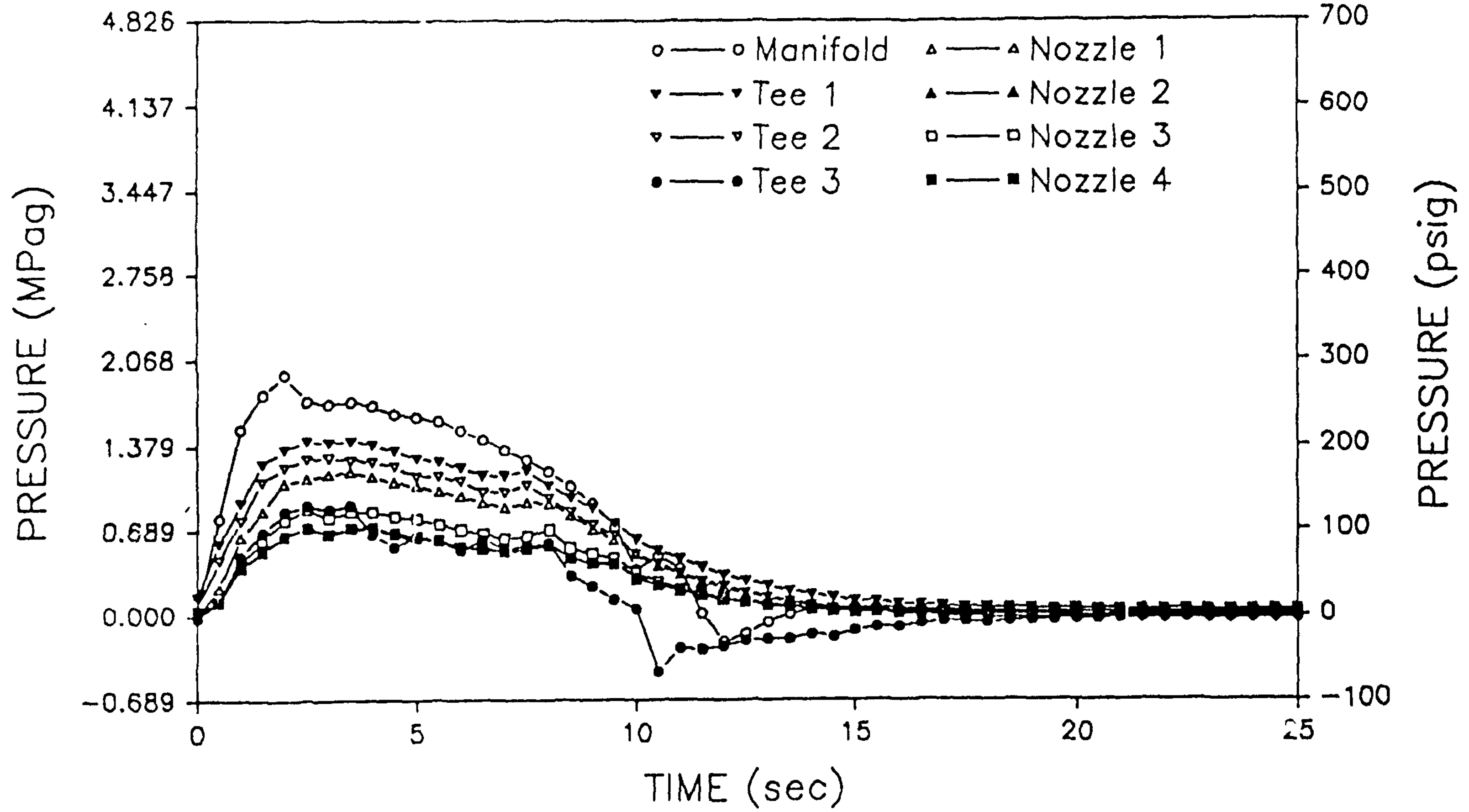


Fig. 52 — Pressure traces for system 5 with R-22

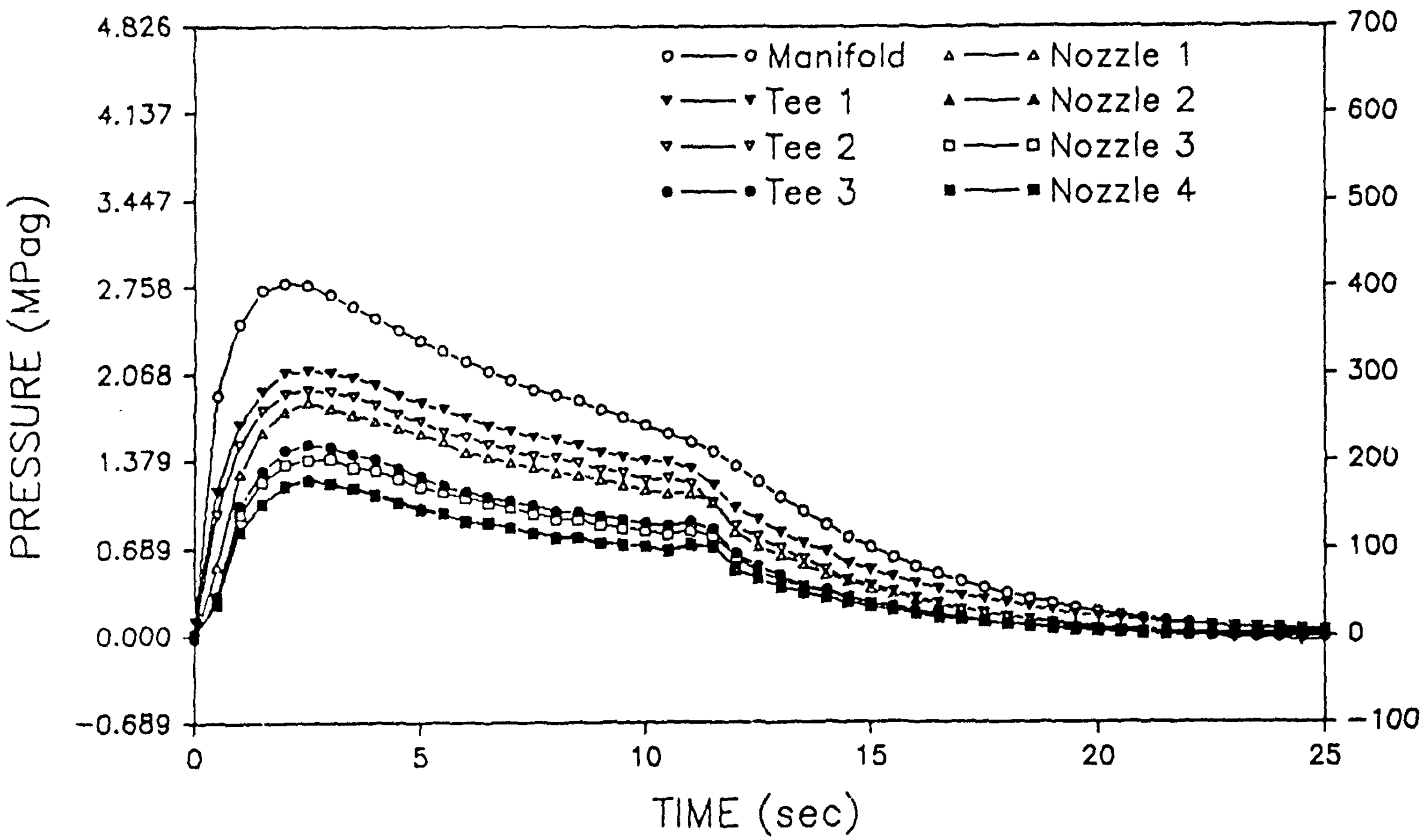


Fig. 53 – Pressure traces for system 5 with SF6

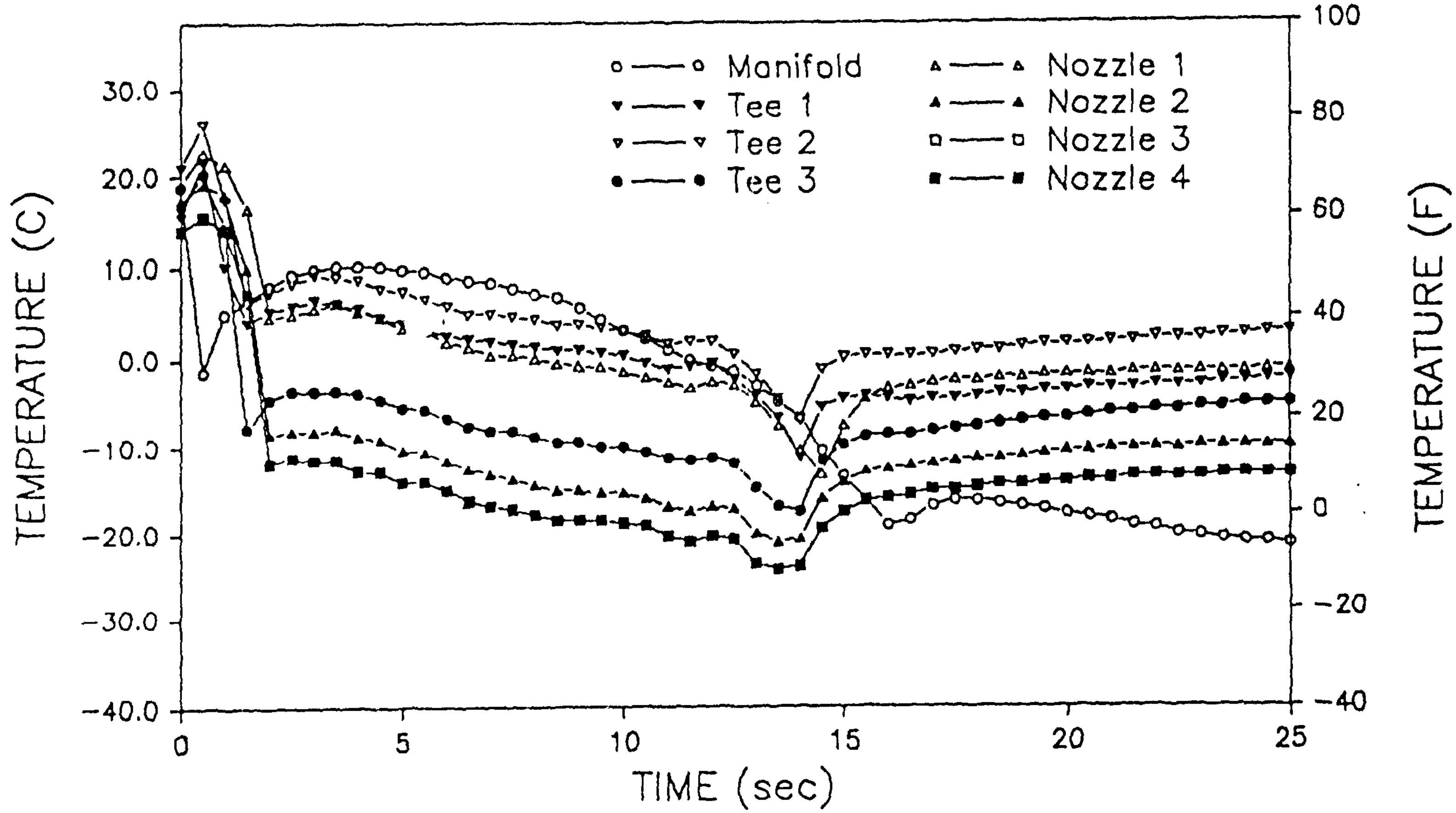


Fig. 54 – Temperature traces for system 5 with Halon 1301

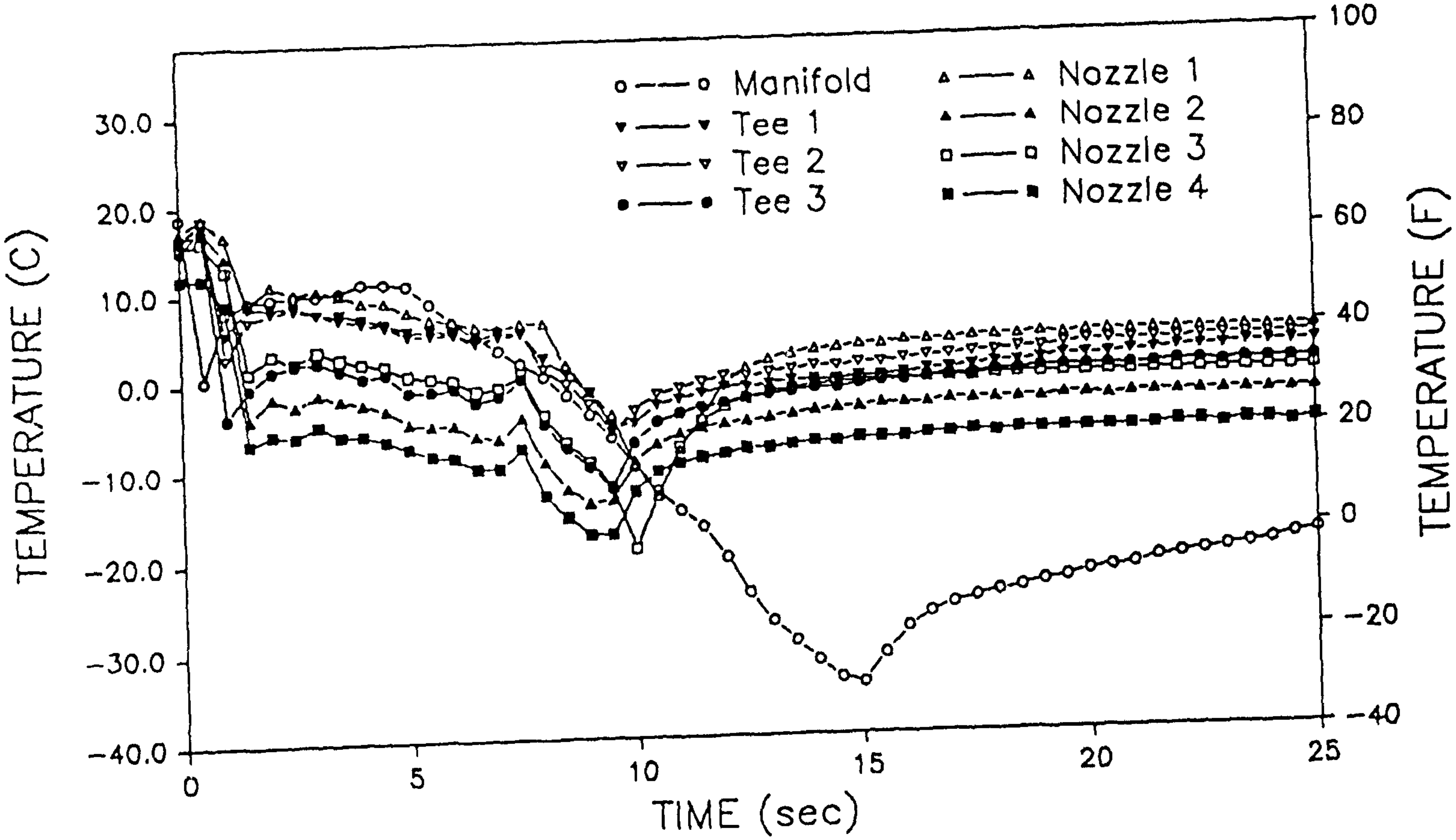


Fig. 55 – Temperature traces for system 5 with R−22

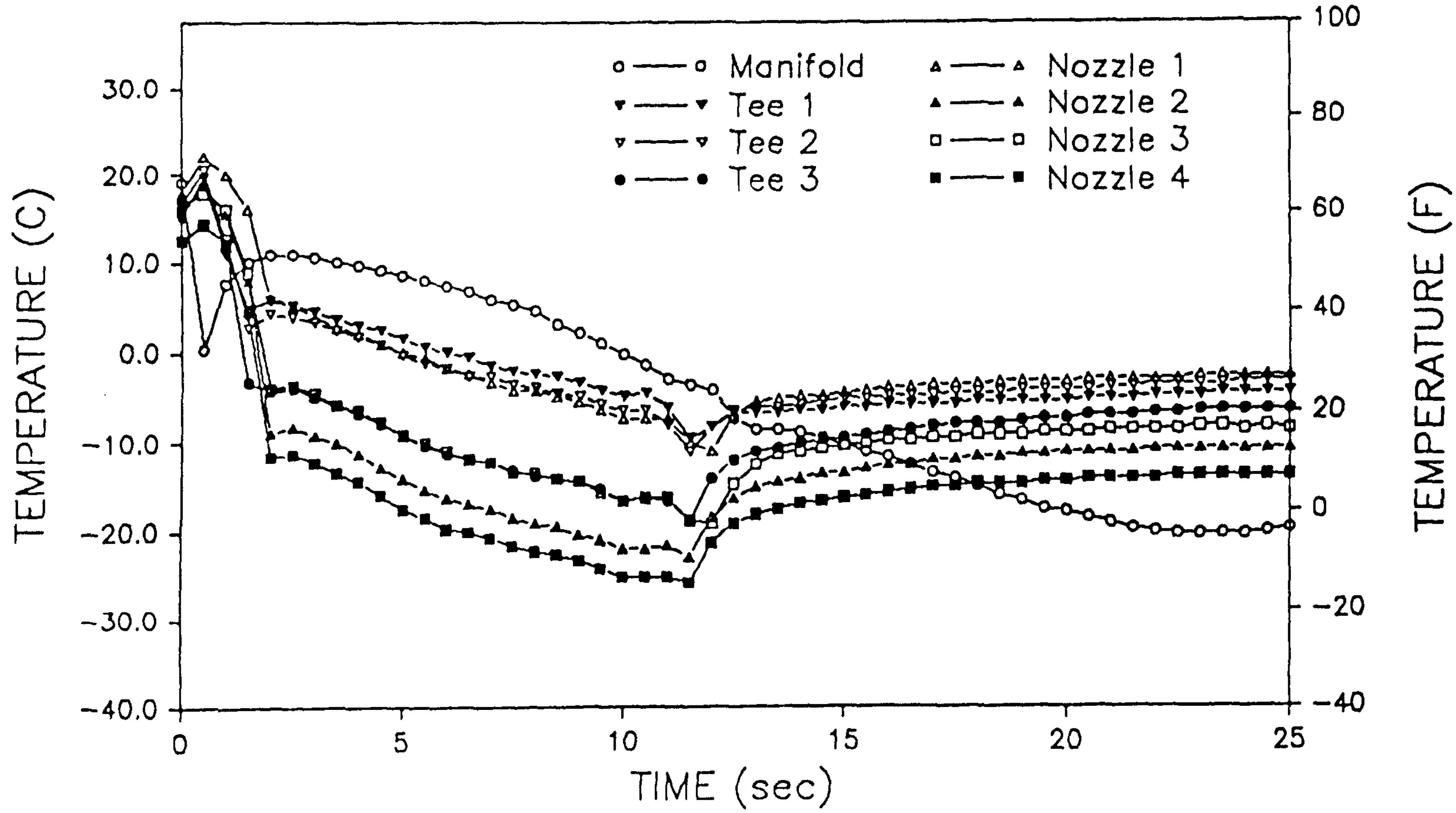


Fig. 56 – Temperature traces for system 5 with SF6

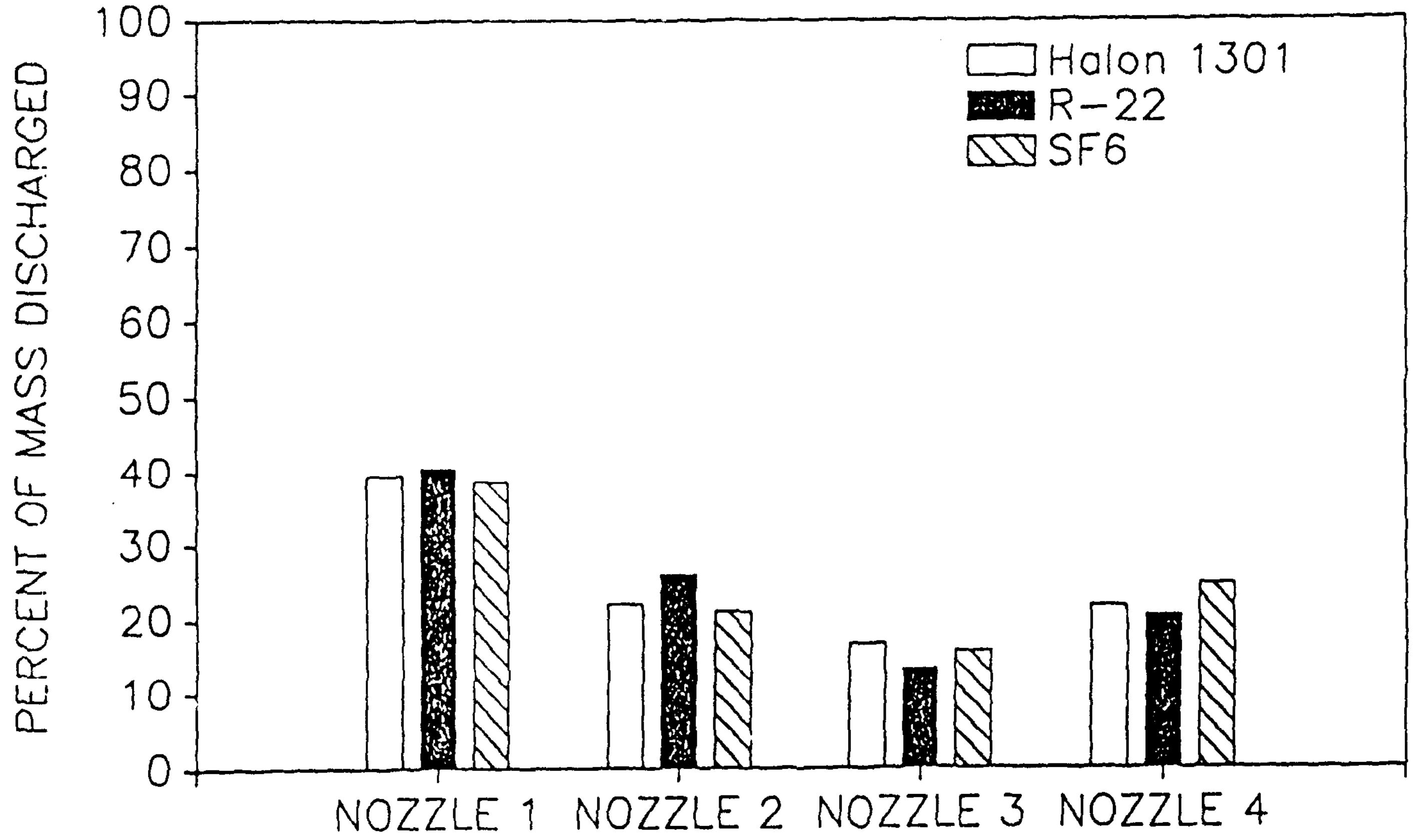


Fig. 57 – Mass distribution for system 6

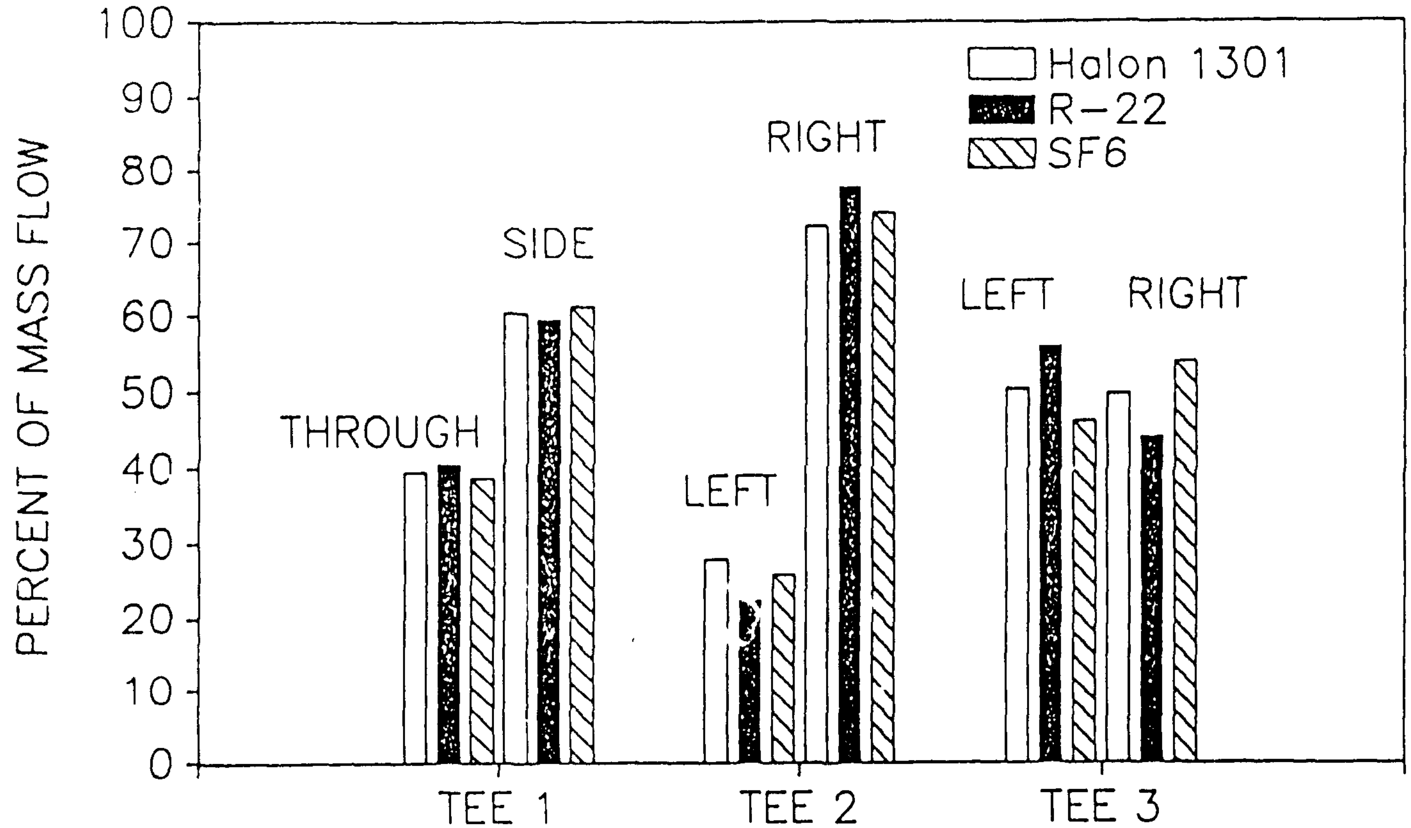


Fig. 58 — Mass flow distribution for system 6

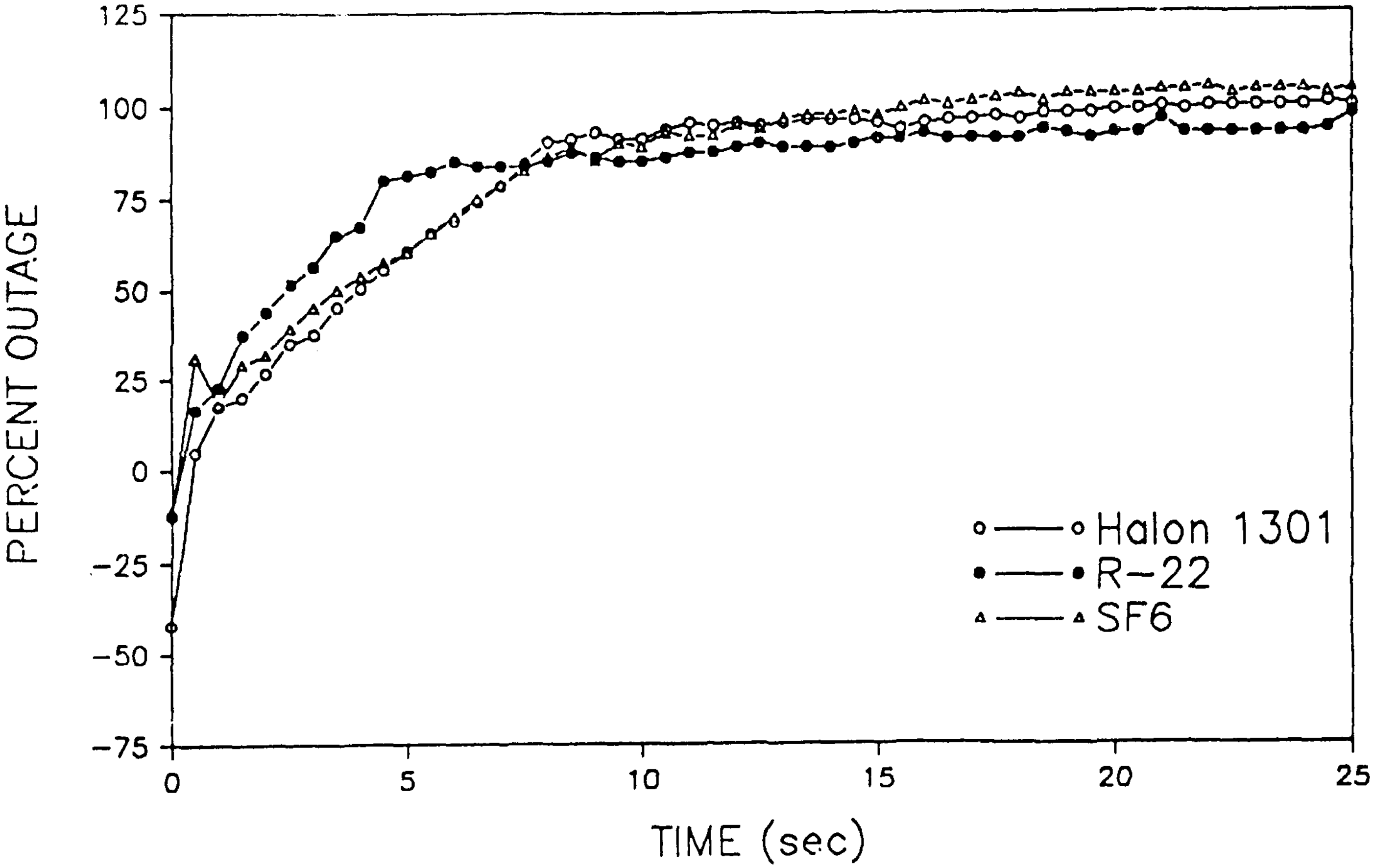


Fig. 59 — Percent outage for system 6

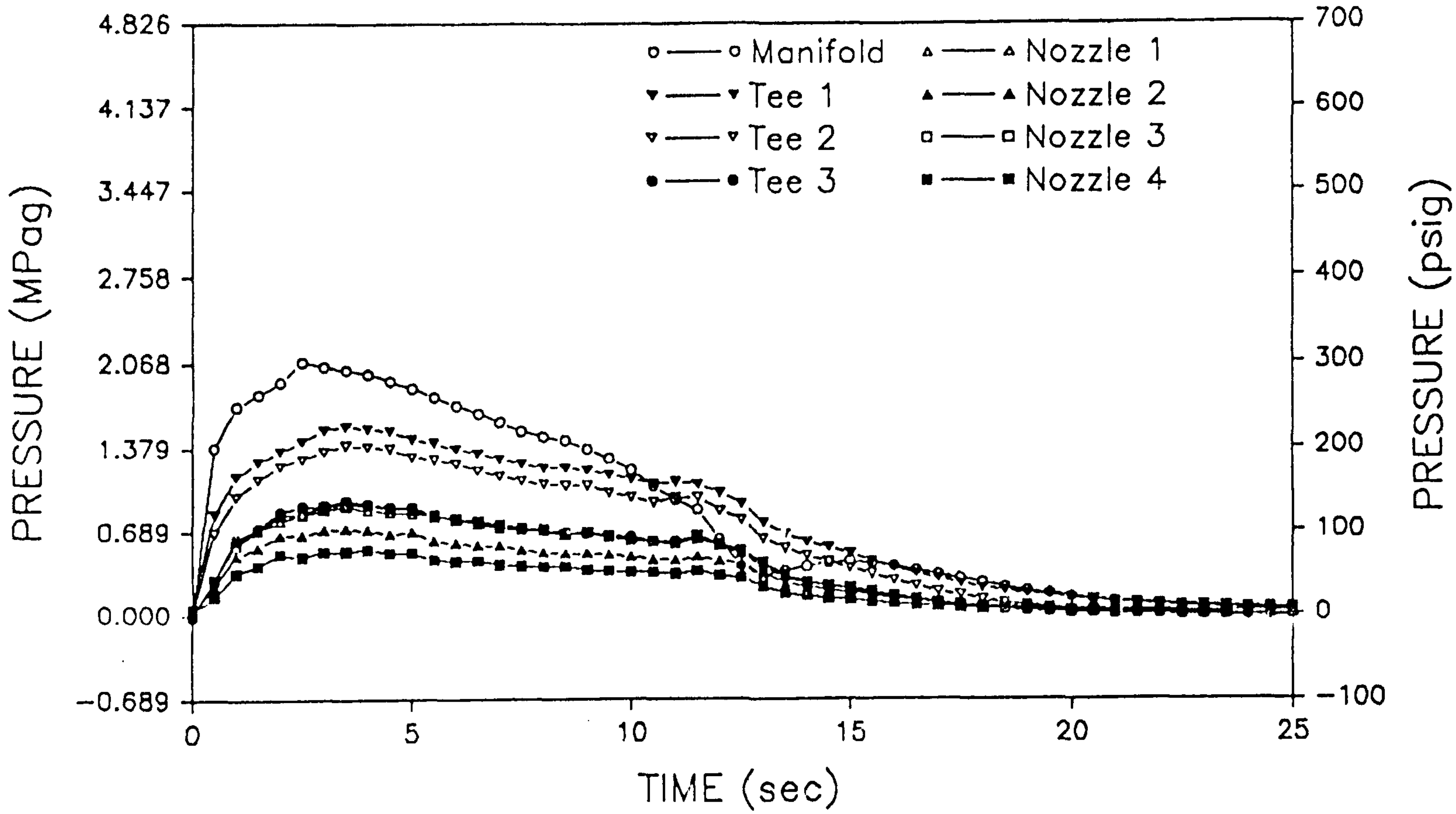


Fig. 60 – Pressure traces for system 6 with Halon 1301

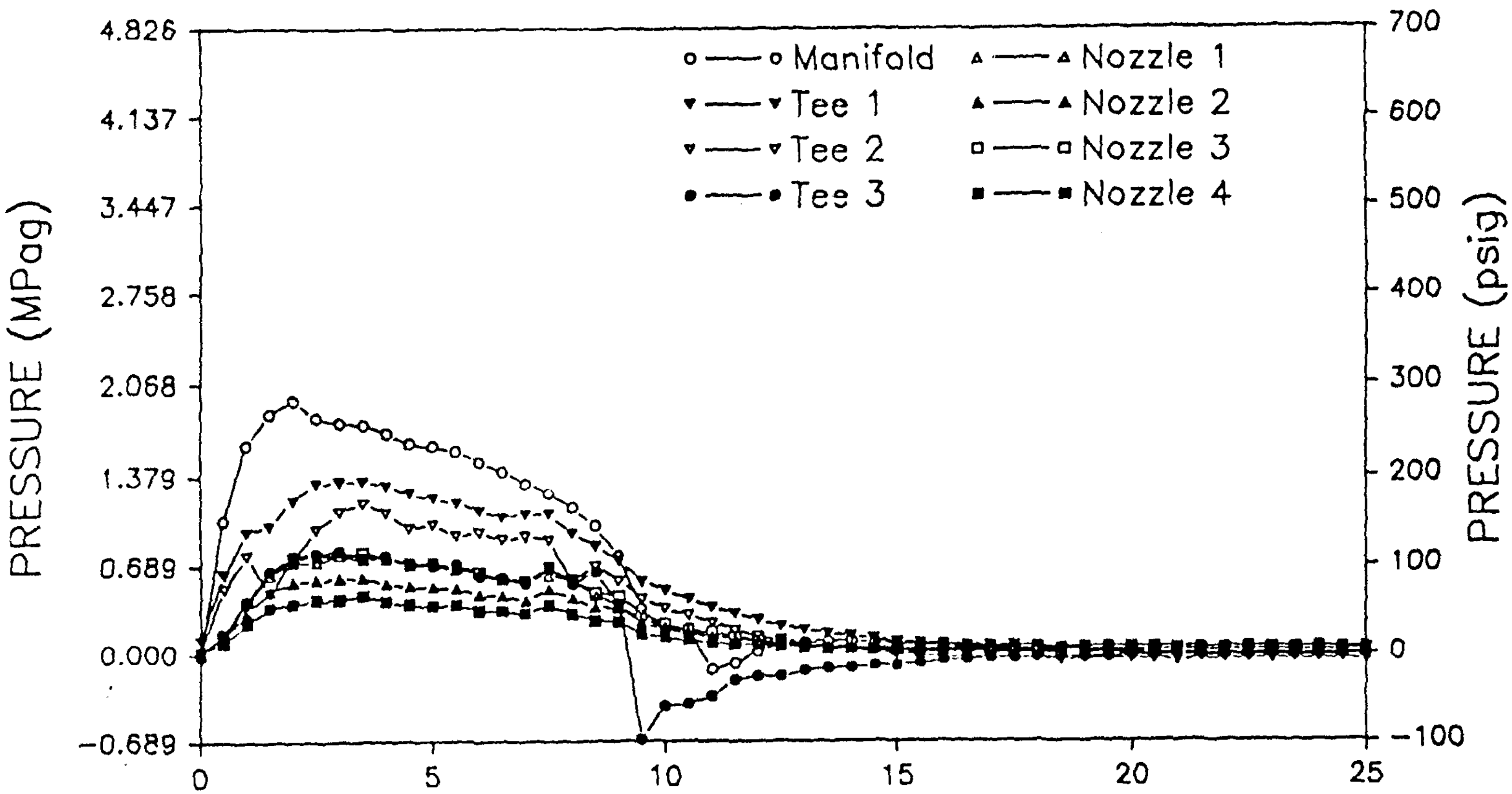


Fig. 61 – Pressure traces for system 6 with R–22

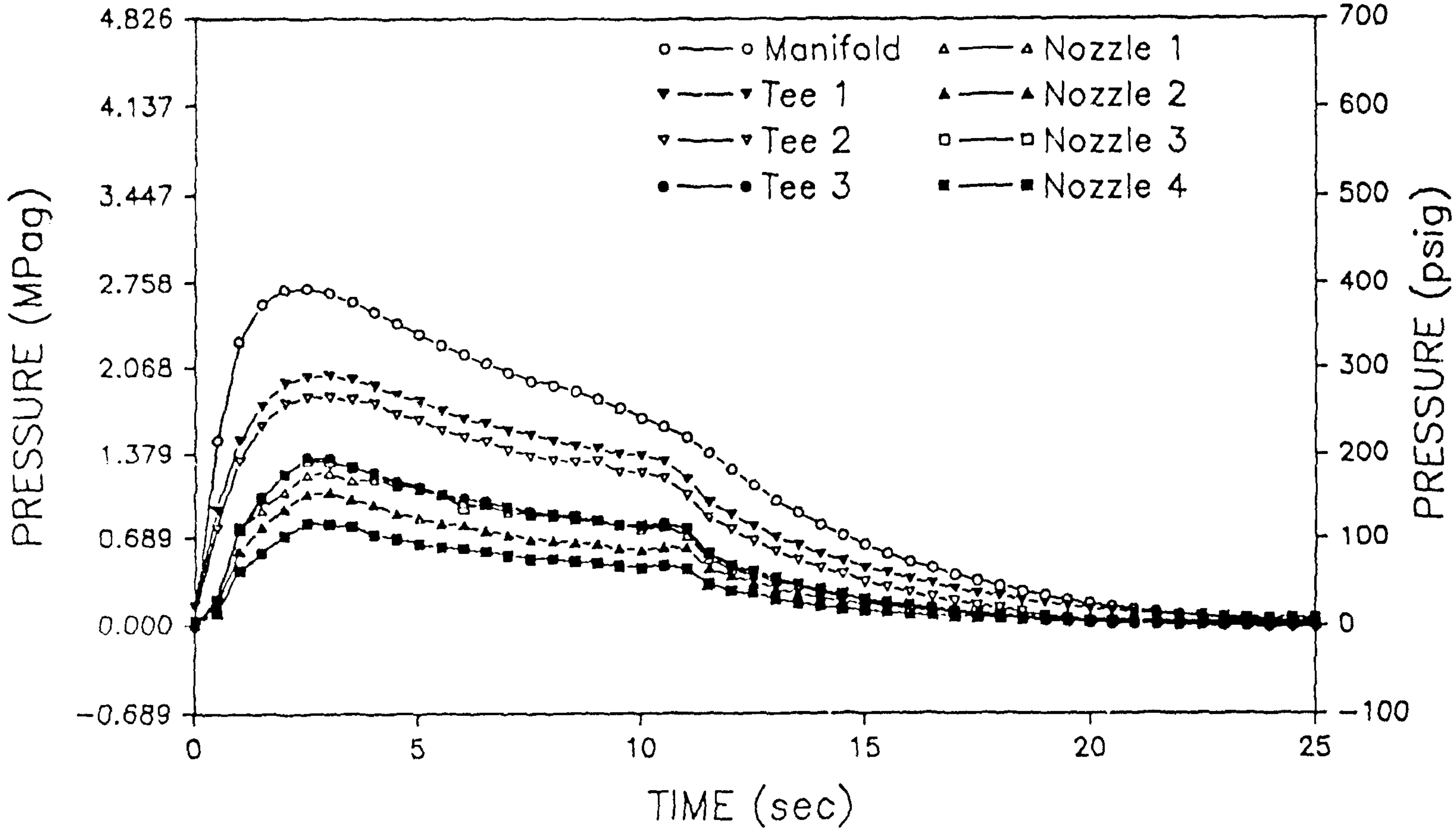


Fig. 62 – Pressure traces for system 6 with SF6

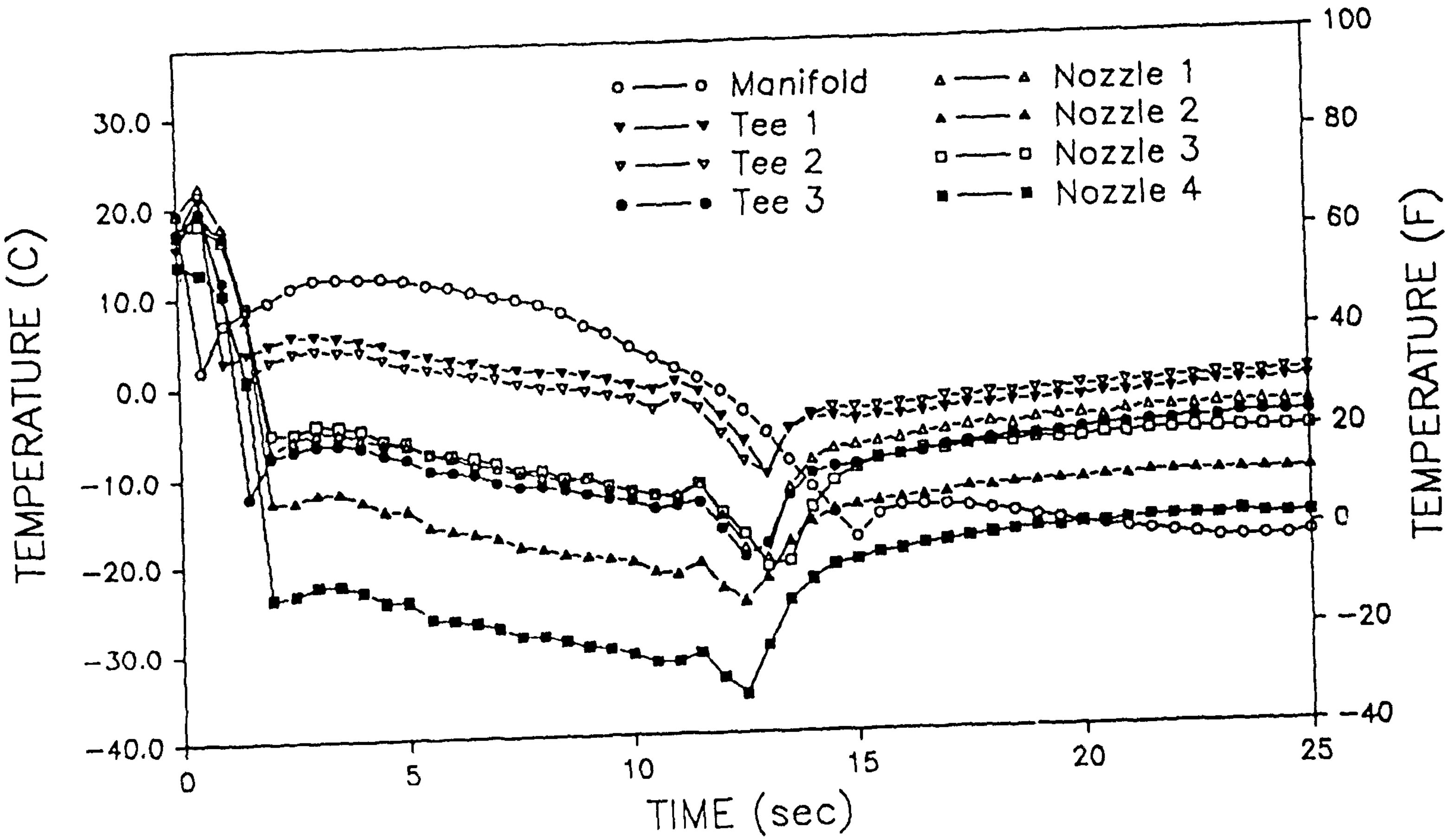


Fig. 63 – Temperature traces for system 6 with Halon 1301

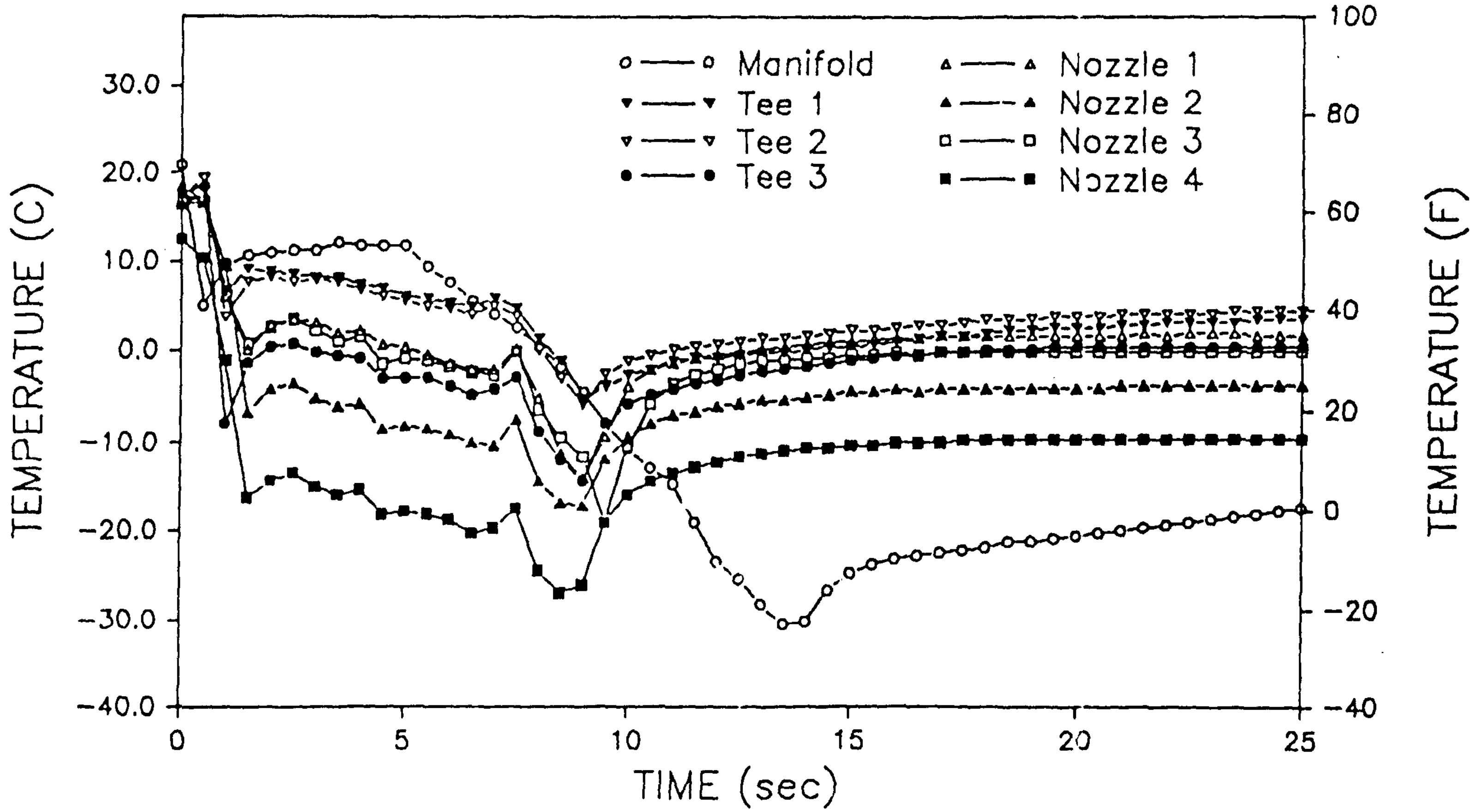


Fig. 64 — Temperature traces for system 6 with R−22

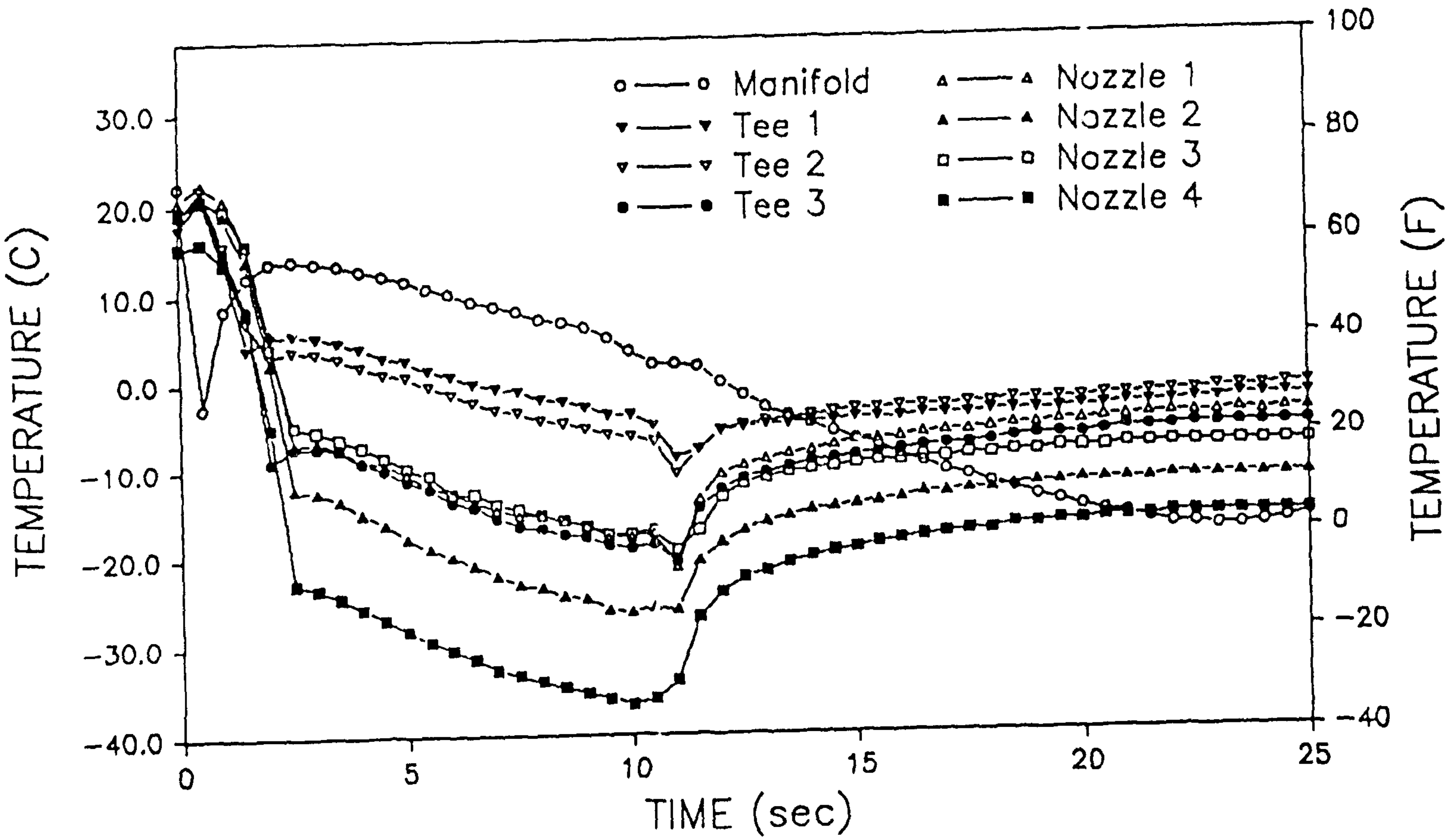


Fig. 65 – Temperature traces for system 6 with SF6

## 6.0 CONCLUSION

Together with previous work on leakage from an enclosure and initial mixing [4,10], these tests have shown that sulfur hexafluoride is an excellent simulant for Halon 1301 in total flooding system discharge tests. $SF_6$ has been shown to discharge at a similar rate, to distribute through a piping network in a similar manner, to leak from an enclosure similarly, and to mix with air in a similar manner to Halon 1301.

## 7.0 RECOMMENDATIONS FOR FURTHER WORK

Further study is needed in order to broaden the scope of these conclusions. These investigations include additional pipe networks, leakage flows, initial mixing and increased scale.

### 7.1 Additional Pipe Networks

An investigation into the effects of a broader range of discharge network parameters on the simulation of Halon 1301 flows is needed. These parameters include the percent of agent in the pipe network, cylinder fill densities, pressure drop in the pipe network, and intial cylinder charge pressure.

### 7.2 Leakage Flows and Initial Mixing

A broader approach to these two phenomena are needed. The effects of various ventilation schemes, and more representative enclosure geometries need to be investigated.

### 7.3 Increased Scale

Full scale, shipboard testing is needed to confirm the results obtained.

## REFERENCES

1. "Update on the Halon-Ozone Issue, "Fire Journal, 82(2), 1988.

2. Taylor, G., "Achieving the Best Use of Halons," Fire Journal, 81(3), 1987.

3. Willey, A.E., "The NFPA's Perspective on Halons and the Environment," Fire Journal, 81(3), 1987.

4. Carhart, H.W., Leonard, J.T., DiNenno, P.J., Starchville, M.D., Forssell, E.W., and Wong, J.T., "Tests of Halon 1301 Test Gas Simulants," NRL Memorandum Report 6424, Naval Research Laboratory, Washington, DC, 1989.

5. DuPont Company, "Halon 1301 Fire Extinguishant Product Information Library," Vols 1 and 2, Wilmington, DE.

6. Air Products and Chemicals, Inc., "$SF_6$, An Applications and Technical Manual," Air Products and Chemicals, Specialty Gas Department, Allentown, PA.

7. Allied Chemicals, "Accu Div $SF_6$," Technical Bulletin, Morristown, NJ.

8. DuPont Company, "Thermodynamic Properties of 'FREON' 22 Refrigerant," Wilmington, DE.

9. DuPont Company, "'FREON' Fluorocarbons, Properties and Applications," Wilmington, DE.

10. DiNenno, P.J., Starchville, M.D., Forssell, E.W. and Carhart, H.W., "Initial Mixing Tests of Halon 1301 Test Gas Simulants," NRL Memorandum Report, Naval Research Laboratory, Washington, DC., 1989.

11. National Fire Protection Association, "Standard on Halogenated Extinguishing Agent Systems - Halon 1301," NFPA No. 12A, Batterymarch Park, Quincy, MA, 1987.

12. Navy Sea Systems Command, "Halon 1301 - Modular System," Standard Drawing No. 803-5773930, Washington, DC.

13. Navy Sea Systems Command, "Halon 1301 - Banked System," Standard Drawing No. 803-5959326, Washington, DC.

14. DiNenno, P.J. and Budnick, E.K., "A Review of Halon 1301 Total Flooding Systems," National Fire Protection Association Research Foundation, 1988.

15. Robenson, J.A. and Crowe, C.T., Engineering Fluid Mechanics, 2nd Ed., Houghton Mifflin Company, Boston MA 1980.

# APPENDIX A

## Comparison with NFPA 12A

The National Fire Protection Association (NFPA) provides a method to estimate the pressure drop in the piping network of a Halon 1301 total flooding system in their standard 12A [A-1]. This method utilizes mid-discharge conditions (50% of initial mass discharged) and average flow rates. The mid-discharge point is determined in an iterative manner from a cylinder recession curve with the 50% outage point adjusted by the amount of agent in the piping network.

This method estimates the pressure drop in a section of pipe by the following equation:

$$Y_2 = Y_1 + LQ^2/(1.013D^{5.25}) + 7.97\ (Z_2 - Z_1)\ Q^2/D^4$$

where L is the equivalent length of the section in feet (actual length adjusted to account for fittings), Q is the average mass flow rate in lbm/sec and D is the inside diameter of the pipe in inches [A-1]. Y and Z are functions of the pipe line static pressure and are presented in tabular form in NFPA Standard 12A [A-1]. As Y and Z also depend on what occurs both before and after the mid-discharge point, a separate Y and Z Table is given for each initial charge pressure and a range of fill densities. The subscripts $_1$ and $_2$ refer to beginning and ending conditions respectively.

The first step in using this method is to estimate the percent agent in piping. This is accomplished by the following equation:

$$pnp = K_1/[(W/V_p) + K_2]$$

where pnp is the estimated percent agent in piping, W is the initial charge weight and $V_p$ is total internal pipe volume [A-1]. $K_1$ and $K_2$ are constants depending on the initial charge pressure and fill density. The mid-discharge storage pressure is then determined from the appropriate pressure recession curve with the percent cylinder outage being equal to the sum of 50% and the percent agent in pipe. The piping network is then divided into sections and the equivalent length and flow rate for each section determined. $Y_1$ and $Z_1$ for the first section are then determined by interpolation with the mid-discharge storage pressure, in the appropriate table. $Y_2$ is then determined, initially ignoring the contribution of $Z_2$ and correcting the $Y_2$ for it after the ending pressure has been estimated. $Y_2$ and $Z_2$ become $Y_1$ and $Z_1$ for the next section and the process repeats until the final section is completed. At this point the percent agent in piping estimate must be refined by the following equation,

$$pnp = 100\ \Sigma(V_n\ p_n)/W$$

where $V_n$ is the internal volume of Section n, and $p_n$ is the average density in section n determined graphically from 12A [A-1]. The whole procedure is then iterated until there is no change in the percent agent in pipe.

The nozzles are then sized from a characteristic curve provided by a nozzle manufacturer. In this particular case; the nozzles were sized by the Navy's specified characteristic curve [A-2].

This method was used to predict the pressure at various locations in the piping network used in the banked system tests. The flow splits and discharge times were adjusted until the nozzle sizes calculated agreed with the actual nozzles used.

In Tables 11 through 16, the predicted pressures are shown together with the measured peak pressures, and those measured at three cylinder outage percents. As the percent agent in pipe is approximately 40% in each system, the 90% outage measurement corresponds to the specified mid-discharge point.

As can be seen from this, the predicted pressures at the nozzles are higher than even the measured peak pressures. The discharge times calculated are consequently shorter than those measured.

A more rigorous approach needs to be taken to accurately predict the pressure drops in these systems. The NFPA

Table 11 - Pressure Decay for System 1

| | Pressure in MPag (psig) | | Percent Outage | | |
|---|---|---|---|---|---|
| Location | 12-A Calculation | Peak | 50% | 70% | 90% |
| Manifold | 1.98 (287) | 2.65 (384) | 2.56 (372) | 2.11 (306) | 1.75 (254) |
| Tee | 1.60 (232) | 1.63 (237) | 1.62 (235) | 1.39 (201) | 1.23 (179) |
| Nozzle 1 | 1.48 (214) | 1.35 (196) | 1.34 (195) | 1.13 (164) | 1.01 (146) |
| Nozzle 2 | 1.48 (214) | 1.37 (198) | 1.37 (198) | 1.11 (161) | 0.99 (143) |
| Time of Occurance [seconds] | | | | | |
| | | | 3.0 | 4.8 | 6.5 |
| Discharge Time [seconds] | | | | | |
| | 10.65 | | 10.6 [Temperature Method] | | |

Table 12 - Pressure Decay for System 2

| | Pressure in MPag (psig) | | Percent Outage | | |
|---|---|---|---|---|---|
| Location | 12-A Calculation | Peak | 50% | 70% | 90% |
| Bottle | 2.01 (291) | 4.05 (587) | 2.47 (358) | 2.12 (308) | 1.74 (252) |
| Tee | 1.74 (253) | 1.84 (267) | 1.81 (262) | 1.57 (228) | 1.30 (188) |
| Nozzle 1 | 1.72 (249) | 1.73 (251) | 1.72 (249) | 1.48 (215) | 1.22 (177) |
| Nozzle 2 | 1.59 (231) | 1.45 (210) | 1.37 (198) | 1.22 (177) | 0.98 (142) |
| Time of Occurance [seconds] | | | | | |
| | | | 3.4 | 5.4 | 8.4 |
| Discharge Time [seconds] | | | | | |
| | 12.60 | | 11.6 [Temperature Method] | | |

Table 13 - Pressure Decay for System 3

| Location | Pressure in MPag (psig) 12-A Calculation | Percent Outage Peak | 50% | 70% | 90% |
|---|---|---|---|---|---|
| Manifold | 1.96 (284) | 2.30 (334) | 2.12 (308) | 1.79 (259) | 0.75 (109) |
| Tee 1 | 1.65 (240) | 1.70 (247) | 1.63 (237) | 1.37 (199) | 0.80 (116) |
| Tee 2 | 1.61 (233) | 1.64 (238) | 1.59 (230) | 1.33 (193) | 0.82 (119) |
| Tee 3 | 1.61 (233) | 1.64 (238) | 1.58 (229) | 0.69 (100)* | 0.11 (17)* |
| Nozzle 1 | 1.48 (215) | 1.28 (186) | 1.25 (181) | 1.04 (151) | 0.65 (94) |
| Nozzle 2 | 1.48 (215) | 1.32 (192) | 1.26 (183) | 1.05 (152) | 0.61 (89) |
| Nozzle 3 | 1.48 (215) | 1.17 (169) | 1.12 (162) | 0.94 (137) | 0.56 (81) |
| Nozzle 4 | 1.48 (215) | 1.25 (181) | 1.21 (176) | 0.99 (143) | 0.60 (87) |
| Time of Occurance [seconds] | | | 3.9 | 5.9 | 11.8** |

Discharge Time [seconds]

9.96

10.7 [Temperature Method]

* Affected by a leak in pipe
** Beyond liquid runout

Table 14 - Pressure Decay for System 4

| | Pressure in MPag (psig) | | Percent Outage | | |
|---|---|---|---|---|---|
| Location | 12-A Calculation | Peak | 50% | 70% | 90% |
| Manifold | 1.94 (282) | 2.28 (330) | 2.23 (323) | 2.01 (292) | 1.70 (246) |
| Tee 1 | 1.66 (241) | 1.63 (236) | 1.59 (231) | 1.54 (223) | 1.35 (196) |
| Tee 2 | 1.61 (233) | 1.48 (215) | 1.44 (209) | 1.40 (203) | 1.21 (175) |
| Tee 3 | 1.55 (225) | 1.56 (226) | 1.53 (222) | 1.14 (166) | 1.01 (147) |
| Nozzle 1 | 1.43 (208) | 1.17 (170) | 1.16 (168) | 1.12 (162) | 0.96 (139) |
| Nozzle 2 | 1.43 (208) | 1.23 (178) | 1.22 (177) | 1.12 (162) | 0.98 (142) |
| Nozzle 3 | 1.48 (215) | 1.14 (165) | 1.04 (151) | 1.01 (147) | 0.94 (136) |
| Nozzle 4 | 1.48 (215) | 1.12 (162) | 1.06 (154) | 1.03 (149) | 0.89 (129) |
| Time of Occurance [seconds] | | | 2.9 | 4.6 | 6.4 |
| Discharge Time [seconds] | 10.26 | | 11.2 [Temperature Method] | | |

Table 15 - Pressure Decay for System 5

| | Pressure in MPag (psig) | | Percent Outage | | |
|---|---|---|---|---|---|
| Location | 12-A Calculation | Peak | 50% | 70% | 90% |
| Manifold | 1.95 (283) | 2.04 (296) | 1.93 (280) | 1.65 (239) | 1.25 (182) |
| Tee 1 | 1.68 (243) | 1.59 (231) | 1.57 (227) | 1.37 (198) | 1.13 (164) |
| Tee 2 | 1.57 (227) | 1.44 (209) | 1.41 (205) | 1.22 (177) | 1.01 (147) |
| Tee 3 | 1.50 (217) | 1.05 (153) | 1.05 (152) | 0.89 (129) | 0.71 (103) |
| Nozzle 1 | 1.50 (217) | 1.32 (192) | 1.30 (189) | 1.12 (163) | 0.94 (137) |
| Nozzle 2 | 1.43 (207) | 0.84 (122) | 0.83 (121) | 0.71 (103) | 0.57 (83) |
| Nozzle 3 | 1.45 (210) | 0.99 (144) | 0.99 (144) | 0.84 (122) | 0.68 (98) |
| Nozzle 4 | 1.43 (207) | 0.83 (120) | 0.83 (120) | 0.70 (102) | 0.57 (83) |
| Time of Occurance [seconds] | | | 3.8 | 6.2 | 10.3 |
| Discharge Time [seconds] | 10.35 | | 12.4 [Temperature Method] | | |

Table 16 - Pressure Decay for System 6

| Location | 12-A Calculation (MPag) | (psig) | Peak (MPag) | (psig) | 50% (MPag) | (psig) | 70% (MPag) | (psig) | 90% (MPag) | (psig) |
|---|---|---|---|---|---|---|---|---|---|---|
| | Pressure in MPag (psig) | | | | Percent Outage | | | | | |
| Manifold | 1.94 | (282) | 2.10 | (305) | 1.99 | (289) | 1.72 | (249) | 1.48 | (215) |
| Tee 1 | 1.59 | (231) | 1.57 | (228) | 1.54 | (224) | 1.37 | (199) | 1.22 | (177) |
| Tee 2 | 1.46 | (212) | 1.42 | (206) | 1.40 | (203) | 1.22 | (177) | 1.10 | (160) |
| Tee 3 | 1.36 | (197) | 0.95 | (138) | 0.91 | (132) | 0.79 | (115) | 0.71 | (103) |
| Nozzle 1 | 1.25 | (181) | 0.90 | (130) | 0.87 | (126) | 0.74 | (108) | 0.68 | (99) |
| Nozzle 2 | 1.31 | (190) | 0.72 | (105) | 0.69 | (100) | 0.59 | (86) | 0.53 | (77) |
| Nozzle 3 | 1.38 | (200) | 0.94 | (136) | 0.87 | (126) | 0.79 | (114) | 0.70 | (101) |
| Nozzle 4 | 1.20 | (174) | 0.55 | (80) | 0.52 | (75) | 0.46 | (67) | 0.39 | (57) |
| Time of Occurance [seconds] | | | | | 3.9 | | 6.1 | | 7.8 | |
| Discharge Time [seconds] | 9.4 | | | | | | 11.3 [Temperature Method] | | | |

standard 12A method should be relegated to first cut estimations only.

## REFERENCES


A-1 National Fire Protection Association "Standard on Halogenated Extinguishing Agent Systems - Halon 1301," NFPA No. 12-A, Batterymarch Park, Quincy, MA, 1987.

A-2 Navy Sea Systems Command, "Halon 1301 - Banked System," Standard Drawing No. 803-5959326, Washington, DC.